FRICTION STIR WELDING OF SIMILAR AND DISSIMILAR 2024-6061 ALUMINIUM ALLOYS

2024
MASTER THESIS
METALLUGICAL AND MATERIALS ENGINEERING

Hamid Mohammed Kodi KODI

Thesis Advisors
Assoc. Prof. Dr. Hüseyin DEMİRTAŞ
Prof. Dr. Adel K. MAHMOUD

FRICTION STIR WELDING OF SIMILAR AND DISSIMILAR 2024-6061 ALUMINIUM ALLOYS

Hamid Mohammed Kodi KODI

T.C.
Karabuk University
Institute of Graduate Programs
Department of Metallurgical and Materials Engineering
Master Thesis

Thesis Advisors
Assoc. Prof. Dr. Hüseyin DEMİRTAŞ
Prof. Dr. Adel K. MAHMOUD

KARABUK
June 2024

I certify that in my opinion the thesis submitted by Hamid Mohammed Kodi KODI titled "FRICTION STIR WELDING OF SIMILAR AND DISSIMILAR 2024-6061 ALUMINIUM ALLOYS" is fully adequate in scope and in quality as a thesis for the degree of Master of Metallurgical and Materials Engineering.

Assoc. Prof. Dr. Hüseyin DEMİRTAŞ   ....

Prof. Dr. Adel K. MAHMOUD   ....

Thesis Advisor, Department of Metallurgical and Materials Engineering This thesis is accepted by the examining committee with a unanimous vote in the Department of Metallurgical and Materials Engineering as a Master of Science thesis. June 25, 2024

Examining Committee Members (Institutions)   Signature

Chairman: Assoc. Prof. Dr. Harun ÇUĞ (KBU)   ....

Member: Assist. Prof. Dr. Cihangir Tevfik SEZGİN (KÜ)   ....

Member: Assoc. Prof. Dr. Hüseyin DEMİRTAŞ (KBU)   ....

The degree of Master of Engineering by the thesis submitted is approved by the Administrative Board of the Institute of Graduate Programs, Karabuk University.

Assoc. Prof. Dr. Zeynep ÖZCAN   ....
Director of the Institute of Graduate Program

"I declare that all the information that has been presented in this thesis was gathered and presented in accordance with ethical principles and academic regulations and I have according to requirements of those regulations and principles that were cited all those which don't originate in this work too."

Hamid Mohammed Kodi KODI

ABSTRACT

Master Thesis

FRICTION STIR WELDING OF SIMILAR AND DISSIMILAR 2024-6061 ALUMINIUM ALLOYS

Hamid Mohammed Kodi KODI

Karabuk University
Institute of Graduate Programs
Department of Metallurgical and Materials Engineering

Thesis Advisors:
Assoc. Prof. Dr. Hüseyin DEMİRTAŞ
Prof. Dr. Adel K. MAHMOUD
June 2024, 114 pages

Friction stir welding (FSW) is a relatively modern joining technology and solid-state welding process used for welding similar and dissimilar aluminum alloys such as 2xxx and 6xxx series. In this study the friction stir welding is conducted on similar and dissimilar Al alloys (AA6061-T6 and AA2024-T3) of 2mm thick plates at three different tool Rotating Speeds (450,710 and 1400 RPM) and three various travel speeds or Travel Speed (45,71 and 112mm/min). with using cylindrical pin geometry and tilt angle was 2 degree.

Many tests and inspections are carried out such as X-ray radiography and tensile test to evaluate the joint quality and the soundness of weldments. Microstructure and microhardness test were done on cross section of welds in order to study the welding zones and their microstructure and hardness distribution on various welding zones.

SEM-EDS instruments were used to study the fractography of tensile fracture surface. Also, EDS was used to know the elemental analysis in weld zones after fracture.

Tensile test is curried out for all welded joints to indicate the weld quality and joint efficiency. Microhardness distributions across section of similar and dissimilar FSW joints are investigated at the best welding conditions. SEM was used to study the fracture surface after tensile and bending test for similar and dissimilar FSW.

It was found the tensile strength for dissimilar FSW joints were (332 MPa) which are higher than that of similar FSW joints which was (322 MPa), both results associated at the same conditions (710 RPM and 112 mm/min). For all samples base alloys and welded joints, result more fracture type (cleavage fracture) because some micro cracks propagation and striation, but some surface fracture type (brittle fracture).

Key Word: Friction stir welding, aluminium alloys, mechanical properties, microstructure.
Science Code: 91511

ÖZET

Yüksek Lisans Tezi

BENZER VE BENZER OLMAYAN 2024-6061 ALÜMİNYUM ALAŞIMLARIN SÜRTÜNME KARIŞTIRMA KAYNAĞI

Hamid Mohammed Kodi KODİ

Karabük Üniversitesi
Lisansüstü Eğitim Enstitüsü
Metalurji ve Malzemeler Mühendisliği Anabilim Dalı

Tez Danışmanları
Doç. Dr. Hüseyin DEMİRTAŞ
Prof. Dr. Adel K. MAHMOUD
Haziran 2024, 114 sayfa

Sürtünme karıştırma kaynağı (FSW), 2xxx ve 6xxx serisi gibi benzer ve farklı alüminyum alaşımlarının kaynaklanması için kullanılan nispeten modern bir birleştirme teknolojisi ve katı hal kaynak işlemidir. Bu çalışmada, 2 mm kalınlığındaki benzer ve farklı Al alaşımları (AA6061-T6 ve AA2024-T3), farklı üç takım dönüş hızında (450,710 ve 1400 RPM) ve üç farklı kaynak hızı veya ilerleme hızında (45, 71 ve 112 mm/dak) sürtünme karıştırma kaynağı yapılmıştır. Çalışmada karıştırıcı uç 2 derece eğim açısında ve silindirik geometride kullanılmıştır.

Birleşim kalitesini ve kaynakların sağlamlığını değerlendirmek için X-ışını radyografisi ve çekme testi gibi birçok test ve muayene yapılmaktadır. Kaynak bölgelerindeki mikro yapı ve sertlik dağılımlarını incelemek amacıyla kaynakların kesitinde mikro yapı ve mikro sertlik testleri yapılmıştır. Kırılma yüzeyini incelemek

için SEM-EDS kullanılmıştır. Ayrıca kaynak bölgelerinde kırılma sonrası element dağılımının tespiti için EDS kullanılmıştır.

Kaynak kalitesini ve bağlantı verimliliğini belirlemek için tüm kaynaklı bağlantılar için çekme testi yapıldı. Benzer ve farklı FSW bağlantılarının kesitleri boyunca mikro sertlik dağılımları en iyi kaynak koşullarında araştırılmıştır. Benzer ve farklı FSW için çekme ve bükme testinden sonra kırılma yüzeyini incelemek için SEM kullanıldı.

Benzer olmayan FSW bağlantı noktalarının gerilme mukavemetinin (332 MPa), benzer FSW bağlantı noktalarından (322 MPa) daha yüksek olduğu bulunmuştur. Her iki sonuç da aynı koşullarla (710 RPM ve 112 mm/dak) ilişkilidir. Tüm numuneler için baz alaşımları ve kaynaklı bağlantılar, bazı mikro çatlakların yayılması ve çizgilenme nedeniyle daha fazla klivaj kırılması tipi ile sonuçlandı, ancak bazı yüzeyler gevrek kırılma tipi ile sonuçlandı.

Anahtar Sözcükler: Sürtünme karıştırma kaynağı, alüminyum alaşımları, mekanik özellikler, mikro yapı

Bilim Kodu:　　　91511

ACKNOWLEDGMENT

CONTENTS

LIST OF TABLES

LIST OF FIGURES

ABBREVIATIONS AND SYMBOLS

AA.	:	Aluminum Association Designation
Al_2O_3	:	Aluminum Oxide or Alumina Solution
ASTM	:	American Society for Testing and Materials
AWS	:	American Welding Society
BM	:	Base Metal
CNC	:	Computer Numerical Control
FSP	:	Friction Stir Processing
FSSW	:	Friction Stir Spot Welding
HAZ	:	Heat Affected Zone
HCl	:	Hydrochloric Acid
Hf	:	Hydrofluoric Acid
HNO_3	:	Nitric Acid
HV	:	Vickers Hardness
MMCs	:	Metal Matrix Composites
NDT	:	Non-Destructive Test
NZ	:	Nugget Zone
RPM	:	Revolution per Minute
TMAZ	:	Thermo-Mechanically Affected Zone
TWI	:	The Welding Institute
VT	:	Visual Test
WN	:	Weld Nugget Zone Symbols
ω	:	Rotational Speed
υ	:	Welding Speed
θ	:	Tool Tilt Angle
ε	:	Strain
D	:	Shoulder Diameter

PART 1

INTRODUCTION

1.1. BACKGROUND

Aluminum alloys have wide area of engineering applications, because of its light weight and excellent weight to strength ratio, it has a huge range of usages in aircraft, automobile manufacturing, railway vehicles, bridges, and high-speed shipping. Generally, welding term reflect the joining method, posing a significant challenge for designers and technicians. There are numerous challenges associated with this type of joint process, mostly due to the presence of an oxide layer, high thermal conductivity, a high coefficient of thermal expansion, solidification shrinkage, and the high solubility of hydrogen and other gases during the molten state. The further problem appears when emphasis is focused on heat-treatable alloys, where the heat generation during the welding process is responsible for deterioration mechanical property deterioration due to phase transitions and softening [1]. However, heat treatable aluminum alloys are very sensitive to the elevated temperature, which makes the traditional fusion welding techniques incompetent to produce efficient joints. This was the main problem that led to originate non-fusion welding approaches, such as friction welding which was used in limited industrial applications. In this process, a frictional heat is generated by a relative rotational or linear motion between the compressed materials to be welded. This heat softens the workpieces at the contact region and assist to produce the weldment by increasing the applied pressure [1].

Friction Stir Welding (FSW) techniques is an innovative solid phase welding technique created at The Welding Institute (TWI _ Cambridge, UK) in 1991. The FSW method functions work beneath the solidus line temperature of the metallic element that are joined, hence no melting occurs.

1

The procedure is a modification of traditional friction welding and is used to create continuous welded joints layers for plate manufacturing. Since its creation in 1991, many researchers have made continuing efforts to understand, use, and improve this technique [2]. This technique may enhance joint mechanical characteristics such as strength, by reducing the number of brittle compounds near the contact. Friction and plastic deformation between the tool (pin and shoulder) and the workpieces induce localized heat. Friction stir welding was developed as a welding technology to be utilized for high strength alloys that were difficult to join using traditional methods [3]. During fusion welding, complex thermal and mechanical stresses develop in the weld and surrounding heat and accompanying constraint. Following fusion welding, residual stresses commonly approach the yield strength of the base material. It is generally believed that residual stresses are low in friction stir welds due to low temperature solid-state process of FSW [3]. This approach is mainly useful for aluminum alloys however can also be applied to other items such as stainless steel, copper and its alloys, lead, titanium and its alloys, magnesium and its alloys, zinc, plastics, and mild steel. This process can also be used to weld many different shapes, including plates, sheets, and hollow pipes [4].

AA6061 aluminum alloy (Al-Mg-Si alloys) is the most extensively used medium strength aluminum alloy and has gained great recognition in the manufacture of light-weight structures [4]. AA2024 is an alloy introduced in 1931. It employs copper as its greatest secondary element, increasing the strength of an aluminum alloy and facilitating precipitation hardening. Other trace elements include magnesium and manganese, both of which boost the material's strength. It demonstrates good strength throughout a wide temperature range. However, 2024 doesn't demonstrate good corrosion resistance. Actually, containing copper as the major alloy component makes 2024 particularly susceptible to corrosion and less ductile. As a consequence, 2024 is typically not appropriate for welding [5].

Several geometrical and technological aspects greatly influence the FSW process; tool geometry affects heat generation and metal flow consequently of friction forces. The fluxing heat applied at the joint controlled by the tool's rotation and travel speed.

Furthermore, tool design, rotation, and travel speed all have a significant impact on mechanical properties [6].

However, there is no concurred optimum tool design in use presently, because a specific tool might generate various outcomes when an identical set of input variables are employed on other materials or with varying plate thicknesses [6]. The material frequently experiences different load circumstances, and fatigue failure is a serious problem. Choice of welding procedure (clamping condition) can significantly influence the fatigue life. In transportation and under varying load conditions fatigue failure is an important issue. There are many factors that make the weld critical under fatigue loading conditions. For instance, stress concentrations such as residual stresses, unfavorable Weld failure in service is caused primarily by the mechanical properties of the weld nugget and probable defects in the weld.

1.2. AIMS of PRESENT WORK

The present work deal with the following considerations:

1. Study the effect of rotating speed on the tensile, bending strength, microhardness and microstructure for similar and dissimilar 6061, 2024 Al alloys.

2. Study the effect of travel speed on tensile, bending strength, microhardness and microstructure for similar and dissimilar 6061, 2024 Al alloys.

3. Study the metallurgical phases that presents in welding zones after FSW process.

4. Evaluation of the properties and weld quality depending on many of inspection tests.

5. Study the effect of preheat treatment on the tensile strength of 6061, 2024 Al alloy before FSW process.

6. Fracture analysis is done by scanning electron microscopy (SEM-EDS).

7. Evaluation the welding efficiency for some selected parameter.

1.3. LAYOUT of the THESIS

In order to research the aim of this work many steps are carried out as following:

1. Chapter one includes background about aluminum and friction stir welding, also include the aim of thesis.

2. Chapter two include some research about friction stir welding and choosing parameters to result best efficiency.

3. Chapter three include theoretical about type of aluminum and friction stir welding, also application and advantage of friction stir welding.

4. Chapter four includes experimental work and machine parameters and all inspection and tests.

5. Chapter five has results of inspection and discussion all data.

6. Chapter six includes conclusion and recommendation.

PART 2

LITERATURE REVIEW

2.1. INTRODUCTION

Numerous studies have concentrated on the variables that affect friction stir welding, as it is a quite new procedure that is quickly replacing older methods of welding. These characteristics include the tool rotational speed and the welding speed, among others.

In this section, the examination of how different friction stir welding settings influence the features of the resulting aluminum alloy joints. Also, go into research on the wear and tear characteristics of FSW.

Here is a quick rundown of studies that have looked into comparable and different types of friction stir welding.

2.2. COMPARABLE FRICTION STIR WELDED JOINTS

Here are a few findings from studies conducted by researchers and investigators who looked into the FSW, with an emphasis on those who dealt with aluminum alloys and the 2xxx and 6xxx series in particular.

Adamowski and Szkodo (2007) [7]**;** examined how modifying process parameters influenced the mechanical characteristics and microstructural changes of friction stir welds in the aluminum alloy AA 6082-T6. The tensile strength of the joints that were manufactured was measured, and the relationship with the process parameters was evaluated. Optical microscopy and microhardness measurements were used to display and evaluate microstructures of different zones of FSW welds.

As the speed of welding process increased while the rotating speed remained constant, they discovered that the mechanical qualities of the test welds improved. Comparatively, fusion welds result in superior material softening across the zone impacted by heat and weld nugget. It was determined and studied where the tunnel faults originated.

Babu et al. (2008) [8]; Examined the impact of factors involved in processing on the mechanical and microstructural features of friction stir welded (FSW) joints made of aluminum alloy AA 6082-T6. The welding speeds and rotational velocities were varied to create a variety of welded specimens. A connection between the process parameter and the tensile strength of the welded joints was evaluated at room temperature. The microstructures of different zones of FSW welds were shown and examined using optical microscopy and microhardness tests. The experimental findings revealed that the process parameters greatly impact the mechanical characteristics and weld macrostructure of this particular joint.

Kumbhar and Bhanumurthy (2008) [9]; A vertical type milling machine was utilized to conduct FSW tests on the Al 6061 alloy. An almost perfectly flat welded interface was achieved by meticulously selecting and fabricating the tool's shape. a) axial force is a significant process parameter that affects weld quality. b) tool tilt angle; c) traverse speed; and d) Rotating Speed was fine-tuned to produce welded connections free of defects. Friction stir welding causes significant distortion in the nugget zone, and the resulting microstructure has a major impact on the joint's mechanical characteristics. The mechanical characteristics and microstructural changes that occur during and after FSW and post-weld heat treatment (PWHT) were the focus of the current investigations. Through the use of electron probe microanalysis (EPMA), orientation imaging microscopy (OIM), and secondary electron microscopy (SEM), The research discussed process parameter optimization, the resulting microstructure was described. Highlighting the impact of PWHT on the microstructure, composition variation across the interface, and mechanical attributes of FSW 6061 Al alloy.

Sammer Jasim AL-Joud (2009) [10]; Investigated the impact of geometrical shape and diameter of the tool pin on the microstructure and mechanical characteristics of

2218-T72 aluminum alloy and made an effort to comprehend it. The connection was constructed using five variations of tool pin profiles: threaded cylindrical, straight cylindrical, square, triangular, and threaded cylindrical with flat. The pin diameters utilized for the fabrication were 3, 4, and 5 mm. Various mechanical investigations including as tensile, bending, and microhardness examinations, were used to evaluate the impact of the tool pin profile on the mechanical characteristics of the welded connections. With a tool pin profile of threaded cylindrical with a flat, a Rotating Speed of 900 RPM, and a welding speed of 30mm/min, the findings established that the (FSW) process could weld aluminum alloy (2218-T72) with a maximum welding efficiency of 86.55% in terms of ultimate tensile strength and 83.21% in terms of bending force.

Rajakumar et al. (2010) [11]; shown the widespread preference for the Al (6061-T6) alloy in friction stir welding the ability for offering a lightweight joint with superior mechanical qualities, including high strength and great corrosion resistance. Joint strength may be affected by grain size and the strength of the nugget zone, as he demonstrated. Therefore. An empirical relationship was derived by him that predicts the tensile strength and grain size of an Al (6061-T6) joint that is friction stir welded.

Perumalla et al. (2013) [12]; Examined the load-extension behavior during in-plane stretching of AA6061 FSW blanks as a function of tool shoulder diameter, plunge depth, tool Rotating Speed, and welding speed. The necessary load was almost same for the two divergent drop depths. The shoulder diameter, plunge depth, welding speed, and tool rotating speed all had an effect on the extension, while the base metal had the opposite effect, experiencing maximum stress with little extension. With the exception of the failure start, the failure pattern for both welded and unwelded blanks was identical.

Aval et al. (2013) [13]; This study looked into friction stir-welded AA6061-T6 to see how it aged mechanically, microstructurally, and in terms of residual stresses. Optical metallography, transmission electron microscopy, X-ray diffraction to determine residual stresses, tensile testing, and hardness measurements were used to characterize the mechanical properties and microstructure of the friction stir-welded joints in both

the as-welded and post-welded states. The research concluded that the applied heat input per unit length is the primary determinant of the post-weld hardness and weld strength changes. On the other hand, the effects of natural aging on the welded samples become much less pronounced after 14 days of aging, and they become rather visible during the first 14 days. There is a notable decrease in residual stress of around 22 MPa as a result of natural aging, according to the measurements of residual stress. This decrease is clear appear in the stir zone and the thermos mechanically impacted zone.

Saad et al. (2015) [14]**;** Explored FSW AA2024-T3's mechanical and microstructure characteristics. An effort has been made to comprehend how the welding process mode and tool profile impact the weldment strength. For the purpose of welding the joint zone, seven distinct tool pin profiles were used, including straight cylindrical, threaded cylindrical, tapered cylindrical, threaded taper, triangular, hexagonal, and square. Additionally, two distinct shoulder surfaces, flat and concave, were employed. Single and double-sided welding were accomplished using two different approaches. Maintained a steady Rotating speed of 1000 RPM and a welding pace of 28 mm/min. The angle of the tool spindle three degrees toward the weld line. The hexagonal pin shape with a concave shoulder and a single-side welding method yielded the optimum mechanical performance. Maximum tensile strength (89.4% efficiency) and bending force (85.71% efficiency) were achieved during welding. When comparing the straight cylinder tool profile to the others, the weaknesses in tensile strength and bending force were discovered. For both single- and double-side welding, the concave shoulder surface outperformed the flat surface in terms of tensile strength and bending force. In comparison to the base metal, the weld zone has a greater hardness value.

Ahmed Waheeb Shafey (2016) [15]**;** Studying the impact of friction stir welding on the mechanical characteristics of aluminum AA1050 plates, we found that parameters like tool Rotating Speed and travel speed had an essential impact on the results. Then used destructive cutting length to conduct a microscope examination of the welding stirring zone, which revealed welding defects and residual stress. It founded that the most common stresses formed during friction stir welding are compressive types, and that welding speed influences the resultant residual stress. Finally, we used the finite

element software ANSYS to model the welding process and predict the welding temperature and distribution.

Sergey et al. (2016) [16]; Investigated the process of friction stir welding a 3 mm thick aluminum (6061-T6) sheet. The technique included subjecting it to heat treatment, which involves aging and solid solution. The specimens were heated in the furnace to 550 ℃ for an hour to achieve a solid solution, and then they were quenched with water. The specimens were held in the furnace at 160 C for 8 hours to age them. The primary goal of this research was to examine the relationship between the mechanical characteristics and variables such as speed of welding and heat treatment technique, particularly aging response. This welding process made use of three distinct travel speeds: 125, 380, and 760 mm/min. The ductility was less than 3% and the joint efficiency was more than 93% at a travel speed of 760 mm/min. According to the results of the micro hardness test, the nugget zone hardness of the aged specimens was lower than the base metal hardness.

Mahdi Masoumi Khalilabad (2017) [17]; The study aimed to develop hybrid constructions comprised of AA2198 and AA2024 materials using friction stir welding (FSW). In order to enhance the joint's mechanical characteristics, several tool designs, welding speed parameters, base metal heat treatments (T8 and T3), and post weld heat treatments (PWHT) were tried. In regard to yield strength and elongation, the ideal tool design configuration was a tapered cylindrical pin with an elevated fan shoulder. The best tool design for finding the right welding circumstances was then determined by studying a variety of welding speed factors. The optimal welding speed variables are 750 RPM and 450 mm.min-1, which may increase the joint efficiency to 78%. Because of the mechanical property loss in the (TMAZ)/(HAZ) of the AA2198 side, it is found that using the plates in T3 or T8 would result in joints with identical mechanical characteristics.

The mechanical properties of the joint regions were recovered by applying T8 PWHT, with or without pre-straining, to welded samples under T3 conditions. While both T8 PWHT processes increased the hardness of the AA2198 side of the (TMAZ)/(HAZ), they had no beneficial impact on the AA2024 side and had no influence on the final

8

mechanical parameters. Results for the AA2024-AA2198 dissimilar joint indicate that T8 PWHT is ineffective. Additionally, the distribution of the workpiece's temperature was accomplished by means of FEM modeling. By reducing peak temperature and heat exposure duration, cooling during welding might improve the mechanical qualities of the joint, according to the simulation.

Ridha et al. (2020) [18]; Used the stir welding technique to join two 1.2 mm thick 2024-T4 Al sheets, checked their microstructure and mechanical properties. The procedure required a cylindrical tool and a specially made fixture. Welding aluminum alloy thin sheets is a complex procedure that requires both old and new techniques. Friction stir welding (FSW) is used in this method. To evaluate the finished product's qualities, tensile testing and microstructure testing were carried out. For the purpose of welding aluminum alloys, the cylindrical tool was used to form a junction. All samples that were evaluated were determined to be free of flaws. The specimens' mechanical characteristics reveal that their ultimate tensile strength is lower than that of the basic metal. Welding Travel Speeds of 20, 40, and 80 mm/min were used in conjunction with two different rotating speeds of 900 and 1400 RPM, respectively. The pin diameter of the tool is 1.2 mm, with a height of 1 mm, and the shoulder diameter is 8 mm. The highest-grade product, with an increase of 72% in ultimate tensile strength was produced at a Travel Speed of 40 mm/min and a rotating speed of 900 RPM.

2.3. STIR WELDED JOINTS with DIFFERENT FRICTION

One novel welding process, friction stir welding, has the unique capability to join metals that are chemically incompatible, such as aluminum and steel, or even different series of aluminum.

Li et al. (1999) [19]; Intercalated, lamellar-like flow patterns are produced during friction stir welding (FSW) of 0.6 cm plates of 2024 Al (140 HV) to 6061 Al (100 HV). The weld zone contains residual, equiaxed grains with average sizes ranging from 1 to 15 mm, which show growth process of grain from dynamically recrystallized grains. The contrast between the 2024 Al and 6061 Al, created by differential etching,

allows one to see these flow patterns. The flow patterns exhibit a variety of shapes and sizes, including intricate spirals and vortex-like structures. These patterns also show some systematic variation, varying from 400 to 1200 RPM, depending on the orientation of the tool. The microstructures of the equiaxed grain and sub-grain change in relation to the predicted temperature profiles, which range from 0.6 to 0.8 TM where TM is the absolute melting point) as measured relative to the rotation axis of the tool. At higher speeds (800 RPM), dislocation climb occurs in the 2024 Al intercalation regions within the weld zones, and residual microhardness profiles follow microstructural variations. As a result, the microhardness of the 6061 Al workpiece is reduced by 40% and that of the 2024 Al workpiece is reduced by 50% just outside the FSW zone.

Vilaca et al. (2005) [20]**;** The article begins by contrasting the welding characteristics that are important for industrial use as a consequence of fusion welding and FSW, two methods often used to join aluminum alloys. There's hope that FSW may enhance custom blank construction. This study presents the outcomes of metallurgical analysis, surface finishing, residual deformation, and static strength efficiency for joints produced by FSW, GMAW, and GTAW on AA1050, AA2024-T3, and AA5083-H111 welding plates of varying thicknesses.

Fujii et al. (2006) [21]**;** Researchers looked at how different tool shapes affected the microstructure and mechanical characteristics of welded aluminum plates that were 5 millimeters thick. The three different kinds of aluminum alloys were welded using probes with the simplest form (a cylinder without threads), the conventional form (a column with threads), and the triangular prism form. Due to the poor deformation resistance of 1050-H24, a threadless cylinder tool generates a weld with excellent mechanical qualities. In the case of AA6061-T6, the shape of the tool has little impact on the microstructures and mechanical properties. The weldability of AA5083-O is greatly impacted by the Rotating Speed. At low Rotating Speed s (600 RPM), the geometry of the tool has little to no effect on the mechanical characteristics and microstructures of the joints.

Balasubramanian (2007) [22]; Made an effort to determine which FSW process parameters were related to which features of the base material. Five distinct aluminum alloy grades (AA1050, AA6061, AA2024, AA7039, and AA7075) have been used in FSW joints, each with its own unique set of manufacturing conditions. There are known empirical correlations between the welding speed, tool rotating speed, and base metal characteristics. Weld quality of FSW joints is heavily affected by the hardness, yield strength, and ductility of the aluminum alloys. Making advantage of the known base metal characteristics of aluminum alloys, the empirical connections found in this work may be utilized to efficiently anticipate the FSW process parameters needed to produce joints free of defects.

Filho et al. (2007) [23]; An alloy called AA2024-T351 and another called AA6056-T4 were joined via friction stir welding. The process parameters that were varied to produce butt joints were the welding speed (150-400 mm/min) and the rotating speed (500-1200 RPM), with the axial force and tool geometry kept constant. Parameter optimization, informed by microhardness testing and micrographic analysis, found that a welding speed of 150 mm/min and a rotating speed of 800 RPM produced sound joints. A lamellar material flow pattern was seen by light and scanning electron microscopy in many locations, indicating that mechanical mixing of materials occurred inside the agitated zone as a result of the differential flow. A dynamically recrystallized stirring zone with refined grains was produced by subjecting the material to high levels of strain and temperatures, often exceeding 400 C. The strength may reach 90% of the weakest connecting partner 6056-T4, according to tensile tests conducted on common flat L-T samples. The annealed structure of alloy 6056-T4 caused a drop in microhardness, which is where the fracture occurred in the thermomechanical heat impacted zone. Micro flat tensile testing corroborated this tendency by showing that strain increased along with a decrease in tensile strength in areas where microhardness dropped. According to this research, in a dissimilar friction stir weld, the joint's performance is dictated by the weaker component, and failure occurs at the area of the joint where the strength is reduced the most due to annealing. Mechanical mixing seems to be the primary material flow process into the involving stirred zone, according to microscopic study and assessment of local mechanical parameters.

R.M. Leal and A. Loureiro (2008) [24]**;** Investigated how geometrical aspect of the tool affects material flow during heterogeneous friction stir welding in AA6016-T4 and AA5182-H111 aluminum alloy plates that are 1mm thick. There were two varieties of tool shoulders used: one with a conical chamber and one with scrolls. While the first tool produced welds that looked great, they were thinner than they otherwise would have been. The weld nugget's properties were mostly dictated by the pin-driven flow in these welds; the plasticized material fluxed surrounding the pin and through the plate thickness, creating an onion ring structure. Because it uses two separate processes operating concurrently at the weld crown and the leading side of the weld to draw material into the shear layer that generates the weld nugget, the shoulder has a significant impact on the formation of the weld. The scrolling shoulder tool welds were less smooth and didn't show any decrease in thickness compared to the base plates. The weld structure was determined by the interplay between pin-driven and shoulder-driven material flow, which was considerable in these welds. Welds in the second series had much greater amounts of material transferred from the tool's advancing to its retreating sides. The degree to which the weld material is plastically deformed determines the degree to which the second set of welds exhibit significant property variability.

Moreira et al. (2009) [25]**;** After comparing it to AA6061-T6 and 6082-T6, the friction stir welded dissimilar joint showed intermediate mechanical performance. Butt joints formed by friction stir welding the aluminum alloys 6061-T6 and 6082-T6 were studied mechanically and metallurgically. The process included analyzing the joints' microstructure and microhardness as well as conducting tensile and bending tests on each one. By factoring in the spatial dependency of the tensile strength characteristics, an approximate finite element model of the joint was created. Friction stir welding AA6082-T6 reduced ultimate and yield stresses, but non-similar joints showed intermediate behavior. Near the edge line of welding, where the hardness amount was found to be minimal, failures occurred in the tensile testing. During tensile testing, the dissimilar joints showed the lowest hardness profiles compared to all other joints on the side of the AA6082-T6 alloy plate. This is where the fracture occurred. However, in the nugget zone, the values of all three joints are identical. This research definitively

shown that friction stir welding causes microstructural alterations. Additionally, the dissimilar joint analysis clearly shows that the two alloys were mixed since the etching responses of the two alloys were different. A rough approximation of the finite element model allowed for the prediction of the joint bending behavior. The simulation showed a good agreement with the actual testing up to around maximum load when compared.

Pa et al. (2014) [26]**;** Examined the physical characteristics and mechanical properties of a friction stir welding (FSW) joint between two different kinds of aluminum plates, AA2024 and AA6061, with a thickness of 5 grams each. A statistical technique was utilized to establish the ideal process parameters for the joints. The impact of rotational and traversal speeds on microstructural and tensile characteristics has been studied using five distinct tool designs. Welded connections with great efficiency and no defects were created by adjusting the process parameters. The most important element is the ratio of the tool's pin diameter with respect the shoulder diameter. The microstructural examination clearly shows that the nugget area is dominated by the material deposited on the advancing side. During the tensile tests, the welded connections failed because the 6061 (HAZ) had the lowest hardness.

Abdulwadoodi (2014) [27]**;** Due to the heat produced by the welding thermal cycle, which might impact the heat treatments of base metals, investigated fusion welding is not recommended for 2024-T3 and 6061-T6 alloys. So, to combine these different alloys, the friction stir welding (FSW) procedure is often used due to its solid-state nature. An experimental work was conducted to examine the impact of varying rotational and traverse speeds on the hardness, bending, and tensile characteristics of FSW-produced joints between 2024-T3 and 6061-T6 alloys. From 3 mm thick pieces of these alloys, high-quality, defect-free friction stir welded joints were successfully formed, according to experimental data.

Venkatesh and Shunmathi (2021) [28]**;** This article compares the solid-state welding procedure versus fusion welding for combining aluminum alloys that are chemically different. Fusion welds are known to create more flaws when uniting materials that are chemically different. Welding parameters such as weld current, hold time, weld force, etc. may be impacted by the microstructure and mechanical features of the two

different metals used in the process. Friction Stir Welding (FSW) is a viable alternative to traditional welding methods for eliminating faults; unlike other methods, it does not use consumable tools and consistently produces welds free of defects. Combining two different types of aluminum alloys—2024 and 6061—is the goal of this thesis. D2 tool steel, an octagonal probing tool composed of high carbon and high chromium steel, is used to attach the plates. Problems with welding different types of aluminum alloys also arise from changes in phase transition and the parameters used for the welding process (such as rotational speed, transversal speed, pin diameter, shoulder diameter, D/d ratio, and others). Welding at lower speeds (500 RPM) at the beginning stage resulted in better weld quality after thermo-mechanical heating, as compared to welds at higher speeds (710 RPM) and 1000 RPM (with the same transversal speed of 20 mm/min), according to a trail experiment conducted with 2024 and 6061 aluminum alloys using an octagon probe tool made by the HC-HCR tool.

2.4. CONCLUDING REMARKS

From the previous brief survey, several remarks can be drawn:

1. Researchers demonstrated that all process parameters significantly impact the weld macrostructure and mechanical characteristics of welded joints.

2. The hardness values are higher in the weld zone compared to that in base metal.

3. Failure under monotonic or cyclic loadings occurs in the nugget zone, or in the transitional region between (TMAZ) and (HAZ).

PART 3

THEORETICAL BACKGROUND

3.1. INTRODUCTION

Every nation has a surplus of aluminum. It is widely used, much like steel. Some industries utilize steel or other metals for their compensatory properties. The metal is lightweight, flexible, corrosion-resistant, and has high electrical conductivity. Aluminum, an engineering metal with a superior strength-to-weight ratio compared to steel, is a common component of metallic cables and a thermal and electrical conductor. Alloys provide efficient and cost-effective solutions for many industrial applications such aluminum cutting, shape, sheet and rod manufacture, and other large-scale uses. Lightweight, very fluid, good melting and surface expansion qualities, and a high degree of polis [30,31].

Aluminum has a higher thermal conductivity than steel, whereas aluminum is about three times less strong (elastic modulus 70 GPa). To reduce weight without compromising strength, design changes are often necessary [29]. Reinforcing imparts beneficial qualities to aluminum and its alloys, making them valuable in many sectors. The main advantages of aluminum alloys over pre-reinforced materials are:

1. When certain components are incorporated into aluminum, it enhances its strength and hardness.
2. The density is moderate.
3. It remains stable even when exposed to extreme heat.
4. Its thermal expansion coefficient is within reasonable manageable.

5. It has excellent electrical conductivity. Moreover, it has exceptional versatility.
6. Excellent abrasion and friction resistance relative to its density [33, 34].

Aluminum's properties mechanical strengthening enhances properties such as electrical conductivity, hardness, fatigue resistance, tensile strength, pressure resistance and components. These components contribute to positive outcomes. When reinforcement components are included into aluminum alloys, certain defects arise. A drop in hardness, corrosion resistance, or tensile strength could result from the defects influenced by the unique characteristics of the additives. Aluminum's corrosion resistance is attributed to the oxide layer that forms on its surface when exposed to air. Alkalis and acids cannot corrode metal due to this protective coating. It is insoluble in water and alcohol. Under certain conditions, it may partly dissolve in water. The FCC axis is the cubic face that links its component atoms. There are nine isotopes of aluminum. Aluminum powder is used in creating silver plating and highly reflecting mirrors because of its silver-reflective characteristics. Making aluminum alloys with other elements, such silicon, copper, and magnesium, to increase the metal's tensile strength [30].

Friction stir welding is a solid-state technique used to connect sheets and plates made of aluminum that do not need filler wire or shielding gas. Friction stir welding has proven successful on several materials including aluminum alloys, copper, magnesium, lead, and zinc. Friction stir welding has shown efficacy with almost all types of aluminum alloys [32,36].

3.2. ALUMINUM APPLICATIONS

Aluminum is an essential chemical element for modern industry due to its distinct properties such as high strength, low density, formability, hardness and resistance to environmental factors including corrosion. The transportation sector, aircraft, naval vessels and projectiles makes use of it. Utilizing aluminum alloys in construction projects. It is used in door and window frames, as well as household appliances. The field that involves electrical conductors. Since aluminum is not poisonous to humans, it poses no threat to their well-being [31].

Aluminum's superior properties enable it to propel ships and steer them. Aluminum's exceptional electrical conductivity distinguishes it. Therefore, it has the full right to rival copper. It has substituted pricier alternatives while maintaining almost same electrical conductivity. The main use of this material is in manufacturing microcircuit components, particularly in the field of microelectronics. Aluminum has several possible applications. It was the first of its type to be used in manufacturing airplane frames and critical components. Minimizing weight is a critical feature of aircraft design. The Boeing 787 increased its efficiency by 20% mostly via reducing its overall weight. The missile, food processing and machining industries are also engaged. Its use in the automobile industry is very extensive. The average automobile manufacture in North America now utilizes 90 kg of aluminum. Adhesion sites might be subjected to higher temperatures due to the formation of an insulating layer. When use aluminum as a conductor, certain rules must be followed. Aluminum alloys are used in a variety of applications such as automobiles, aircraft, construction equipment, appliances, structures, cookware, and hoods because to their cost-effectiveness. Utilized for pressure containment in cryogenic applications and several other settings, including those related to electrical equipment [32].

3.3. ALUMINUM ALLOY CLASSIFICATION

3.3.1. Aluminum Alloys

Table 3.1 displays a system of nine series for wrought aluminum alloy designations. These expressions are often used in the aluminum industrial applications.

Table 3.1. The designation scheme for wrought aluminum alloys [32].

Grades	Key component of the alloy
1xxx	Aluminum, 99% min. or more
2xxx	Copper Cu min.2.2% to max. 6.8%
3xxx	Manganese min. 0.05% to max.1.8 %
4xxx	Silicon min 3.6% to 13.5 %
5xxx	Magnesium min. 0.5% to max.5.6% and Manganese
6xxx	Magnesium min.0.35% to max. 1.8% and silicon
7xxx	Zinc min. 0.8% to max.8% and Magnesium
8xxx	Fe min.0.5%to max. 8.6% and other elements
9xxx	Reserved Alloys (Unused series).

There are two fundamental categories of aluminum: pure aluminum and aluminum alloys. The quid book is divided into two sections: one for cast alloys and another for wrought alloys. One component might be seen as the alloys that receive heat treatment, while the other part consists of the alloys that do not subject to heat treatments.

3.3.2. Casting Alloy

Compared to cast iron and steel, cast aluminum alloys have lower melting temperatures, are largely insoluble in all gases except hydrogen, exhibit high fluidity, and possess a smooth, polished surface. However, when these alloys are rapidly cooled or cemented, they undergo significant shrinkage of up to 7%. Figure 3.1 illustrated cast aluminum alloys.
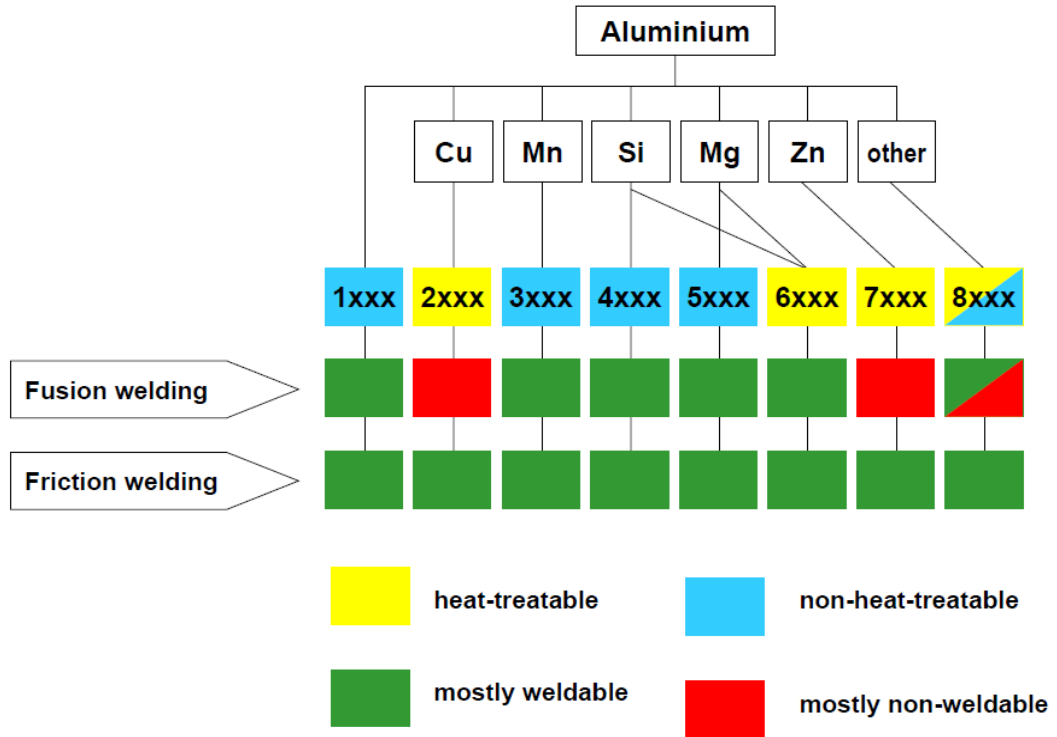
Figure 3.1. Aluminum different alloys and weldability [39].

This category includes both heat-treatable and non-heat-treatable alloys, consisting of several series. Aluminum alloys with varying compositions of copper, silicon, magnesium, and zinc are present in the following ratios: 2:1, 3:1, 4:1, 5:1, 6:1, 7:1, and 8:1. Accelerated hardening may be used to strengthen 2xxx, 3xxx, 7xxx, and 8xxx alloys. The heat treatment process enhances their properties significantly; however, they do not reach the same level as those found in alloys produced by manufacturers [33].

3.3.3. Non Heat Treatable Aluminum Alloys

Figure 3.1 summarizes the aluminum alloys that were produced. The alloy has undergone certain manufacturing processes, Thermomechanical processing mill products include slabs, billets, plate extrusions, wires, and ingots led to the formation of shaped ingots. Heat treatment may improve the properties of alloys produced by precipitation hardening, but it cannot strengthen these alloys. Challenging work in cold conditions might perhaps enhance their abilities. You may heat treat the commercially pure aluminum alloys of 1xxx, Mn + Al 3xxx, and Si + Al 4xxx. Cold working might

cause it to become harder. Heat treatment may increase the hardness of Al + Mg 5xxx alloy [33].

3.3.4. Heat-Treatable Alloys

In order to make the alloy stronger, heat treatment is used. This category includes the following series of lithium-ion alloys. The aluminum alloys include range from 2xxx Al-Cu and Al-Cu-Mg, 6xxx Al-Mg-Si, 7xxx Al-Zn-Mg and Al-Zn-Mg-Cu, and Al-8xxx. 275 grams of bullion. This enables us to use these alloys at a very high degree of strength. Aluminum alloys are distinguished by a four-digit number identification system that enables regulation of impurity levels, characteristics of hardening, including cooling rate, and particle size.

3.4. ALUMINUM ALLOY 2024

The 2024 aluminum alloy is well-suited for use in automobiles and aircraft due to its exceptional workability, great mechanical strength, and the ability to be coated to prevent corrosion.

It excels when used in structural applications. The heat treatment process is excellent. AA2024 is a durable alloy known for its high strength and resistance to corrosion. The strength of aluminum alloys is greatly increased by the inclusion of copper, manganese, and magnesium. Adding a significant amount of copper to alloy 2024 modifies the characteristics of aluminum, leading to enhanced corrosion resistance and tensile strength, along with other advantages. This alloy is often used in trucks, aircraft bodies, vehicles, cylinders, pistons, machine components, recreational equipment, and fasteners. Iron, zinc, and silicon in trace amounts.

Table 3.2. The effect of alloying elements on aluminum alloy 2024

Alloying Element 2024	Effect on the Mechanical Properties
Copper (Cu) (3.8-4.9 wt.%)	• Increase strenth , hardness and fatigue • Increase the deformation resistance of aluminum alloy

	• Increase susccptibility to corrosion craking
	• Reduce ductility and elongation
	• Facilitatates precipitation hardening
	• Reduce corrosion resistance
Magnesium (Mg) (1.2-1.8 wt. %)	• Increase strenth without noticeable dicreseasing ductility
	• Improves good weldability and machinability
	• Improves good corrosion resistance

3.4.1. Mechanical and Physical Characteristics of Aluminum Alloy 2024

Aluminum alloys may be identified by examining their mechanical properties. The density of the material is 2.77 g/cm^3, slightly higher than that of the pure aluminum which is 2.7 g/cm^3. Aluminum 2024 has excellent workability, making it suitable for a variety of applications [40,41].

Possible applications, strengths, and workability of aluminum alloy may be deduced from its unique characteristics [34]. Aluminum alloy 2024 is appropriate for high-strength structural components because of its tensile strength of 324 MPa. The mechanical characteristics of Al 2024 can be summarized as following [35]:

1. Resistant to shear pressures, often known as "cutting" stresses, or shear strength. Aluminum alloy is renowned for its shear strength of 283 MPa in AA2024-T3.
2. Fatigue strength refers to a material's capacity to endure loading cycles below its yield point without developing cracks. Aluminum 2024 has a fatigue strength of 138 MPa [44,45].
3. Given the modulus of elasticity and shear modulus of aluminum alloy 2024, you can determine the tensile elasticity, or deformation. The modulus of elasticity is 73.1 GPa. The shear modulus is 28 GPa [36].
4. Aluminum 2024 is a high-strength structural material known for its tensile strength of 324 MPa [35].

3.4.2. Applications of Aluminum 2024

Aluminum AA 2024-T3 is widely used in several industries, with aviation and aerospace sectors being particularly common. Components such as gears, cylinders with pistons, tires for vehicles, and a tennis racket. Its uses are diverse [25]. Matrix metal composites (MMCs) provide exceptional characteristics such as superior corrosion resistance, lightweight, high strength, and little thermal expansion, which are not found in pure metals. Both liquid and solid-state procedures are recognized methods for making metal matrix composites (MMCs). Key challenges in MMC manufacture and fabrication include issues like as wettability, low density, grain agglomeration, and undesired interactions, all of which diminish material properties [37].

3.5. ALUMINUM ALLOY 6061-T6

The 6xxx alloys are heat treatable alloy. It requires silicon and magnesium in the necessary proportions to form magnesium silicide (Mg_2Si). The 6000 series is a common option for medium-strength structural alloys. These alloys are well-suited for automobile body sheets because to their malleability, resistance to corrosion, and weldability [47,48].

This alloy contains 0.2% chromium, providing enhanced corrosion resistance. An overabundance of silicon enhances the age hardening process, but it may lead to lower ductility and intergranular embrittlement if the extra silicon segregates to grain boundaries.

The AA 6061 standard covers a variety of products such as structural shapes, sheets, plates, foil, rods, bars, wires, tubes, and pipes. Among aluminum alloy 6061's many desirable mechanical characteristics are its excellent ductility and good strength-to-weight ratio. The key reasons for using 6061 are its acceptable mechanical properties and the simplicity with which it can be cast, extruded, rolled, and machined [38].

Table 3.3. The effect of alloying elements on aluminum alloy 6061

Alloying Element 6061	Effect on the Mechanical Properties
Magnesium (Mg) (0.8-1.2 wt.%)	• Increase strength without noticeable decreseasing ductility • Improves good weldability and machinability • Improves good corrosion resistance
Silicon (Si) (0.4-0.8 wt.%)	• The silicon makes the aluminum alloy more fluid without breaking • The silicon actually lowers the aluminum's melting point • Increase strength • Reduce coefficient of thermal expansion • Reduce specific gravity

3.6. WELDABILITY of ALUMINUM ALLOYS

Aluminum poses issues in electric arc welding because of its high heat coefficient and protective oxide layer. To prevent unnecessary thermal expansion in the products, it is necessary to break and eliminate the oxide layer and quickly apply heat. Friction stir welding resolves the common challenges associated with dealing with aluminum. As shown in Figure 3.1. illustrates certain wrought aluminum alloys' fusion and friction stir welding capabilities [29].

3.7. FRICTION STIR WELDING PROCESS

Friction stir welding was invented by Wayne Thomas at TWI in 1991, with patents filed in Europe, the USA, Japan and Australia. Further work to study the process was undertaken at TWI in 1992 with the project titled, "Development of the New Friction Stir Technique for Welding Aluminum." Industrial production using FSW was in progress by the mid-1990s, making it one of the shortest time periods for any welding process to go from invention to widespread use. FSW has been used for a variety of applications across industries ranging from aerospace to shipbuilding and rail to electronics, including EV battery trays. Figure 3.2 illustrates the Friction Stir Welding (FSW) technique, introducing new areas in welding technology [39].
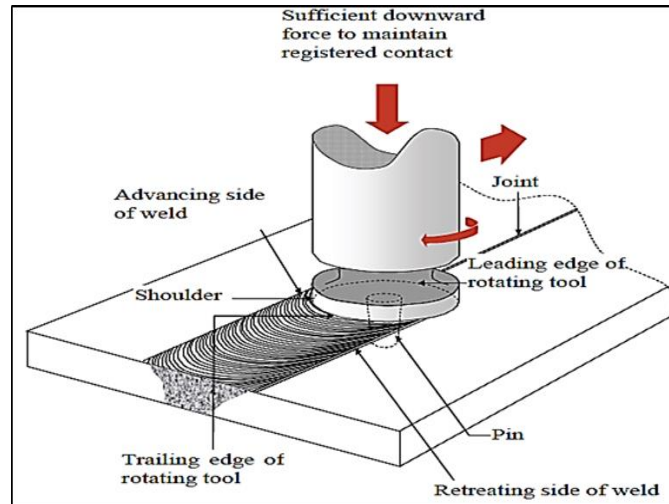
Figure 3.2. Friction stirs welding process schematic [50].

The tool, which has a cylindrical shoulder and a profiled pin, is turned in friction stir welding when it enters the area where two sheets or plates of material meet. To prevent separation of the joint faces, ensure that the components are securely connected. The wear-resistant welding tool may travel along the weld line as the work components soften due to frictional heat, rather than melting. When the tool shoulder and pin profile touch closely, the plasticized material moves to the trailing edge of the tool pin and is forged. As it cools, a solid phase connection develops between the two components.

Friction stir welding may be used to join aluminum sheets and plates without requiring more metal. Full penetration welding from one side is achievable without porosity or internal cavities in materials with thicknesses between 0.8 and 65mm. Aluminum alloys, copper, magnesium, lead, and zinc have all been effectively friction stir welded so far. Figure 3.3 illustrates that a 75 mm thick aluminum plate may be friction stir welded on both sides at varying thicknesses [32,51].
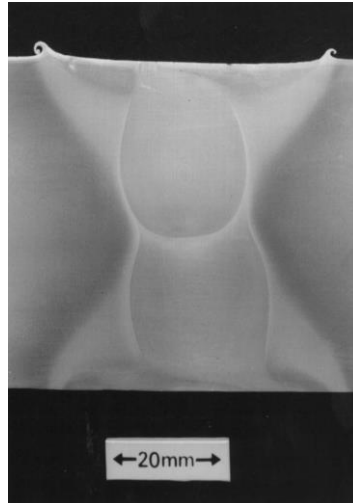
Figure 3.3. Aluminum extrusion 75 mm thick subjected to a double-sided friction stir welding process [51].

3.8. THE MAIN DEFINITIONS USED in FSW

Figure 3.4. displays a list of vocabulary used in the FSW process, with descriptions provided below:

Tool pin: The portion of a welding instrument that, when in use, extends from the shoulder and makes contact with the joint line (fixed, sliding).

Tool shoulder: The base of a welding tool is often in the shape of a disk. The weld cap is created when the shoulder comes into contact with the plate intended for welding.

Backing plate: A thick metal sheet positioned behind the welding components. The backing plate and tool combine to form the junction that is welded.

Advancing side: The region of the tool where the transfer motion and the local surface direction are at right angles.

Retreating side: Tool side opposes the direction of transfer motion when the tool surface rotates in the opposite direction.

Plunge depth: The pin can only penetrate the plate to the extent permitted by its plunge depth. The tool is often oriented towards its trailing edge.

Rotating Speed: The number of full angular rotations a tool completes around its axis during a certain time period is referred to as its Rotating Speed.

Welding speed (Travel speed): Welding speed is the pace at which welding occurs, measured in millimeters per minute at which the tool moves along the weld joint line [40].
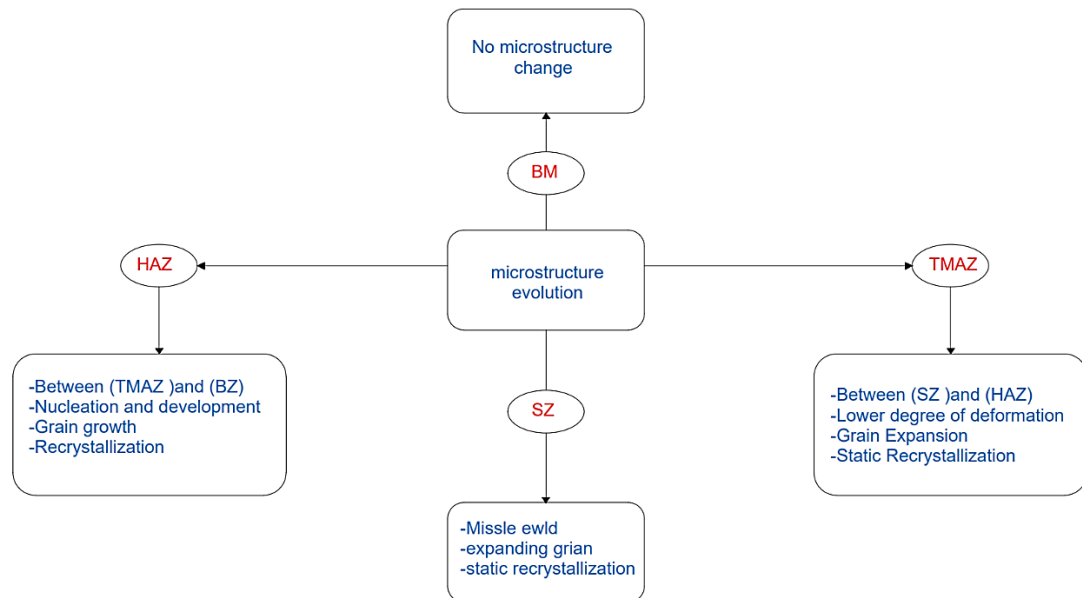
Figure 3.4. The main definitions used in FSW.

3.9. WELDING PARAMETERS

Rotating speed is considered the most crucial welding parameter, however transverse speed and plunge depth are also recognized as important factors. The speed of rotation impacts both the input heat and temperature. This impacts the mechanical properties and microstructure of the FSW welds. Additional welding factors besides the distance between the FSW weld and the side of the plate include tilt angle, spindle power, torque, down force, tool geometry, and tool shape [41].

When using FSW, you may vary the following parameters: down force (N), welding speed (mm/min), tool Rotating speed (RPM), and tilting angle (θ). Table 3.2 displays the key process parameters and their impact on friction stir welding [41].

Table 3.4. Main friction stir welding process parameters [52].

Parameters	Effects on
The rate of rotation	Frictional heat, "stirring", breaking oxides and combining the materials
Tilting angle	To optimize the transfer of material from the front to the back of the pin
Welding speed	Appearance, heat control.
Welding axil force	Cause the tool and workpiece contact, Frictional is the primary heat

Another crucial process parameter is the spindle or tool tilt angle in relation to the workpiece surface. To optimize the transfer of material from the front to the back of the pin, it is crucial to tilt the spindle towards the trailing direction. This will ensure that the material remains disturbed by the tool's shoulder [42].

Sometimes the tool is slightly inclined, while in other circumstances, the shoulder is inserted deeper into the workpiece. In shoulder anatomy, the "heel" is the deepest part. The surface of a work piece is defined as the "heel plunge depth" if the shoulder cannot penetrate it beyond that point. The tilt angle, often known as the travel angle, refers to the angle of tilt. Figure 3.5 depicts a scenario where the tool is tilted to one side; this tilt is known as the "work angle" or "sideways tilt angle". You may use the following formula to calculate the depth of a heel plunge:

$P = 0.5\ D \sin \theta$ (3.1)

Where: P=shoulder plunge (mm), D=shoulder diameter (mm) and θ= tilt angle (degree).
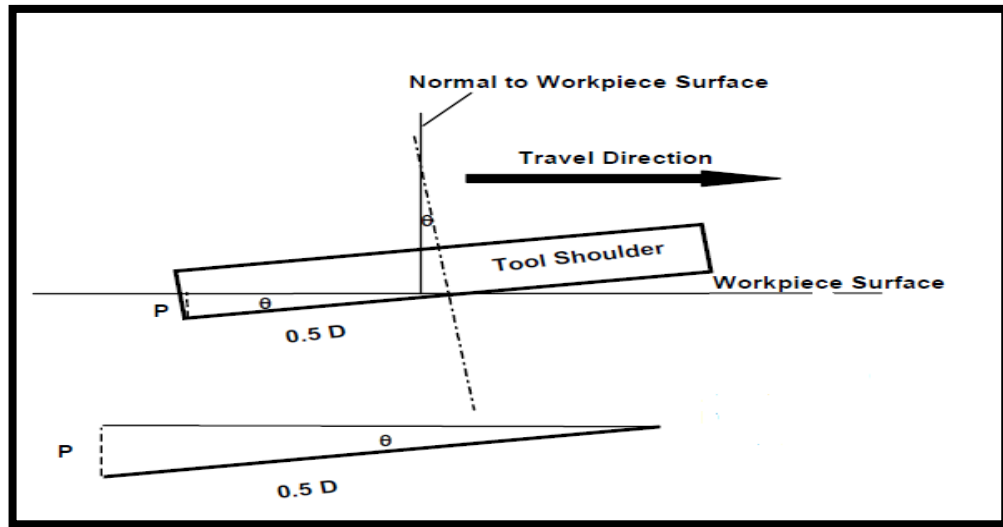
Figure 3.5. A schematic depicting the depth of the shoulder plunges [54].

The two primary parameters of the FSW process are the traversal speed and the rotational speed. The tool is rotated and moved forward to mix and swirl the substance. When moving at too slow of rates, excessive heat may be generated, resulting in a large weld bead and poor penetration. On the other hand, when traveling at too rapid of speeds, a narrow weld with inadequate weld toe tie-in is produced. For each particular weld joint, it is critical to keep the speed constant.

$$Q = \frac{4}{3}\pi^2 \alpha \mu P R^3 \frac{\omega}{v}$$

In this context, Q represents the heat input per unit of length, whereas α, P, R, and v denote heat input efficiency, tool pressure on the joint, shoulder radius, and travel speed, respectively. The speeds of rotation are denoted by w and traversal by v. A substantially greater ω/v may be deduced. Increasing the heat input ratio allows for more metal around the pin to attain a plastic state flow and recrystallize as the pin rotates. Consequently, when the ratio of W/V increases, the weld nugget and (HAZ) regions become comparatively broader. One of the key process characteristics that will cause the tool and work piece to come into contact with one another is axial force. Throughout the welding process, this friction is the primary source of heat. A force controller that controls the direction of welding is necessary for a successful FSW operation. The unit of measurement for the friction stir welding force is the KN.

28

Workpiece, thickness, material, welding setup, and applied force all play a role in the calculation [52].

3.10. FRICTION STIR WELDING ZONES

This is an analysis of what may be seen by a meticulous investigation of the material microstructure in the joint section of two sheets. figure 3.6 [43].

(a) Parent material The material stays unaltered and has an average grain size of 3.6 nano micro. The microstructure and mechanical characteristics remain unchanged due to the heat flow.

(b) Heat Affected Zone (HAZ) In every metal joining operation, this zone is visible. This area, which is not mechanically damaged but is impacted by the heat cycles created during the joining process, is what friction stir welding is all about. The recrystallization temperature of the material is exceeded in this area, leading to coarsening of the grains and a decrease in the density of the strengthening agents in the alloy. In a friction stir welded joint, this area often has low strength [53]. The low strength area changes from (HAZ) to (TMAZ) in a joint when the temperature there is lower than the recrystallization temperature. Invariably, the hardness rating of this area is lower than that of the based metal (figure 3.6 b).

(c) Thermo-Mechanically Affected Zone (TMAZ) The heat-affected zone (HAZ) and the stir zone (SZ) are separated by this zone. Except for the nugget zone, this is the whole malformed area beneath the shoulder. The rotational motion of the tool shoulder causes mechanical deformation and heat cycles in this area. The lower degree of deformation and partial recrystallization of grains in this area is indicative of the relatively smaller thermal impacts compared to the stir zone. As a result of grain expansion and partial precipitate dissolving brought about by reaching high temperatures in this area of (TMAZ) show in figure 3.6 c, hardness reaches its lowest value here [54].

(d) Nugget. This area is impacted by the tool pin's rotational and traversal movements. The tool pin's diameter determines the area's size. Due to the dynamic recrystallization, this area goes through grain refining. The equiaxed grains found in SZ are much smaller than those in BM. This area may exhibit a structure similar to an onion ring at times, depending on the BM and the process parameters show in figure [3.6]. The hardness values of heat-treatable alloys are often lower than their BM [43].
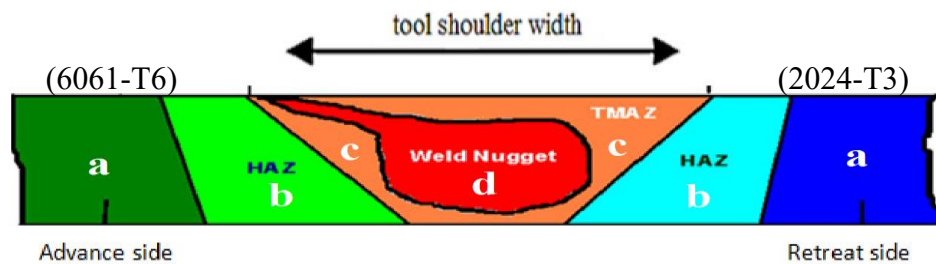
Figure 3.6. Friction stirs welding zones.

3.11. JOINT GEOMETRIES

FSW technology has been used to produce many kinds of welds such as butt, overlap, fillet, and corner welds, as seen in figure 3.7. Further refinement and enhancement of tool designs are required for each of these joint shapes. FSW technology may handle circular, annular, non-linear, or three-dimensional welds. Solid-phase welding have the potential to be used in any orientation, such as vertical, horizontal, above, or orbital, since it is not influenced by gravity [41,56].
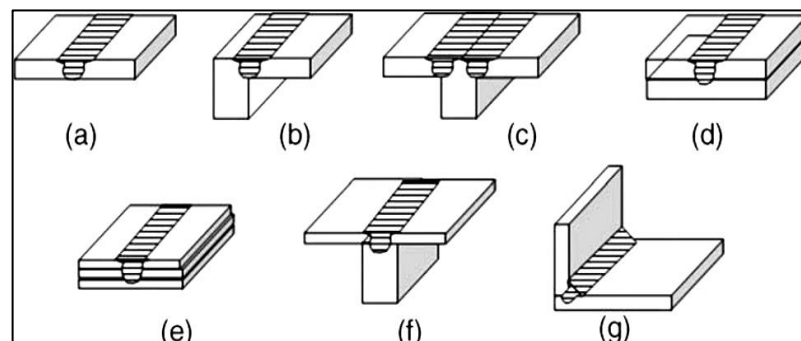
Figure 3.7. A few of FSW joint designs (a) butt weld (b) vertical weld (c) double side vertical weld (d, e) Weld an overlap (f) weld in a T-section (g) joint weld [41,56].

3.12. PLASTIC DISSIPATION HEAT GENERATION

This phenomenon is only apparent when the work material is enclosed under the rotating tool, occurring at elevated temperatures caused by the frictional heat mechanism, namely during the dwelling and welding stages. As the temperature rises below the spinning tool owing to frictional heat, the work material layer at the interface weakens, deforms, adheres, and starts to follow the tool's movement. The shears at the interface of the work material layers are a result of this phenomenon, which further enhances the thermal softening effect due to frictional heat. High strain rate plastic deformation is induced while minimizing the frictional heat process. Dynamic velocity disparities and boundary sliding circumstances result in the work material generating highly concentrated internal heat, separate from the contact between the spinning tool and work material [42,57].

3.13. ADVANTAGES of FSW PROCESS

The advantages may be obtained due to when the materials being connected undergo Friction Stir Welding while still solid and at temperatures below their melting points. One benefit is its ability to join materials that are difficult to fusion weld, such as aluminum alloys. Here are the advantages:

1. With no hot cracking, porosity, or solidification cracks, FSW is a nearly defect-free joining technique since it is a solid-state welding process.

2. The linked material experiences less shrinking and deformation at the lower temperatures because the temperature in FSW less melting degree.
3. Aluminum alloys don't need flux, filler, or shielding gas.
4. The absence of fumes, splatter, and ultraviolet radiation makes FSW a green product.
5. This technique may be easily automated and repeated using machine tool technology, which in turn reduces the requirement for professional welders.
6. Adaptable to any role Straight, circular, or any other welding position.

7. Mechanically sound, with results that are on par with or better than those of rival methods when it comes to aluminum alloys.

8. Energy efficient.

9. Can connect a wide variety of aluminum alloys, including those in the 2xxx, 6xxx, 5xxx, and 7xxx series, which are often considered to be "non-wieldable".

10. Great mechanical characteristics as shown by testing for fatigue, tensile strength, and bending.

11. Certification as a welder is not necessary.

12. When producing in bulk, there is no need to grind, brush, or pickle [41,43].
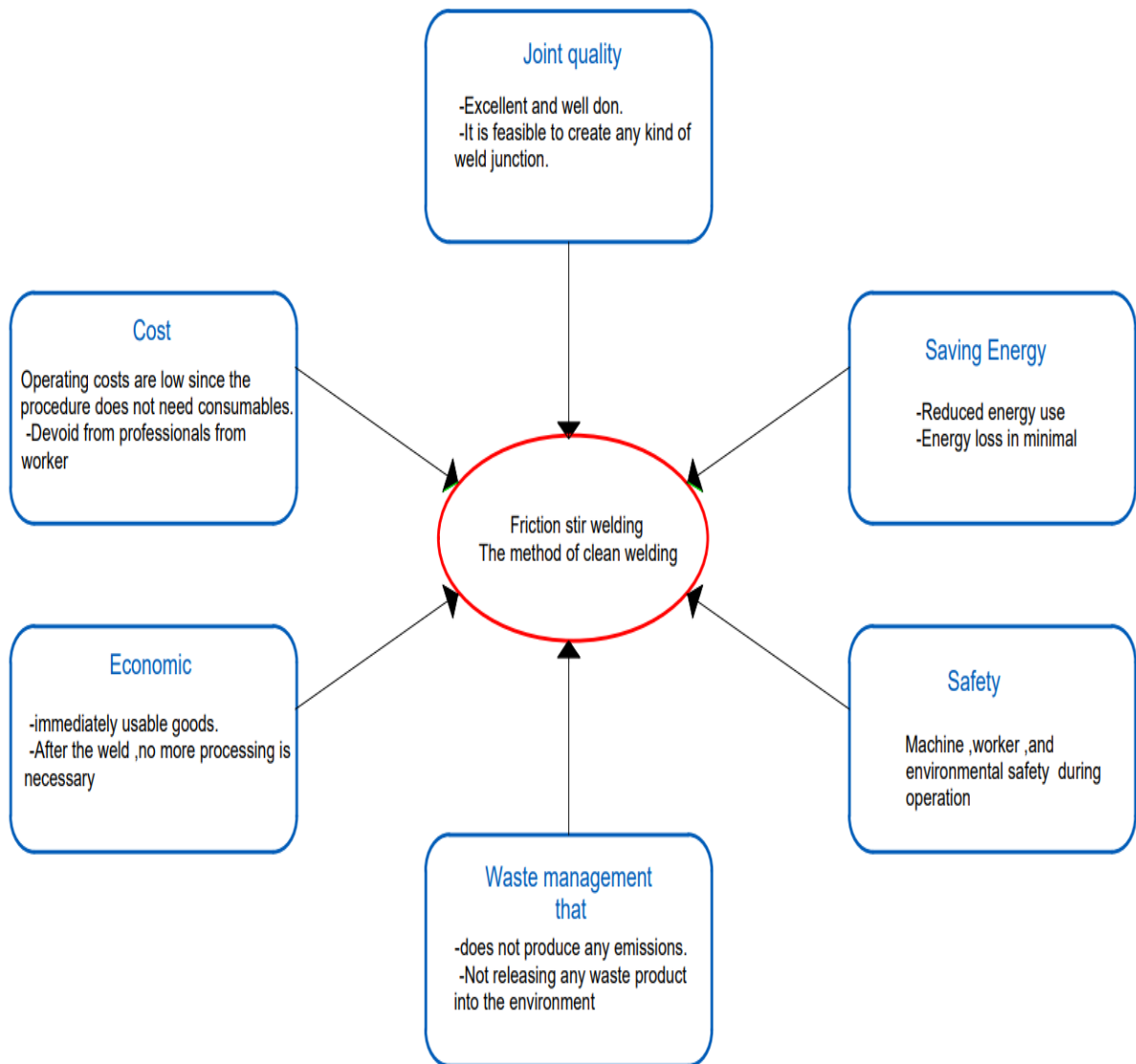
Figure 3.8. Significance of FSW

3.14. FRICTION STIR WELDING LIMITATIONS and DEFECTS

Although friction stir welding has several benefits, it does have some drawbacks. Some examples are:

1. Friction welding is slower than traditional metal welding, The welding rates are somewhat slower compared to some fusion welding methods.

2. The end of every weld has a keyhole this part It is considered damaged and cannot be used [44].

3. Because no filler material is utilized in the procedure, it is necessary to manage the gaps between the pieces that are to be linked.

4. The workpieces need to be secured tightly, Clamping the workpieces to prevent the joint open from moving away especially sample thickness of (2) mm because it folds easily. In order to apply FSW without slipping, a stabilizing mechanism is needed on both sides to counteract the vertical and horizontal pressures.

5. Due to inadequate weld temperatures caused by slow rotation or high traverse rates, the material cannot withstand substantial deformation when welding.

6. A weakened welded junction with voids is the result of welding characteristics such as low friction pressure, short friction time, and low forging pressure.

7. "Kissing bond" describes the degree of tightness of the connection between the two pieces of work. The two sheets will lie side by side.

8. Must the length of pin less than 0.9 thickness of plate.

9. It is essential to have a backing bar.

3.15 APPLICATIONS OF FSW PROCESS

Friction stir welding is widely used across several industrial areas. These are categorized:

1. Shipbuilding and maritime sectors.
2. Aerospace sector.
3. Railway industry.
4. Land transportation.
5. Construction industry.
6. Electrical industry.

PART 4

EXPERIMENTAL WORK

4.1 INTRODUCTION

The chapter provided a definition of the materials, mechanical and chemical qualities, which are used in friction stir welding. It used AA2024-T3 and AA6061-T6 aluminum alloys in our friction stir welding method. Using a procedure that involves fusing comparable materials of AA6061-T6 with AA6061-T6 and dissimilar materials AA6061-T6 with AA2024-T3. To accomplish the welding process with a broad range of rotational and travel speeds, a butt joint arrangement was used. specifically developed backing/clamping mechanisms allowed the trials to be carried out. The ideal mechanical characteristics of the were determined by a tensile test the welded specimens. Welded joint cross sections, whether they are similar and dissimilar, are subjected to microhardness testing. In addition, the experimental effort included imaging the microstructure using optical and scanning electron microscopy with dispersive spectroscopy (SEM-EDS) equipment. XRD inspection also was performed on dissimilar welded joints at the best welding parameters.
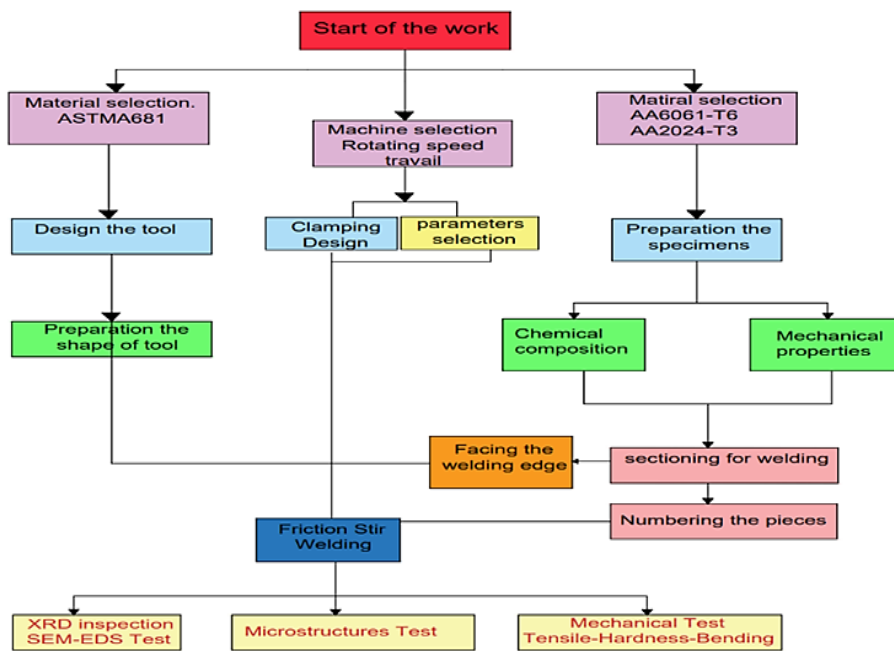
Figure 4.1. Illustrates the experimental process flow diagram

4.2. MATERIALS

Friction stir welding (FSW) is used to join similar and dissimilar aluminum alloys; we used two different types of aluminum alloys: 6061-T6 and 2024-T3. The chemical composition of this material was analyzed in Central Organization for Standardization and Quality Control (C.O.S.Q.C)/Iraqi Ministry of Planning, as shown in Table 4.1 and Table 4.2.

Table 4.1. Chemical composition (wt.%) of AA6061-T6

Cr	Cu	Ti	Fe	Si	Mn	Mg	Zn	Al
0.128	0.207	0.0291	0.362	0.607	0.0471	0.956	0.0445	Rem

Table 4.2. Chemical composition (wt.%) of AA2024-T3

Cr	Cu	Ti	Fe	Si	Mn	Mg	Zn	Al
0.03	4.4	0.02	0.05	0.05	0.46	1.4	0.03	Rem

4.3. PREPARATION of WELDING SAMPLES

The friction stir welding workpieces were made   for two different materials (AA6061-T6 and AA2024-T3) from 2 mm aluminum sheet. The dimensions of each sample are 100x200 mm. The machining process has been done by rolling the direction of samples in perpendicular to the welding direction (direction of length). Samples were cut by hydraulic shear manufactured by Japan it is made in 1988 from Hiraoka iron works company   Figure 4.2 were preparing from two materials (6061- T6, 2024 -T3) and clean the edges of the samples at right angles using sandpaper different size dimensions and also must be measured before cutting, or a standard must be placed behind the hydraulic shear to standardize measurements. In order for the two sheets to adhere completely and without gaps, the edges must be vertical, during the course of conduction before began to friction stir welding. It is important to pay attention to the shape and edges of the samples for the purpose of correct fixation. can see this procedure in Figure 4.5.

Figure 4.2. Hydraulic shear for cutting spearmint

4.4. WELDING TOOL

4.4.1. Welding tool Material

Using the right tool material is a crucial stage in the friction stir welding (FSW) process, because of tool material affected on many different variables. Based on the kinds of base materials utilized, the suitable shoulder and pin (or probe) designs may be chosen. This section details the study's welding tools, including their materials, geometry, and measurements. The next section also explains the processes of fabrication. The friction stir welding tool consists of three parts as body, shoulder, and pin (i.e., probe); As follows; hardening tool steel ASTMA681 O1 type [45]. The chemical composition of this material is shown in Table 4-5. The material of this tool was analyzed in Central Organization for Standardization and Quality Control (C.O.S.Q.C)/Iraqi Ministry of Planning.

Aluminum alloys were chosen from alloys that are difficult to weld by traditional methods, which are alloys 2024-T3, alloy 6061-T6, with a thickness of 2 mm. It noticed that no one used this thickness in previous research due to the difficulty of welding this thickness, the difficulty of fixation, and the ease of movement of the plate with the movement of the tools. The 2 mm thick AA2024-T6 aluminum sheets were imported from Turkey and 6061 T6 was supplied from the local market in Iraq.

Table 4.3. Chemical composition (wt.%) of FSW tool

Cu	V	Cr	W	Mn	Si	C	Fe
0.16	0.18	0.45	0.33	1.38	0.29	1.0	Rem

The hardening and fabricating characteristics of this material are listed in Table 4.4 and Table 4.5 respectively.

Table 4.4. Hardening and tempering characteristics of O1 tool steel type [60].

Approximate hardness HRC	Resistance to cracking	Amount of distortion	Hardening Response	Resistance to decarburization
57-62	Very high	Very low	Medium	High

Table 4.5. Fabrication and service characteristics of O1 tool steel type [60].

Resistance to wear	Resistance to softening	Toughness	Machinability
Medium	Low	Medium	High

4.4.2. Dimensions and Manufacturing Process

The tool's dimensions were considered by several researchers. The dimensions of the tool and other machine parameters determine the amount of heat produced during the welding operation. The most common measurements for a tool are its pin diameter and height, it nearly equivalents to the plate thickness. For optimal mechanical qualities of the welded plate, these dimensions are recommended.

In this work the tool dimensions depend to workpiece which have thickness 2mm, therefore, the following tool dimensions are used in manufacturing the cylindrical tool type because the thickness very thin not need different shape, such as square.

Pin diameter =2 mm.
Pin height = 1.8 mm.
Shoulder diameter =14 mm.

The results of several studies and practical trials reveal that the pin diameter should be more than the plate thickness and height (0.9x thickness of plate) and the shoulder diameter should be greater than three to five times the pin diameter. The steel rod is cut to a length of 100 mm using a disc cutter that uses cooling liquid. The work at Baquba Technical Institute is done entirely by lathe machines. Figure 4.3 presents the manufactured tool.

4.4.2.1. Pin Shapes of Friction Stir Welding

The main functions of the pin are:

1. Create friction heat and deformation.
2. Cutting the material in front of the tool.
3. Turning the material in front of the tool in the friction stir welding process.
4. Damage to the edges of the workpieces.
5. Mixing materials behind the tool

Producing the most basic pin variant, which is cylindrical in form, was necessary due to the (2 mm) metal thickness. The flat design, on the other hand, is the most often utilized friction stir welding method because to its low corrosion resistance, high forming strength, and ease of manufacturing. The shape and dimensions of cylindrical tool is seen at Figure 4.3
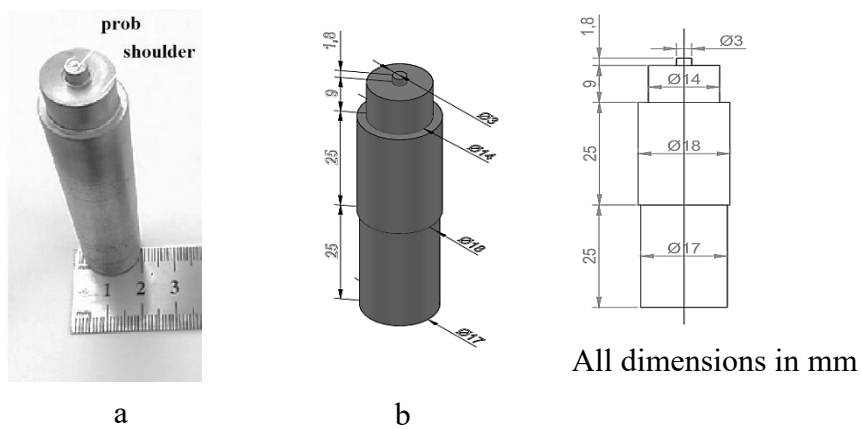
Figure 4.3. Cylindrical tool (a) photograph and (b) Schematic

4.4.3 Heat Treatment

To facilitate machining, manufacture, and the enhancement of characteristics via heat treatment, the majority of tool steel varieties were supplied with an annealing state. Table 4.6 displays the results of the hardening and tempering processes that were used to enhance the tool's characteristics.

Table 4.6. Hardening and tempering procedure of the tool steel [60]

Tempering temperature	Quenching medium	Time at temperature	Hardening temperature	Preheat temperature	Rate of heating
175-260 °C	PVA	10-30 min	790-815 °C	650 °C	Slowly

Figure 4.4 shows the results of the heat treatment procedure. The heating process began at ambient room temperature and increased step-by-step. To reach 800°C, the heating rate was 150–200 °C/h. After maintaining this temperature for about half an hour, the polyvinyl alcohol (PVA) cooling process was quick.
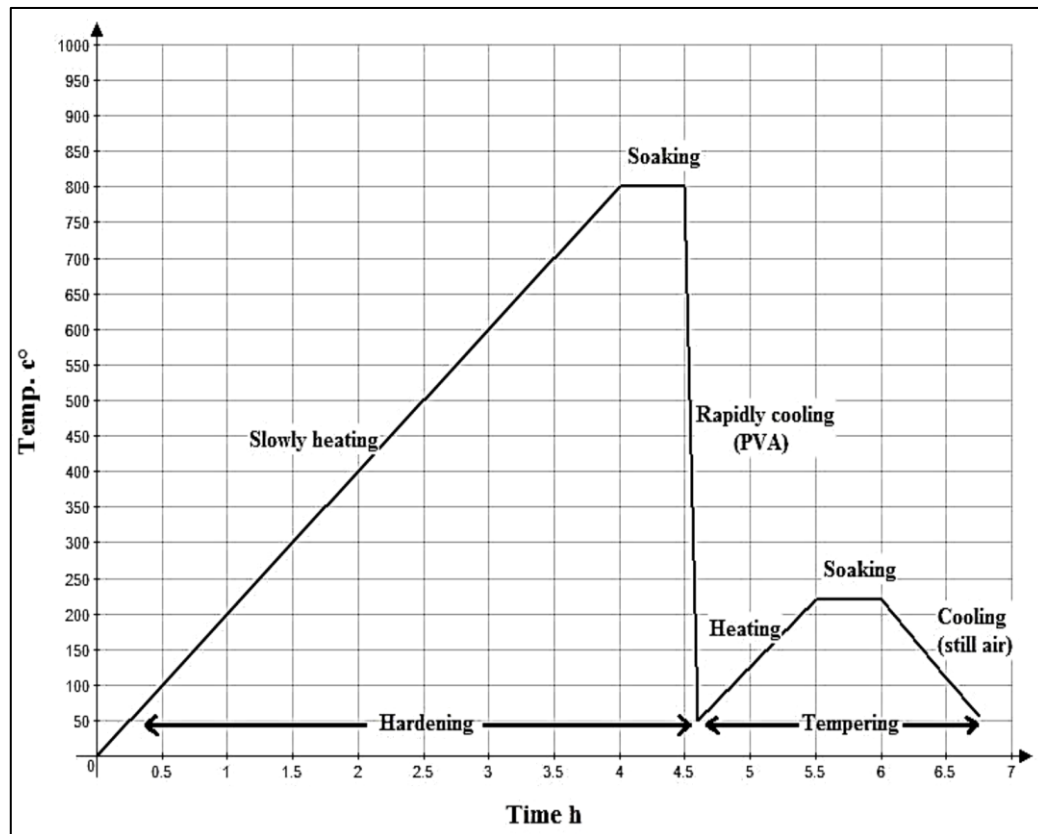
Figure 4.4. Heat treatment curve of the tool

The quenching medium that was employed was a polyvinyl alcohol solution (PVA) rather than oil. The hardening solution was made using a mixture of 2-3 grams of PVA and 1 litter of water [46]. Figure 4.4 shows the results of the tempering process, which was carried out after the quenching process was finished. The heat treatment process was working by furnace name Ney Vulcan available in Laboratory was carried out in

the metallurgy laboratory /Technology University in Baghdad. The tool's hardness increased from 20 HRC before heat treatment to 62 HRC thereafter.

4.5. FIXTURES AND BACKING PLATE

The correct method of fastening the workpieces onto the machine table is extremely necessary in the welding process. A design for fixtures when using the traditional clamping claws, the most prevalent issues that arise during FSW are the abutting plates sliding and separating. Two rectangular plates fastened with four bolts make up lateral restraints. In order to improve heat sinking, these fasteners make it possible to provide consistent side pressure to the adjacent plates. Using a combination of A fixtures, a backing plate, and a series of bolts (both vertical and horizontal), this design makes it simple and inexpensive to secure workpieces on the machine table. The plate must be perfectly level, so that the bottom welding areas are free of defects. to secure the plates (workpieces) that are to be welded onto the table of the milling machine, a specific fixture and backing plate are manufactured. The carbon steel fittings were constructed in two pieces, one for each side, and a backing plate with dimensions of 400x300x20 mm. They are attached to the main plate by screws. This process very important in welding aluminum alloy thickness 2 mm by friction stir welding because in this thickness deviates so we fixed plate four side. The biggest challenge in friction welding of this thickness was the process of fixing the plates, so rulers were manufactured with a thickness of 20 mm and a width of 100 mm to increase the pressure on plate and prevent it from rippling motion with tools move, also the system elements are designed to be readily built, removed, and handled, and it is simple to find the center point above the junction between the adjoining workpiece using motion tools (a pin). It is important to note and clean the backing plate when change workpieces that need to be welded because it is possible for a crack to occur on backing plate as a result of the vertical force on the workpiece It will affect the welding of other samples. A vertical connection was made between the clamping system and the machine table. In Figure 4.6, the assembly are shown.
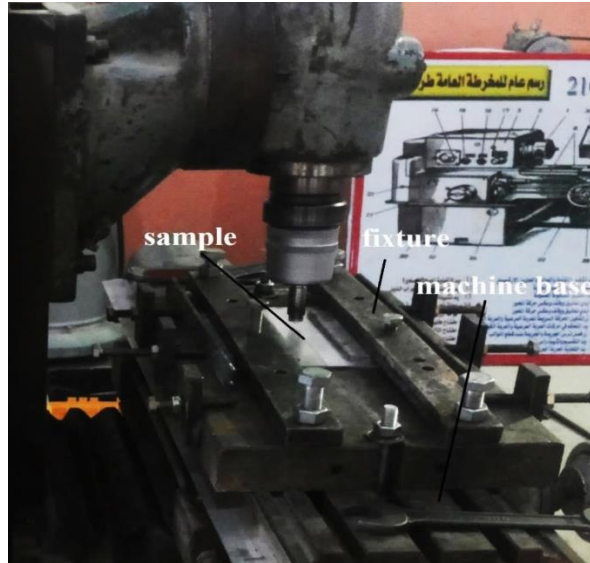
Figure 4. 5. Welding fixture assembly

4.6. FRICTIONS STIR PROCESSING

4.6.1. Introduction

To unite two surfaces of materials without melting them, the friction stir welding procedure employs a non-consumable tool that is harder than the substance being welded [47]. The friction stir welding procedure, shown in Figure 4.7, was patented in December 1991 by Wayne Thomas of The Welding Institute Ltd (TWI _ Cambridge, UK). By reducing the amount of brittle compounds near the contact, this approach may enhance mechanical qualities, including strength, of the joint. Friction and plastic deformation between the tool (i.e., the pin and shoulder) and the work components cause localized heating to occur. As a consequence of plastic deformation and friction, the materials around the pin are stirred and mixed from front to rear. Metals, particularly those in close proximity to the friction stir welding tool, become softer as a result of the friction heat [48]. So, there's no need for external heat sources since mechanical energy is transformed into thermal energy at the contact locations. Work piece heating, material induction and induce material under the shoulder are the main functions of the friction stir welding instrument [63,64]. Because of their unique geometrical properties, the materials that rotate around the pin may be very complex and tool specific. A tool with a specific design—a shank, shoulder, and pin—is the

43

fundamental building block of the friction stir welding idea. A butt or lap joint may be used to implant the pin, which can then be rotated forward along the joint line. In order to create the connection, the friction stir welding tool has a number of benefits, such as heating the work piece surfaces, plastic deformation, material flow, and restriction of heat under the shoulder. It also mixes and stirs the materials surrounding the pin [49]. Due to metallurgical changes and weak joint strength, friction stir welding is not a viable option for joining certain two-phase alloys. Friction stir welding offers numerous advantages over conventional welding methods. These include reduced energy consumption, material waste, environmental friendliness, mechanical properties, pollution, and the ability to join materials that are difficult to fusion weld.
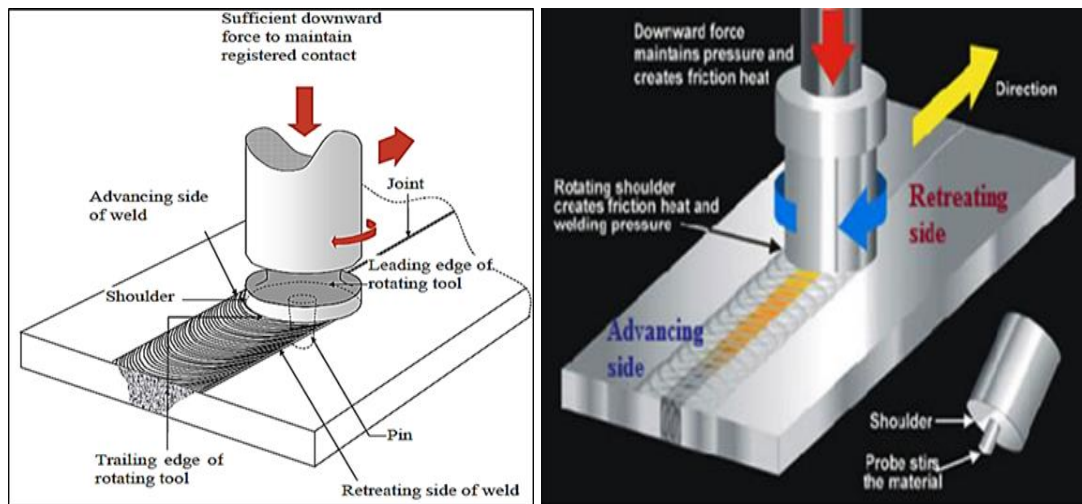
Figure 4.6. Schematic drawing for friction stir welding process

4.6.2. Friction Stir Welding

Choosing the right tool material enhances the weld joint quality and allows for higher maximum welding speeds in the friction stir welding process, which includes spinning the tool at different speeds [50]. To keep metal sheets with exact measurements, such square mating edges, from lifting or separating when welding, clamps are required, as shown in Figure 4.8. It makes no difference what kind of instrument you use for friction stir welding; the fundamental principle is the same.
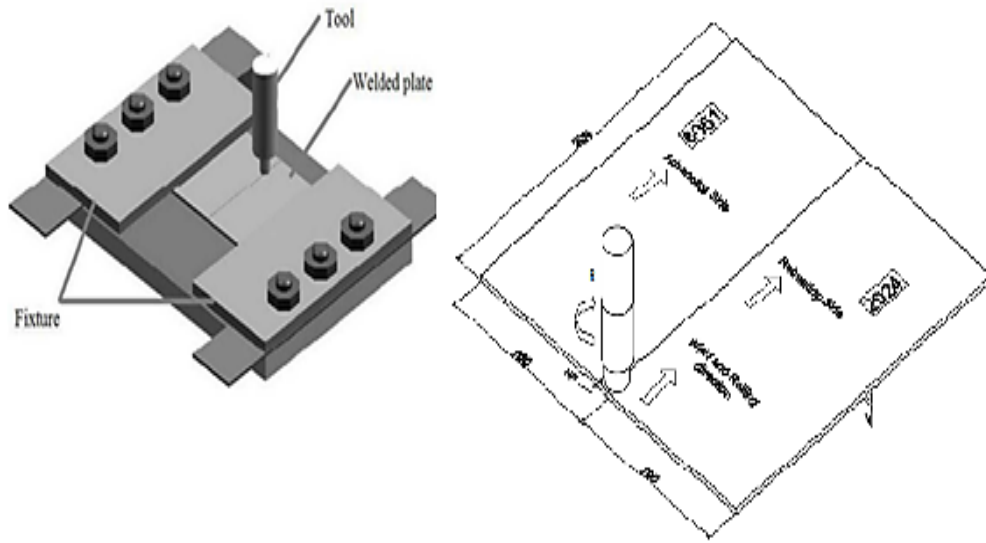
Figure 4 7. Schematic rawing for friction stir welding clamping
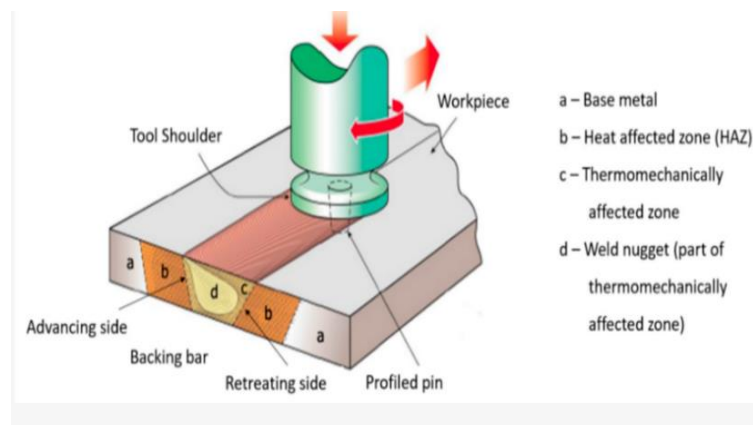
Figure 4.8. Schematic of the friction stirs welding process [50]
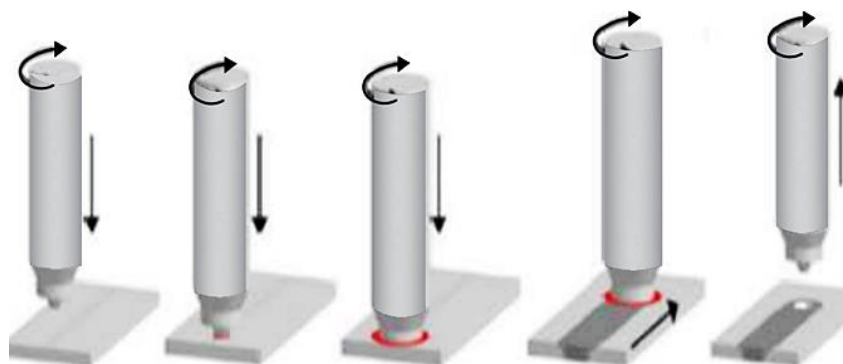
Figure 4.9. Schematic of the friction stirs welding steps [51]

Plunging, dwelling, welding, dwelling, and pulling are the five crucial processes of friction stir welding, as shown in Figure 4.10. To keep the tool's shoulder in touch with the surface of the sheets, the machine forces it to do so. Frictional heat from the shoulder, pin, and work parts reaches over 80% of the melting temperature due to this down force. Speed in relation to a force is also known as travel speed. This kind of tool pulling produces a keyhole, an undesirable outcome in friction stir welding processes. In Figure 4.10 [50] The process (Solid states) describes this procedure. Friction stir welding improves mechanical qualities including residual stress reduction and shrinkage phenomena reduction by keeping temperatures below the melting point.
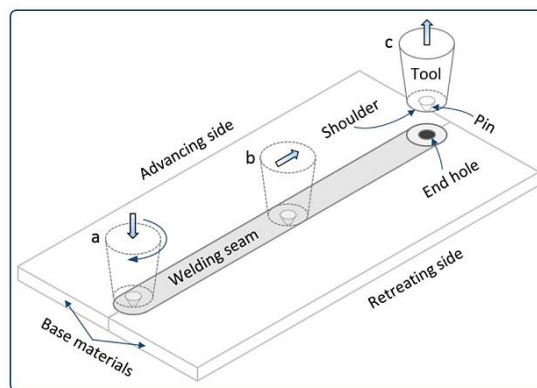
Figure 4.10. Stir welding process shows the exit hole a) plunger and dwell b) stirrer c) tool withdrawal at the end the weld [51]

The advancing side refers to the side where the welding direction and the direction of the rotating tool are congruent which it represents 2024-T3 alloy, while the retreating side refers to the opposite side which it represents 6061-T6. As the pin mixes, it moves the material from the tool's front edge to its back edge, stirring it along the way. Full closure of the bottom section of the joint is ensured when the pin length is smaller than the thickness of the work piece.

4.7. FRICTION STIR WELDING TOOL

The most important part in the friction stir welder is the tool which responsible for welding specifications. The friction stir welding tool consists of three important parts,

and each part has its own task and function: the body, the shoulder and probe (i.e. the pin). The shoulder in friction welding is very important in applying pressure to the workpiece, generating heat and then constricting the material under the shoulder and around the pin. The shoulder in friction stir welding pressing to upper workpieces and generates heat, result plastic deformation because of the friction with the upper work piece's surface, The pin's primary function in a friction stir welding tool is to plasticize, soften, and stir the materials in the stir zone (SZ), which is located in the middle of the welding process [67, 68].

4.7.1. Tool Types

Work piece heating, material flow, heat, and plastic deformation of metal restriction under the shoulder are the primary functions of a friction stir welding tool. Friction is generated by the pin and shoulder's contact with the work pieces. Because we were working with a 2 mm thick plate, we opted for the simpler tool type, which is adaptable to a variety of workspace thicknesses. There are other tools such as square, cube, etc.

4.7.2. Shoulder Shapes

The top surface of the work parts may be heated by the friction force; therefore, tool shoulders should be designed accordingly. For welding integration and to prevent hot material from escaping under the bottom surface, the shoulder's downward forging pressure is crucial. While conical shapes are sometimes employed, the most typical form for the outside of the shoulder is cylindrical. Because it limits material flow from both sides of the shoulder, the friction stir welding procedure often employs tools with concave end surfaces. A pin is used to feed the stirring material into the hollow of the shoulder. When the pin releases flow material, it collects in the concave shoulder. When using a friction stir welding method, the ideal use for this shoulder design is to tilt the tool by 1-3º against to the tool's travel direction. Tilting the tool has various benefits, such as applying a compressive forging force to the welding zone, maintaining material storage continuity beneath the shoulder, reducing hydrostatic pressures, improving the integrity of the nugget or stir zone (NZ) and agitating the substance around the pin.

4.7.3. Pin Shapes

The pin's primary roles in friction stir welding are to heat and distort the materials, cut them ahead of the tool, damage their edges, and mix and stir the materials behind the tool. Pins may have either a flat or a domed end shape; the former is more popular in friction stir welding because to its ease of production. The flat design has the dual benefit of reducing forge force and tool wear while simultaneously providing strong forge force at the plunge stage. Conversely, the tool's shape determines the travel rate and is therefore crucial to the friction stir welding process, particularly with regard to material flow.

4.7.4. Tool Dimensions

In friction stir welding, the dimensions of the tool play a crucial role. Adjusting these parameters alters not just the process outcomes but also the mechanical characteristics. The standard rule of thumb is that the tool pin's diameter should match the workpiece's thickness or a little more workpiece like thickness 2mm we can make diameter from 2mm to 3mm, with the pin's height somewhat below the thickness. In addition, the shoulder's diameters should not be more than three to five times the pin's diameter.

4.7.5. Tool Materials

Select the tool material very important Because it impacts the final product, the quality of the friction stir welding joint is directly related to the substance of the tools used in the process. It is crucial to note the qualities of these materials. There are a lot of considerations when choosing a tool material for FSW, such as the material of the workpiece, the user's performance and expertise, and the expected lifespan of the tool. Consequently, the following characteristics are required of the tool material that is most suited for friction stir welding.

First, the tool's material must have a high level of strength, dimensional stability and creep resistance, are prerequisites for the materials.

Second, the tool must be able to withstand the stresses caused by the machine's forces applied to it, which are more than the compressive yield strength at operating temperature.

Third, the material of the work piece must not react negatively with the substance of the tool.

Fourth, to protect against damage from diving and dwelling, the fracture toughness should be great.

Fifth, to lessen thermal strains, the pin and shoulder material should have a low thermal expansion coefficient.

At last, the price of the tool material shouldn't be too high. For some low-strength materials, such as aluminum alloys, processing and welding techniques have been adequately developed up to this point. These instruments last a long time and don't cost a money.

4.8. FRICTION STIR WELDING PARAMETERS

The first; the rotating speed (w, RPM), which may be either clockwise or counterclockwise, is one of the crucial elements for the friction stir welding process.

The second is the travel speed, which is measured in millimeters per minute along the path to the welding joint. The symbol for travel speed is v, and the unit is mm/min.

The third parameters it is angle of tilt. With the right angle of tilt, the tool's shoulder may grasp the material from both ends of the threaded pin prefer tilt angle from 1-3 degree.

Finally, welding parameters the machine's application of the tool's shoulder's axial force acting downward onto the work piece is the final welding parameter [52].

4.9. THE FRICTION STIR WELDING JOINT'S ZONES

There is usually a predetermined number of zones in a friction stir welding process.

1. Weld stirred zone (SZ) which is located in the middle of the joint and serves as the intersection point for the pin in the workpiece.

2. Thermo- mechanically affected zones (TMAZ) impacted by thermomechanical on each side of the stirred zone is the (TMAZ), an intermediate zone.

3. Heat affected zones areas where heat is felt here in the (HAZ), which is next to the (TMAZ), we encounter temperature cycles but no mechanical shearing.

4. The basic metal (BM) or unaltered parent material.

This means that in terms of fracture initiation, many testing, including tensile strength, will reveal that the heat-affected zone is the weakest. The nugget zone is characterized by a series of concentric semicircular rings because the shoulder makes contact with the top surfaces of the work components. These circles, which are also known as "onion rings," vanish when the rotational speed is raised. Furthermore, threading the instruments is essential for the rings to take place.

4.10. FRICTION STIR WELDING APPLICATIONS

Because of its numerous desirable qualities, including its cheap cost and weight savings, the friction stir welding technique finds use in a wide variety of materials. For instance, the 2XXX and 6XXX series of aluminum alloys are extensively used in the aircraft industry due to their great strength. Welding these metals together using conventional methods is challenging due to the intense cracking that happens during the welding process. Furthermore, certain materials lack the necessary characteristics for some specific applications. Today, an integral part of modern manufacturing technology, particularly in the production of aero planes, is friction stir welding, which

involves joining materials that are chemically or mechanically different. aluminum with aluminum and aluminum to steel connections have extensive use in the aerospace, cryogenic, and petrochemical sectors.

There are many important applications in the friction stir welding are:

1- In the aerospace sector makes extensive use of friction stir welding for a wide variety of components, including but not limited to wings, fuselages, empennages and fuel tanks for space vehicles.

2- Friction stir welding is a useful technique for joining deck, bulkhead, and floor panels and sides in the shipbuilding and marine sectors.

3- The rail industry may make use of friction stir welding for things like container bodies, high-speed trains, carriages, and railway rolling equipment.

4- The electrical industry makes use of friction stir welding for electric motor housings and electrical connections.

5- Electric motor housings and electrical connections are two applications of friction stir welding in the electrical sector.

6- Armor-worthy alloys may be worked with friction stir welding due to their high strength [53].

7- In the realm of land transportation, friction stir welding joints find use in vehicle engine chassis, truck bodywork, and wheel rims.

4. 11 EXPERIMENTED WELDING PARAMETERS USED

The designation numbers (index) of all samples produced in the study, the alloy type and production parameters of the Al sheets are given in Table 4.4. The tilt angle of the stirrer tip was used as 2 degrees in all productions.

Table 4.7. Experimented welding parameters used in this study

Index	Al Alloys	Parameter	
		Rotating speed	Travel speed
1	6061-6061	710 RPM	45 mm/min
2	6061-6061	710 RPM	71 mm/min
3	6061-6061	710 RPM	112 mm/min
4	6061-6061	450 RPM	45 mm/min
5	6061-6061	450 RPM	71 mm/min
6	6061-6061	450 RPM	112 mm/min
7	6061-6061	1400 RPM	45 mm/min
8	6061-6061	1400 RPM	71 mm/min
9	6061-6061	1400 RPM	112 mm/min
10	6061-2024	710 RPM	45 mm/min
11	6061-2024	710 RPM	71 mm/min
12	6061-2024	710 RPM	112 mm/min
13	6061-2024	450 RPM	45 mm/min
14	6061-2024	450 RPM	71 mm/min
15	6061-2024	450 RPM	112 mm/min
16	6061-2024	1400 RPM	45 mm/min
17	6061-2024	1400 RPM	71 mm/min
18	6061-2024	1400 RPM	112 mm/min
19	6061 As received		
20	2024 As received		

In the present work, a vertical milling machine with three travel dimensions (X, Y, and Z-axis) was used; it was semi-automatic and depicted in Figure 4.11. Here are the details of this machine:

1. Motor power: 2 HP.
2. Spindle speeds range:50-1500 RPM.
3. Automatic feed in X, Y and Z axis.
4. Travel speeds range: 50-900 mm/min.
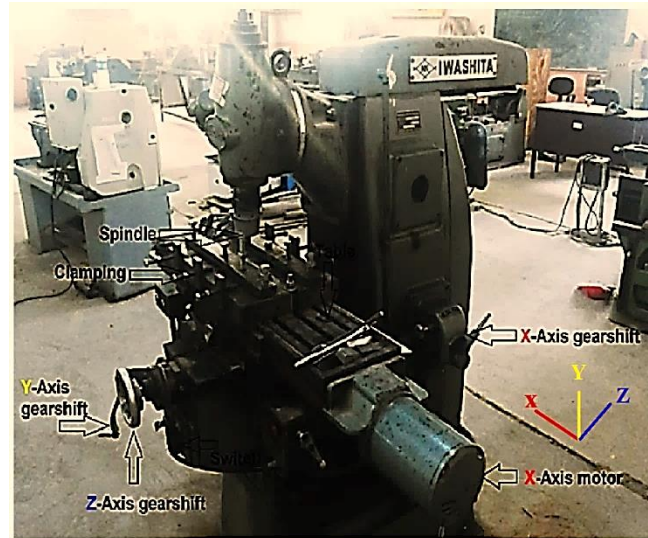
Figure 4.11. The milling machine in FSW

4.12. WELDING MATERAIL AND PROCEDURE

The plan of this work in the welding procedure is to weld two main groups of FSW joints of aluminum alloys material. The first group was similar welds of AA6061-T6, the second group was dissimilar group AA6061-T6 and AA2024-T3.

The rotational speed and Travel Speed varied between instances, and each subgroup was further subdivided into three primary ones.

To achieve the optimal circumstances for the FSW parameters, the specifics of the welding features used for the two sets of welds are shown in Table 4.7.

The tilt angle, travel speed, and rotating speed are different parameters the welding machine characteristics that may be adjusted manually. In the end, the quality of the welded specimens is greatly affected by those characteristics. Adjusting the most efficient welding machine settings (traveling speed and rotational speed) may improve the weld metal's mechanical, metallurgical, and microstructural characteristics as well as those of the thermo-mechanically impacted zone and heat affected zone. Depending on the surface roughness, the amount of heat created between the tool and sample increases as the Rotating Speed decreases and the travel speed increases. Making ensuring the sample gets hot enough to plasticize the material surrounding the tool is

crucial for producing appropriate weld properties. Void and other flaws in the weld line may be created when the temperature is high enough. Weld nugget collapse occurs when a lot of heat is applied [19].

4.13. WELDING PROCEDURES

Once the milling machine's experimental setup is complete, the specimens are fastened tightly using fixtures and placed over the ground plate (anvil). Initially, the FSW tool is heated up by keeping it in touch between the two plates while it is spun at the proper speed. At a rate of about 95% of the plate thickness (t=2 mm), the tool progressively penetrates until its shoulder contacts the work parts. The depth of penetration was about 0.1 mm in order to provide the required welding pressure. Holding the pressure steady for around 20 seconds is necessary to extrude the metal flash surrounding the tool. The next step is to set a specified welding speed and advance the tool along the plate's joints until the item is finished. The tools will be removed at last. Figure 4.12 shows the friction stir welding procedure scheme of operations to conduct and Figure 4.13 shows the stages of the process.
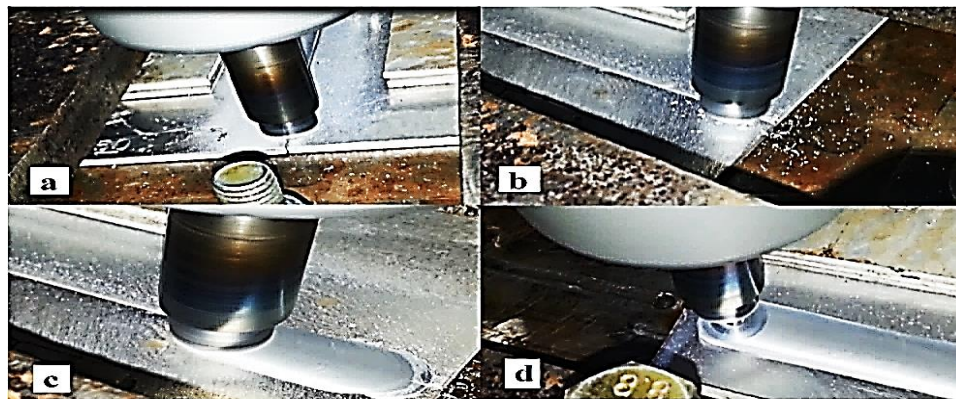
Figure 4.12. The welding steps, (a) Plunging step (b) tool penetration (c) stirring and welding step (d) end of welding.
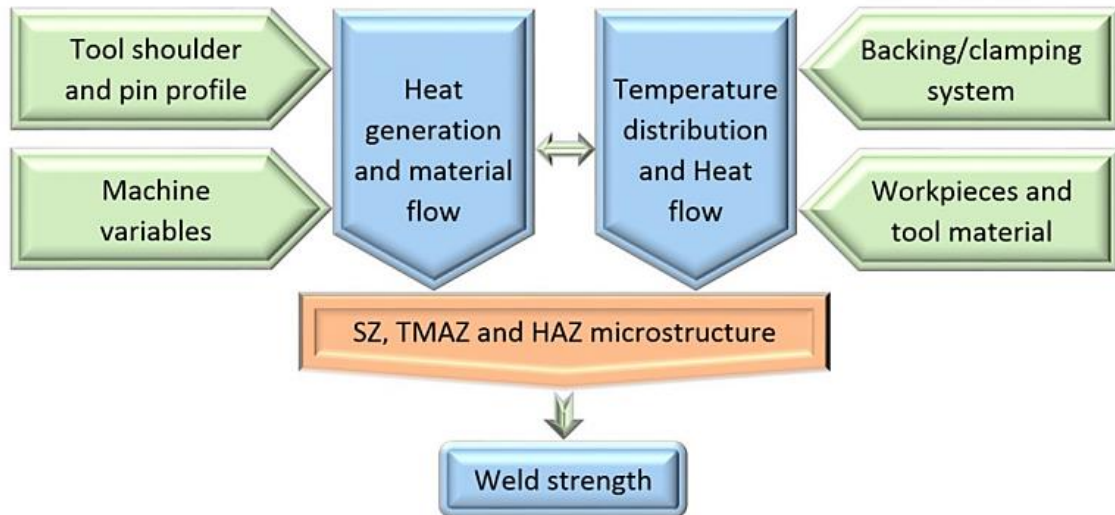
Figure 4.13. Plan of operations to conduct friction stir welding with temperature distribution

4.14. NONDESTRUCTIVE TESTING

4.14.1. Visual Inspection

The first step in diagnosing any welding surface issue, such as misalignment, flash, or lack of penetration, is a visual examination. The subsurface discontinuities cannot be seen by eye examination. From visual inspection of the samples, it is clear that the normal force has a significant effect on the appearance of the side edges of the weld through the appearance flash or lack of penetration. Therefore, care must be taken while welding to give the appropriate vertical force, which depends on the thickness of the workpiece.

4.14.2. X-Ray Inspection

Electromagnetic radiation with very short wavelengths, such as X-rays, may pass through solid materials and be partly absorbed by them. Film or sensitized paper may be used to record the radiation that travels through the substance, and then the results can be shown on a fluorescent screen.

The ideal parameters for this macrograph examination were as follows: 130 volts, 3 milliamperes, 20 seconds of exposure time, and 600 millimeters between the source and film. as referenced in ASTM E747 [54]. The test was conducted at General Company for Research and Development/Ministry and Minerals in Baghdad. Figure 4.15 depicts the X-Ray examination system.

Company: ICM Belgium co.

Model: site –x   250kv

Figure 4.14. X-Ray examination system.

4.14.3. X-Ray Diffraction

A specimen test of 10x10x2 mm, including the stir zone (SZ) and base metals (BM), underwent X-ray diffraction investigation. The X-ray diffraction test is used to ascertain the composition and formation of compounds and phases in all manufactured alloys. The test was performed at General Company for Research and development/Ministry of Industrial and Minerals in Baghdad. The device type (XRD-6000 diffract meter), as shown in Figure 4.16. The used parameters were: 40KV, Current: 30 mA with Cu-Ka radiation as x-ray source and scan speed 1 deg/min.

Table 4. 8: Specification and operating condition of X-ray diffractometer

The diffractometer name	Angstrom Advanced Inc.
Model	ADX 2700
Current	30 Ma
Voltage	40 KV
Divergence slit	1 degree
Scatter slit	1 degree
Source of X-ray	Cu, Ka
Filter element	Ni
Type of X-ray beam	Monochromatic
Wavelength	$\lambda = 1.5410$ A

(a)   (b)

Figure 4.15. (a) XRD device, and (b) X-ray diffract meter

4.15. MICROSTRUCTURE EXAMINATION

4.15.1. Sectioning and Mounting

Pieces suitable for investigation were extracted from the original or welded areas with caution to prevent the introduction of false microstructural findings during the cutting process. Sectioning was performed with utmost care. This surface yielded microstructural information across the vertical cross-section of the specimen at its centreline. The specimens were cold mounted to prevent any minor alterations in the microstructure of the samples due to the heat and pressure involved in the hot-mounting process, such as recrystallization or recovery. The cold mounting was

solidified at ambient temperature, with curing durations ranging from 1 to 2 hours. Therefore, we may succinctly outline the processes according to the following timetable.:

Microscopic Examination

1- Selection
2- Sizing
3- Cutting
4- Mounting
5- Grinding
6- Polishing
7- Etching
8- Microscope

The microstructure examination involves the following steps: -

1. The samples were sliced at the weld line's cross section.

2. Due to the tiny size of the samples, they must be mounted using an epoxy mixture.

3. The wet grinding procedure was carried out using SiC emery sheets with grit sizes of 180, 220, 320, 400, 500, 600, 1000, 1200, 2000, and 2500.

4. A cloth and alumina (Al_2O_3) particles of 0.03 μm in size were used for the polishing process.

5. The etching procedure used Keller's etchant composed of 2ml HF, 6mL HNO3, and 92mL water with a dwell duration of 15-30 seconds. Subsequently rinsing with water and alcohol to halt the reaction. Hot air is used to inhibit surface oxidation, as per ASTM E407-99 [55] .

6. The microstructure investigation was conducted at the Metallurgy Laboratory of the Technical College in Baghdad, which is part of the Middle Technical University in Iraq. Figure 4.16 depicted the placement of the specimens.
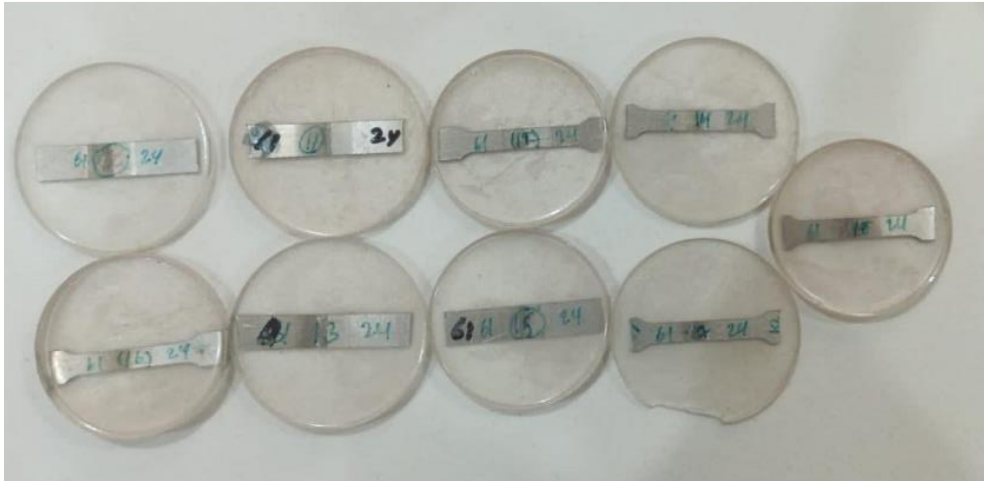
Figure 4.16. Microstructure test specimens

4.16. DESTRUCTIVE TESTING

4.16.1. The Tensile Test

A sample of the tensile test specimen was manufactured by water jet machine. The specimen is made perpendicular to the weld line and including all location of weld according to AWS D17.3/D17.3M:2010 [56]. The standard dimensions of the specimen were shown in Figure 4.20.

Figure 4.17. Standard dimensions of the tension test specimen

Tensile testing was performed at a consistent crosshead speed of 1 mm/min. The transverse sample's deformation was quantified using a computerized 2D curve picture. A standard tensile test specimen was fabricated following the ASTM B557M-02a standard. [57] using a water jet cutting machine. The tensile test was conducted in the Al Fawzi Lab facility located in the industrial district on Sheik Omar St. in Baghdad, Iraq.
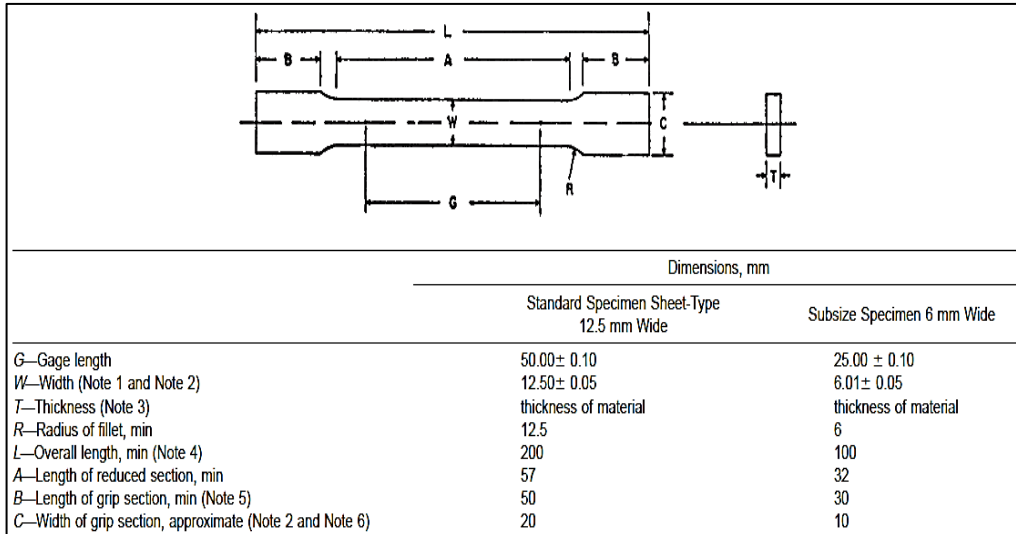
Figure 4.18. Standard dimensions of tensile test specimens [73]

	Dimensions, mm	
	Standard Specimen Sheet-Type 12.5 mm Wide	Subsize Specimen 6 mm Wide
G—Gage length	50.00± 0.10	25.00 ± 0.10
W—Width (Note 1 and Note 2)	12.50± 0.05	6.01± 0.05
T—Thickness (Note 3)	thickness of material	thickness of material
R—Radius of fillet, min	12.5	6
L—Overall length, min (Note 4)	200	100
A—Length of reduced section, min	57	32
B—Length of grip section, min (Note 5)	50	30
C—Width of grip section, approximate (Note 2 and Note 6)	20	10

Figure 4.19. Manufactured tensile test specimen (a) photograph (b) schematic.

61

Figure 4.20. Tensile test specimens of FSW.

A LARYEE computer-controlled electronic-mechanical universal testing equipment, model Time 2012 from LARYEE Technology Co. LTD, with a load capacity ranging from 50 to 300 KN was used for conducting tension tests figure 4.21. The experiments were conducted utilizing dog-bone shaped specimens on the right side. The main objective of the test was to ascertain the stress needed to cause the specimen to fracture, rather than analyzing the whole stress-strain curve. The load to failure was transformed into tensile strength by division by the cross-sectional area. The test gadget was linked to the Bluehill2 software to collect the data. The data was stored in an Excel file including hundreds of readings ranging from 2000 to 6000. The tension test findings indicated that the fracture occurred in the zone of lower strength located between the TMAZ and HAZ.

Figure 4.21. Tensile test device

Table 4. 9. The AA2024-T3 and AA6061-T6 materials' tensile characteristics

Material	Condition	Yield stress (MPa)	Tensile stress (MPa)
AA6061-T6	Measured	224	384
	Standard [7]	276	310
AA2024-T3	Measured	242	384
	Standard [32]	310 Min.	430 Min.

4.16.2. Bending Test

The effects of FSW were investigated by means of three-point bending tests performed on the universal test machine. The material's reaction is evaluated under a basic beam loading arrangement in this test, which is also known as flexural testing or transverse beam testing. By subjecting materials to a combination of compression, shear, and tension, this testing technique determines their ultimate strength yielding valuable data. Parameters including elastic modulus, fracture toughness, flexural strain, and flexural stress may be ascertained by the bending test. Due to differences in loading geometries, the results of bending tests, which measure material properties, will differ from those of tensile and compressive testing. Aside from the 3-point bending test, there are other techniques for assessing materials' flexural stress, such as the 4-point

bending test and the cantilever bending test. Comparing bending behaviors of welded materials to evaluate the impact of welding parameters.
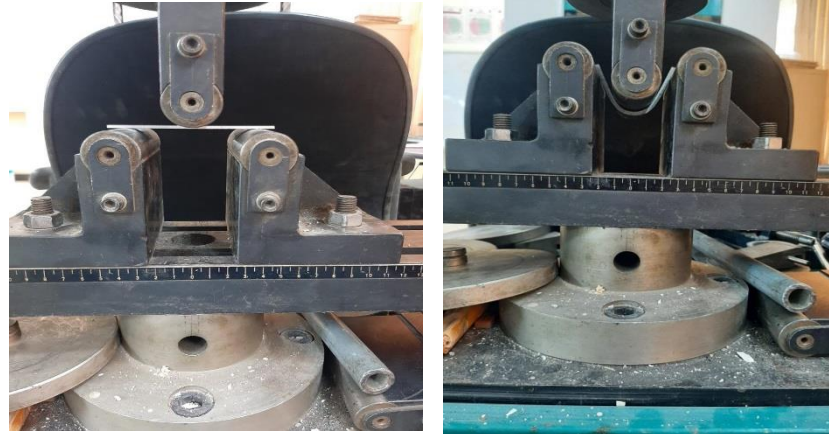
Figure 4.22.   Three points bending test

4.16.3. Microhardness Test

Among the many useful mechanical tests for gauging metal qualities, the hardness test stands out. A material's hardness is often measured by its resistance to permanent deformation. A digital micro hardness tester, Model: HVS-1000 NO. 11200, made in 2011 by Laryee Technology Co., China, was used to measure the hardness of the twenty Al-Al specimens. Once the samples were polished and free of scratches, they were prepared for hardness measurements using straight-sided specimens with dimensions of 100x10x2 mm. Hardness values were measured using a Prinels hardness tester with a 4.5 N load and a 15-second dwell period. Measurements were taken along the center line of the weld cross-section at 0.4 mm intervals. Measurements were taken 3 mm ln contrast to the base metal next to it on either side of the Friction Stir Welding (FSW) zone. Figure 4.23. illustrated the micro hardness instrument and the prepared specimens. A different comparison was conducted with a fixed rotating speed while varying the travel speed parameter.

1. The sample is placed on the platform, and the surface of the sample is shown through the device's lens.

2. The device dial is rotated to select the impact site, then the appropriate load and time for the load are selected.

3. We click on Start to start the process of highlighting the trace and wait for the process to finish.

4. The dial is rotated to select the device lens to determine the diameters of the effect, and the result appears on the device screen.

Figure 4.23. Micro hardness test apparatus and microhardness specimens

4.17. SEM-EDS INSPECTION

Scanning electron microscope Located Corporation and Research Industrial Development / Ministry of Industry was used to analyses the plan view and transverse sections (fractography of fracture surfaces), to examine the microstructure of welding zones of FSW joint [58] .

4.18. EDX

Elements distribution maps may be generated by EDX by scanning the electron beam over the sample and collecting X-ray signals at each spot. Using this method, one may learn about elemental segregation, phase distribution, and sample area of interest identification.

Figure 4.24. SEM/STEM, 5-Axis

PART 5

RESULTS AND DISCUSSION

5.1. NON-DESTRUCTIVE TESTS

5.1.1. Visual Inspection Results

The technology of welding by utilizing FSW is produced by mixing metal under the solid-phase condition to higher temperature that developed from the friction between the tool and specimen. Therefore, defects can be generated internally and externally during the welding process. This type of test explains the surface defects which have been developed after the welding process. There are numerous categories of defects, such as tunnel voids unfinished mixing flash etc. Most of the generated defects result from the incomplete material mixing during the welding procedure. Friction stir welding required an adequate heat input in order to give the optimum conditions of welding. This depends on factors including the tool geometric shape, linear and rotational speed during machine operation. Figure 5.1 presents some of these defects which have been appeared during the welding process.

Figure 5. 1. Surface visual inspection of weldments; (a) similar weld AA6061-T6 at 1400 RPM and 45mm/min (b) dissimilar weld at 450 RPM with 71mm/min.

1. Similar weld (AA6061-T6) at rotating speed 1400 RPM and welding transfer speed 45mm/min include line defect at the end of welding joints because not control load (high load).

2. Dissimilar weld (AA2024 to AA6061-T6) at rotating speed 450RPM and welding 71mm/min. include flush and sound because high load and not good fixing.

The defects in some welding joints at the cross section are presented as Figure 5.2 (a) Incomplete coalescence leads to tunnel defect as in sample as in Figure 5.2 (b) Tunnel defect in the weld root. (C) Void defect shown in advancing side. (D) Free from any defect was examined by visual test. These defects are shown in Figure 5.2.
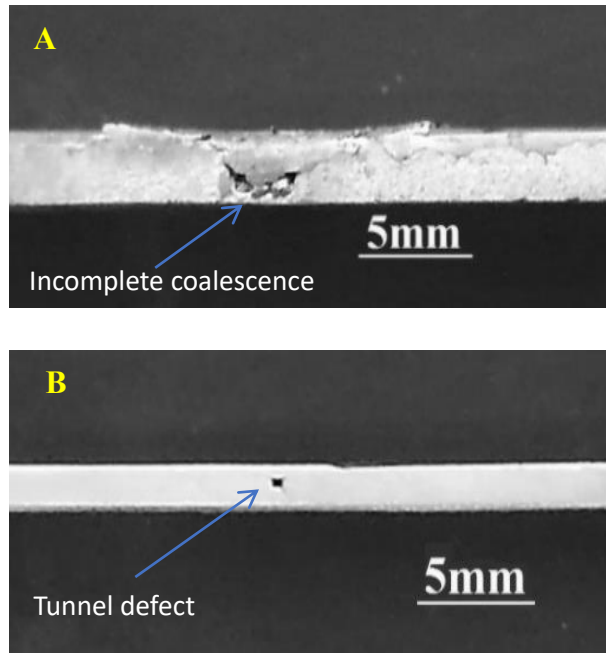
Figure 5.2. Defects in the welded samples cross section. (b) Similar weld (AA6061-T6) 1400RPM and 45mm/min (a) Dissimilar weld (450RPM and 71mm/min).

5.1.2. X-Ray Radiography Inspection Results

A very short-wavelength electromagnetic radiation, specifically X-rays, can penetrate across solid materials and be partially absorbed by it. This passing radiation can be recorded on film or sensitized paper and seen on a fluorescent screen.
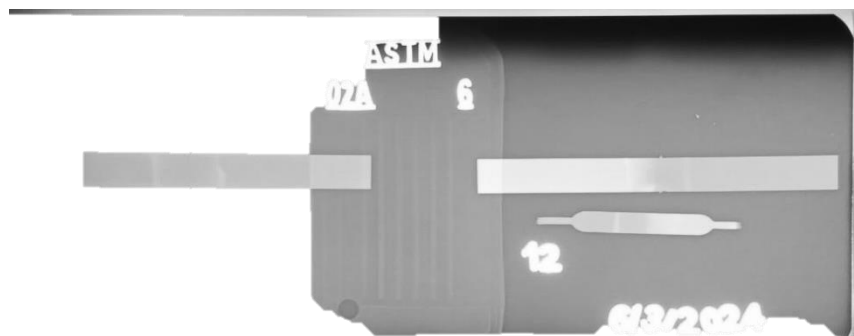
Figure 5.3. Radiographic inspection test for similar and dissimilar welds Al- alloy.

Radiography inspection has been done as shown in Figure 5.3 which represents the x-ray photograph for similar and dissimilar FSW of Al2024 & AL6061; Sample (6061-6061) #3 which represent on side on the left whereas the side on the right represent the (2024– 6061) Sample # 12.

It was seen from both welded samples that there is no crack along weld line (free from defects) when examined by this technique. This supports the given results under the condition (112 mm/min; 710 RPM) for both similar and dissimilar gives the best values among other conditions.

5.2. MICROSTRUCTURE EXAMINATION RESULTS

During FSW, severe plastic deformation and high temperature exposure at the stirred zone contribute to recrystallization and texture development, as well as dissolution and coarsening within and around the stirred zone. Optical macroscopic examination was carried out for in Figure 5-4 and the same examination was repeated on joints welded for identical and different at 710 RPM 112mm/min in figures (5.5, 5.6, and 5.7).

Optical macroscopy demonstrated that the stirred zones of the majority of joints formed contained no porosity or additional defects (such as kissing bonds). The base alloy shows elongated grains according to the rolling direction and an average grain size of 32µm. During FSW, intensive plastic deformation and frictional heating generate fine equiaxed grains through dynamic recrystallization. These grains have an average size of 12µm, consistent with previous findings. Under certain FSW situations, onion ring's shape structure is detected in the NZ. The onion rings have been eliminated from the present study because the welding tool was not threaded.

Some investigators reported that the small, recrystallized grains of the nugget zone have a high density of sub-boundaries, sub-grains, and dislocations [42]. The FSW techniques generates of transition zone TMAZ between the base metal and the nugget zone. During FSW process, the TMAZ undergoes temperature as well as deformation. The TMAZ experienced plastic deformation, however recrystallization was not observed in this zone due to inadequate deformation strain.

However, due to high temperature experience during FSW, dissolution of some precipitates is detected in the TMAZ. The extent of dissolution is affected by the heat impact experienced by TMAZ. This situation is consistent with the observational data

of Mishra et al. [1]. Venugopal et al. [14] establish that the size and morphology of coarser precipitates don't change considerably, but their orientation along the rolling direction, like in the parent metal, is absent in TMAZ.

The HAZ is located next to the TMAZ and has only been exposed to heat, without any plastic deformation. As a result, it has been preserved that, the base alloy's original elongated grain structure, with an average grain size of 18 μm. However, strengthening precipitates may overage and coarsen, degrading the mechanical characteristics of this region, which are related to the position of fracture in tensile tests and the lesser hardness values attained in the HAZ.

Microstructure of the welding base alloys are shown in Figure 5.4 through two different magnifications. The microstructure of all alloys involves of elongated grains (a-solid solution matrix (the bright contrast)) along with inter metallic phases at random distribution of constituent precipitates or small black particles randomly distributed across the aluminum grains [59]. This is in accordance with the standard structure of these advanced aluminum alloys. Some of these intermetallic phases (Al_2Cu and Al_2CuMg) have a coarse plate-like morphology. The typical grain size is approximately 30-32 μm. The XRD investigation of this alloy illustrates the attendance of these intermetallic phases as demonstrated in Figure 5.5.
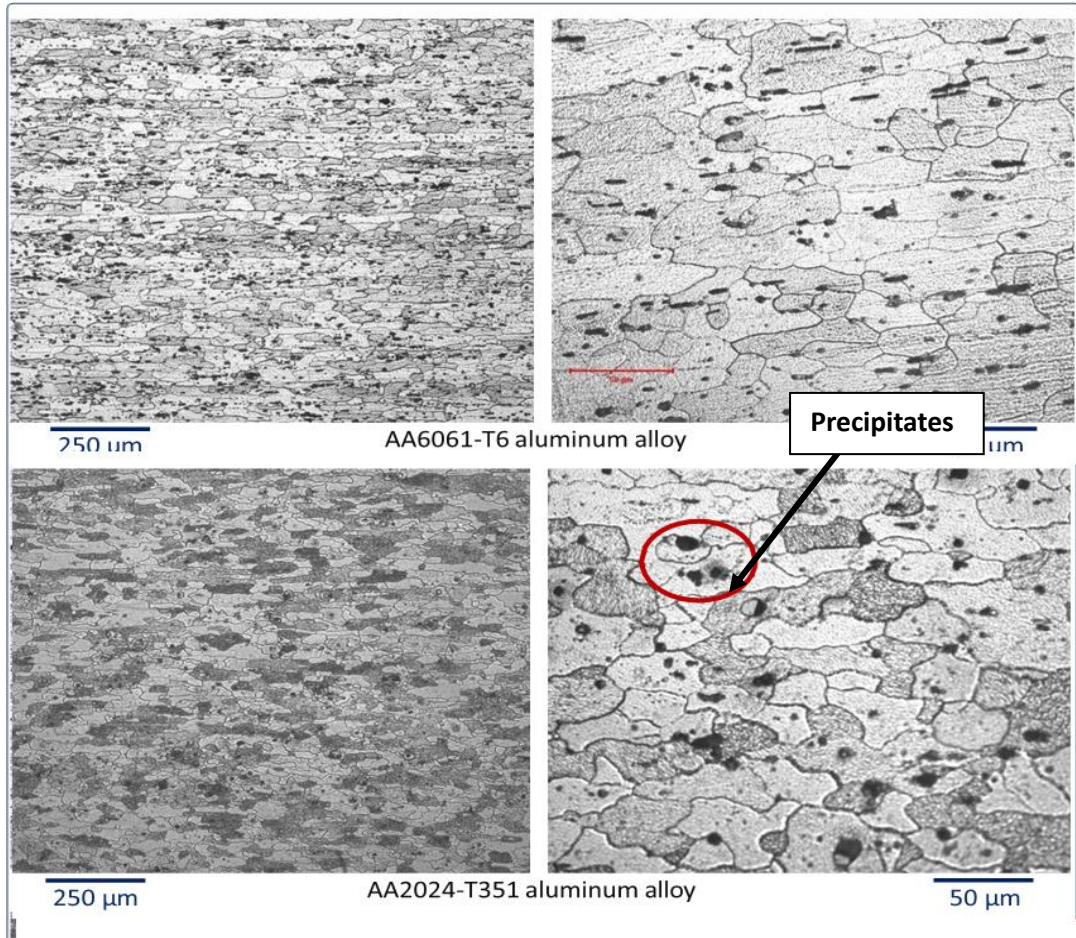
Figure 5.4. Microstructure of welding base materials
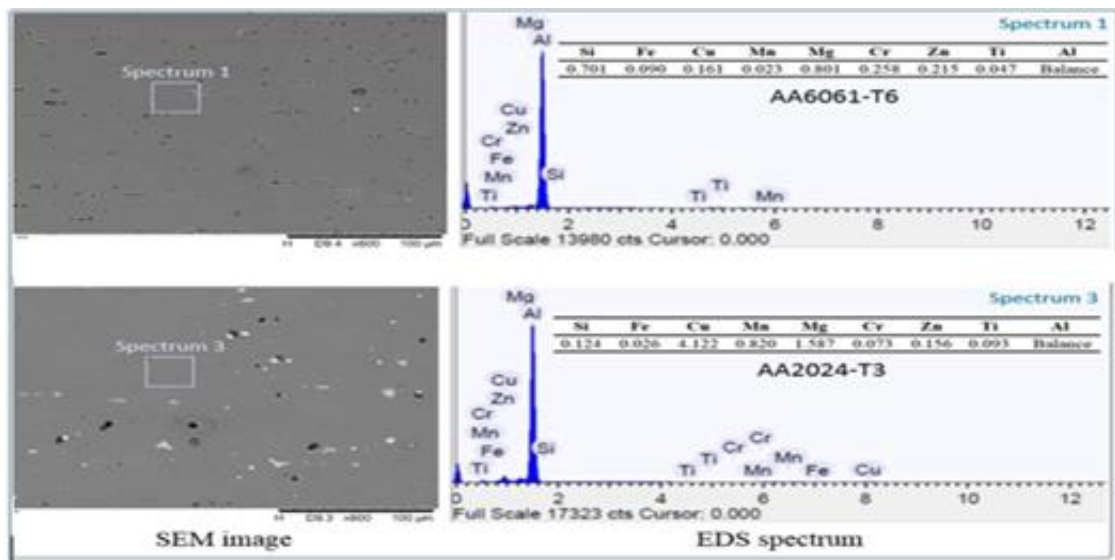
Figure 5.5. The SEM images and EDS spectrums with the acquired chemical compositions of base materials

The microstructure examination results for the aluminum alloy (AA2024-T3, AA6061-T6) specimens which welded by FSW manner are different from the microstructure of the base metal or cast structure of fusion weld, Figure 5.6 shows a sample of this joints.

Figure 5.6. Macro-graphic of welded joint

The (FSW) joint comprised of several zones:

Nugget zone (NZ): it knowing as weld nugget zone, it located at the center of weld and completely re-crystallized region.

Thermo-mechanically affected zone (TMAZ): affected by heat and deformation, but it is not re-crystallized at both side of nugget zone.

Heat affected zone (HAZ): affected by heat only without any plastic deformation between ((TMAZ)) and (BM).

Base metal (BM).

5.2.1. Similar Weld AA6061-T6 to AA6061-T6

Figure 5.7. illustrates the various regions under various welding situations. The stir's zone microstructures comprised of fine equiaxed grains in all samples. The deformed grains of material have a tendency to recrystallize into strain-free grains. As anticipated, the applied strain and heat rates has essential influence on the of grain size variation. The experimental findings illustration that, there is inversely proportional relations between heat flow and final grain size higher the heat flow, results smaller grain sizes. This is identical for both annealed and work hardened circumstances. In the work-hardened samples, the extant plastic strain improves the kinetics of

recrystallization, in addition it observed the present of small grain size in the microstructures of the base metal particularly in TMAZ.
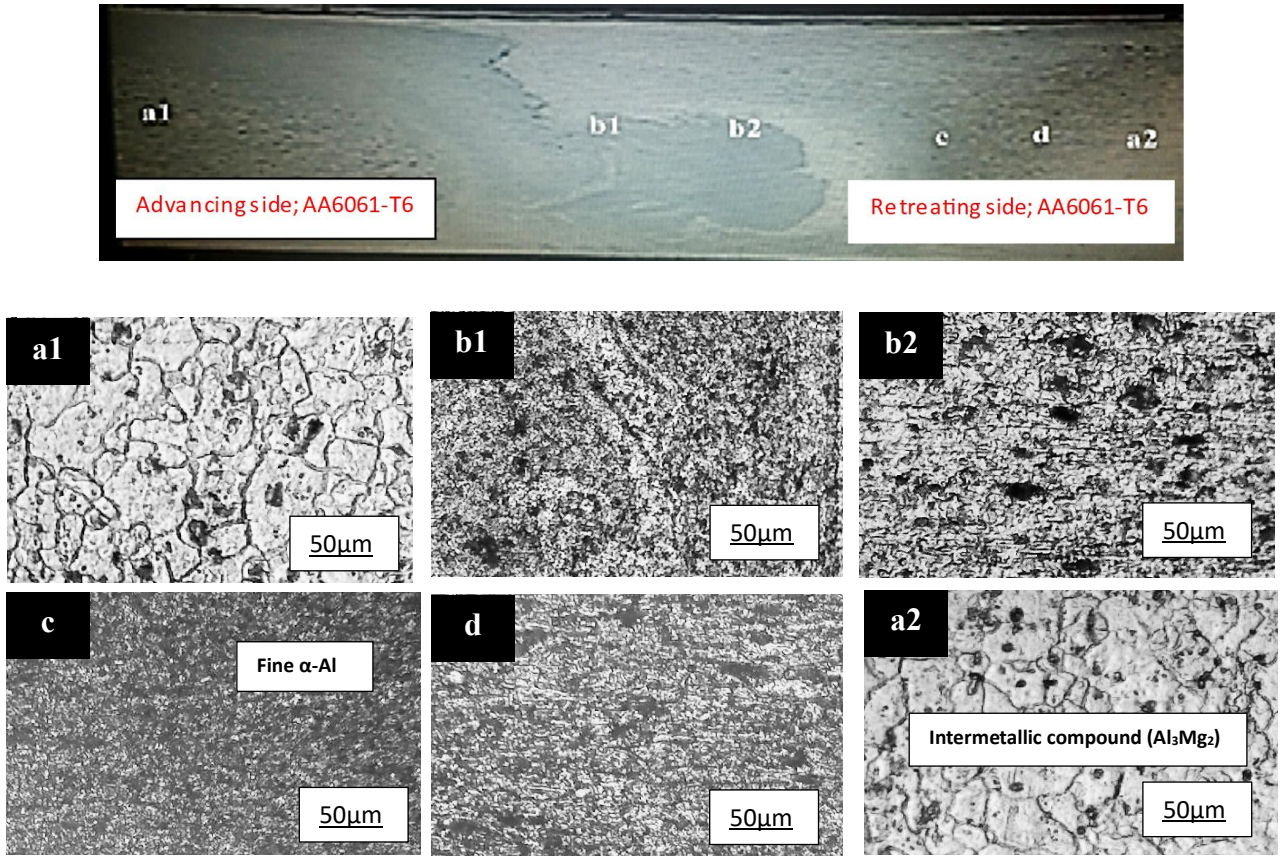
Figure 5.7. Microstructure of various regions in cross section of FSW joint of Al 6061-T6 alloy, (a1, a2) base metal, (d) Heat Affected Zone (HAZ), (c) Thermal Mechanical Affected Zone (TMAZ), (b1, b2) Nugget Zone (NZ) at (710RPM and 112 mm/min).

5.2.2. Dissimilar Weld (AA2024-T3 to AA6061-T6)

Figure 5.8. illustrated the microstructure images related with the dissimilar weld (AA204-T3 with AA6061-T6) by friction stir welded (FSW) procedure. It can be obvious that the refine grain structure was in center of weld zone and presents α-aluminum and Al_3Mg_2.

The microstructures images for different zone of AA2024-T3 and AA6061-T6 base metals sample, under 710 RPM, 112 mm/min are demonstrated in Figure 5.8. a and e. It has been realized that the microstructures of the heat impacted zone HAZ at the

advancing and retreating sides (h), (d) respectively be similar to the base materials without any significant grain coarseness. (g) and (c) images illustrate TMAZ on the advancing and retreating sides, respectively. As shown in the images, the bent and elongated TMAZ grains are more noticeable on the advancing side than those on the retreating side. This could be due to the direction of plastic flow from the advancing to the retreating side, which in turn leading to form a fiber-structure pattern present in wrought metal. Furthermore, in the advancing side of the weld the flow direction of plasticized materials is opposed to that in the base metal, resulting in significant relative deformation and more evident elongated grains on this side also, at the advancing side of the weld It is worth noting that NZ's microstructure is formed from the recrystallized equiaxed grains, with the AA6061 side having finer granules than the AA2024 side. Strain rate and thermal history are the two vital factors influencing recrystallized grain size in NZ. In the case the AA6061 is located on the retreating side of the weld It has been demonstrated, the strain rate distribution in the SZ is approximately uniform. And the temperature on the retreating side is higher than that on the advancing side, thus finer grain size is formed in AA6061.
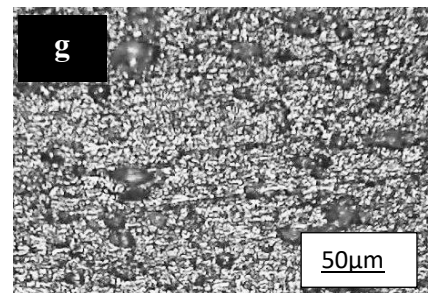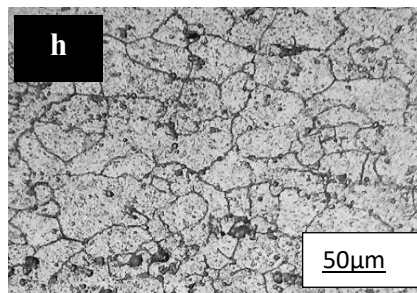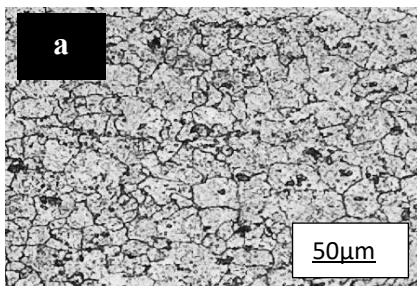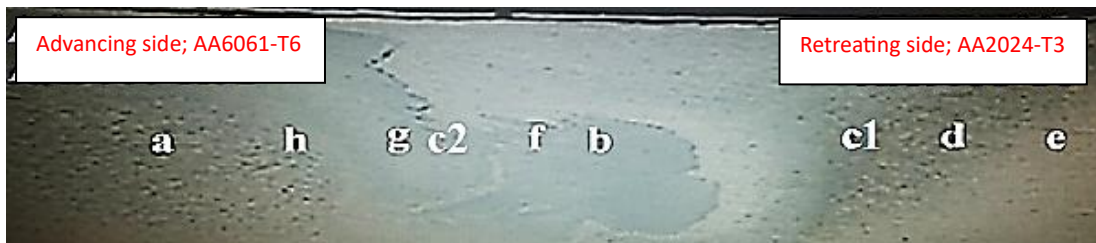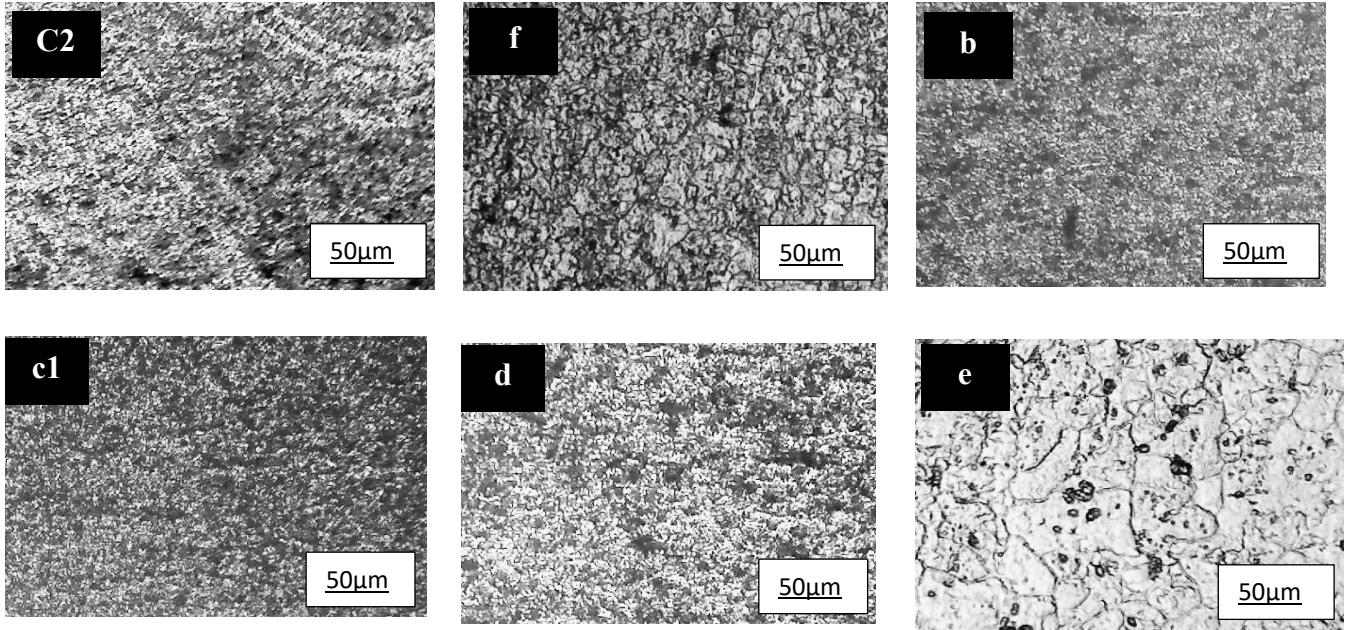
Figure 5. 8. Microstructure of various regions in cross section of FSW joint of Al 6061-T6 to Al-2024-T3 alloys, (a) base metal(AA6061-T6), (e) base metal (AA2024-T3), (h, d) Heat Affected Zone (HAZ) at advance side and retreat side respectively, (g, c1, c2) Thermal Mechanical Affected Zone at advance side and retreat side respectively, (f, h) Nugget Zone at advance side and retreat side respectively at (710RPM and 112 mm/min).

5.3. FRACTURE MORPHOLOGY OF TENSILE SAMPLES

5.3.1. Similar Weld AA6061-T6 to AA6061-T6

Scanning electron microscope (SEM) was utilized to illustrate the surfaces of fracture for FSW specimens after tensile testing. Fracture surface of the (AA6061-AA6061 T6) detected under SEM as shown in Figure 5.9. Fine equiaxed dimples and hemispherical micro voids are observed in the nugget zone, while noticed a microcrack in HAZ region. This indicates that the ductile failure occurred under tensile loading.
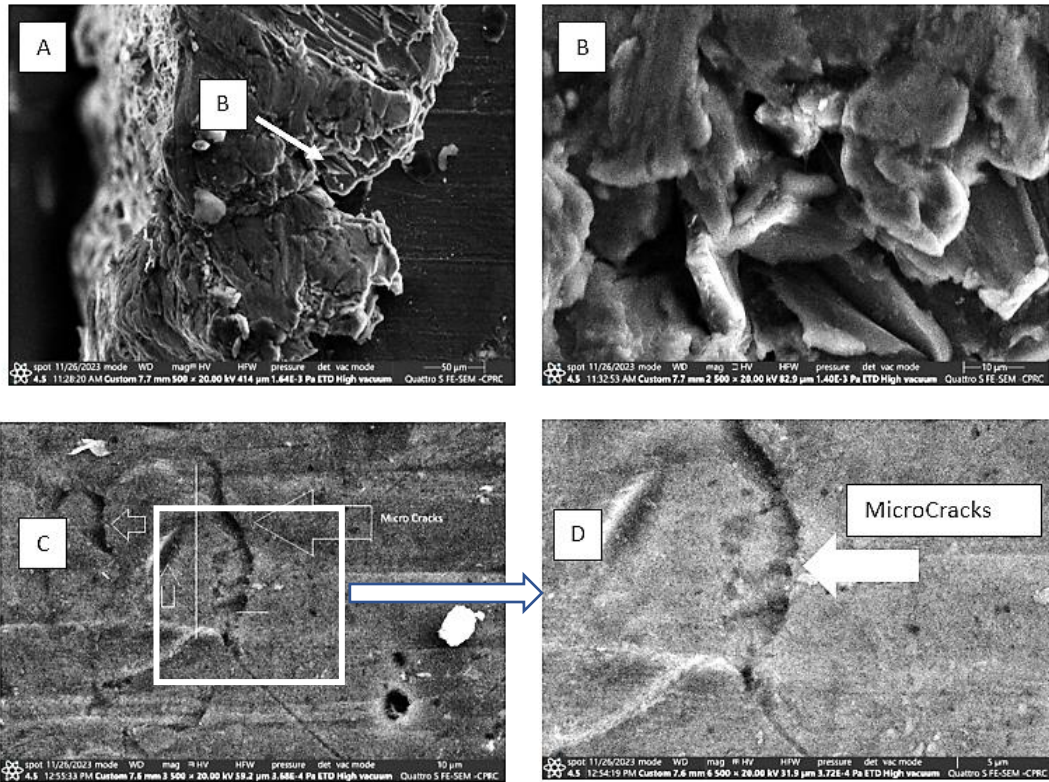
Figure 5.9. Scanning electron micrographs of the AA6061-AA6061 aluminum alloy sheet after tensile testing, (a) Overview of fractured surface, (b) magnified view of region B marked in view showing equiaxed dimples and micro voids in A, (c) magnified view at region of (HAZ) (d) magnified view of region showing microcracks.

5.3.2 Dissimilar Weld AA6061-T6 to AA2024-T3

Figure 5.10 shows fractography of a fracture surface with a striation-like pattern and some scratch marks caused by surface movement. All of these data indicate that the fracture began in this location and spread circumferentially along the weld nugget in a path parallel to the welded specimen's longitudinal direction.
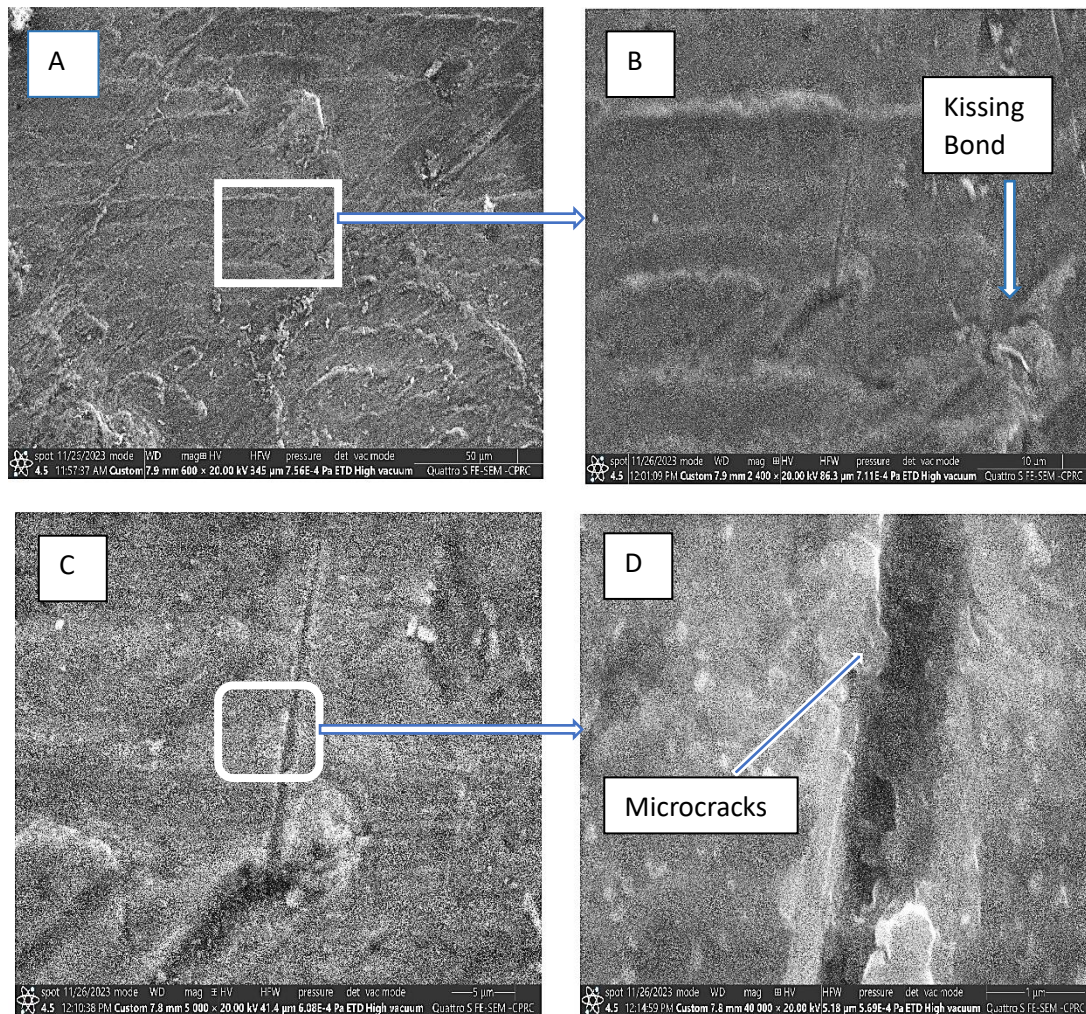
Figure 5.10. Scanning electron micrographs of the AA6061-AA2024 aluminum alloy sheet after tensile testing, (A) Overview of surface in nugget zone (B) magnified view of region B marked in view A showing striation-like pattern, (C) magnified view at region of HAZ (D) magnified view of D region showing microcracks

5.4. ENERGY DISPERSIVE SPECTROSCOPY (EDS) ANALYSIS

The EDS analysis provides useful information regarding the aluminum alloys' chemical composition. The changes in chemical composition in joint zone effect on the adhesion join properties between the elements and furthermore the mechanical performance of the joints.

Figures 5.11 and 5.12 display the EDS spectrum from various zones which represents the element identification in nugget and cracking zone. The surface tension of

aluminum is completely different which in turn effects on the adhesive joining at the interfaces of these two materials.

All EDS analysis results exhibited an item of the Au in their composition, where the surface of the specimens was coated by the gold layer before EDS inspection that's used to enhance the resolution of the SEM photos.

The Al joints of the optimum shear force exhibited the presence of (Al, Si, Fe, Mg) and which represented the major elements at the composite zone in the hole and interface at the Al alloy.

Element	Atomic %	Atomic % Error	Weight %	Weight % Error
Mg	0.9	0.0	0.8	0.0
Al	97.3	0.2	96.2	0.2
Si	0.7	0.0	0.7	0.0
Ti	0.0	---	0.0	---
Cr	0.2	0.0	0.3	0.0
Mn	0.0	0.0	0.1	0.0
Fe	0.7	0.0	1.3	0.1
Ni	0.0	0.0	0.0	0.0
Cu	0.1	0.0	0.3	0.0
Zn	0.1	0.0	0.2	0.0

Element	Atomic %	Atomic % Error	Weight %	Weight % Error
Mg	1.3	0.0	1.1	0.0
Al	98.1	0.2	97.4	0.2
Si	0.0	---	0.0	---
Ti	0.0	0.0	0.1	0.0
Cr	0.1	0.0	0.3	0.0
Mn	0.0	0.0	0.1	0.0
Fe	0.3	0.0	0.6	0.0
Ni	0.0	0.0	0.1	0.0
Cu	0.1	0.0	0.3	0.0
Zn	0.0	0.0	0.1	0.0
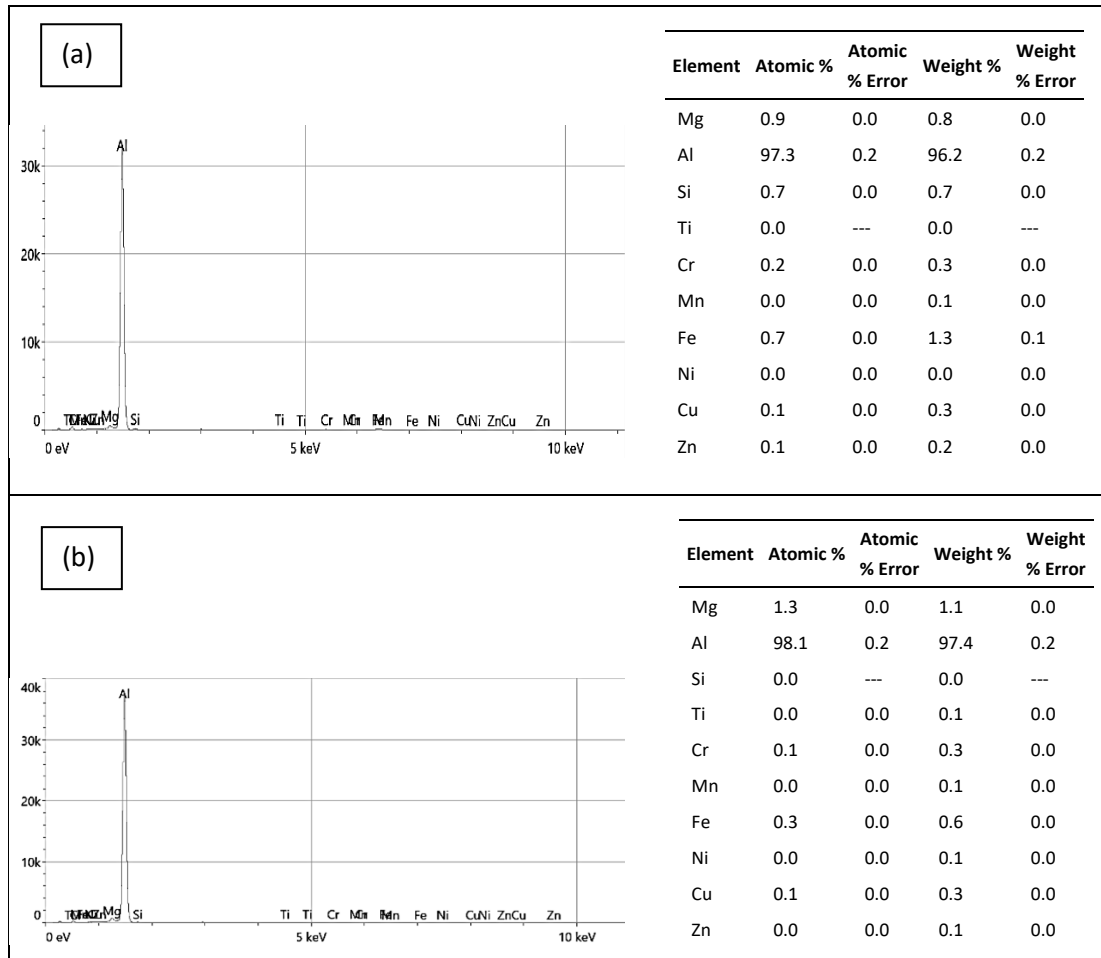
Figure 5.11. EDS for Similar weld AA6061-AA6061 at (a) nugget zone (b) at HAZ

(a)

Element	Atomic %	Atomic % Error	Weight %	Weight % Error
Mg	1.0	0.0	0.9	0.0
Al	97.9	0.2	96.7	0.2
Si	0.0	---	0.0	---
Ti	0.0	0.0	0.0	0.0
Cr	0.1	0.0	0.2	0.0
Mn	0.1	0.0	0.1	0.0
Fe	0.4	0.0	0.7	0.0
Ni	0.1	0.0	0.2	0.0
Cu	0.5	0.0	1.1	0.0
Zn	0.0	---	0.0	---

(b)

Element	Atomic %	Atomic % Error	Weight %	Weight % Error
Mg	0.0	---	0.0	---
Al	99.7	0.2	99.4	0.2
Si	0.0	---	0.0	---
Ti	0.0	0.0	0.1	0.0
Cr	0.0	0.0	0.0	0.0
Mn	0.0	---	0.0	---
Fe	0.3	0.0	0.5	0.0
Ni	0.0	0.0	0.0	0.0
Cu	0.0	0.0	0.0	0.0
Zn	0.0	0.0	0.0	0.0
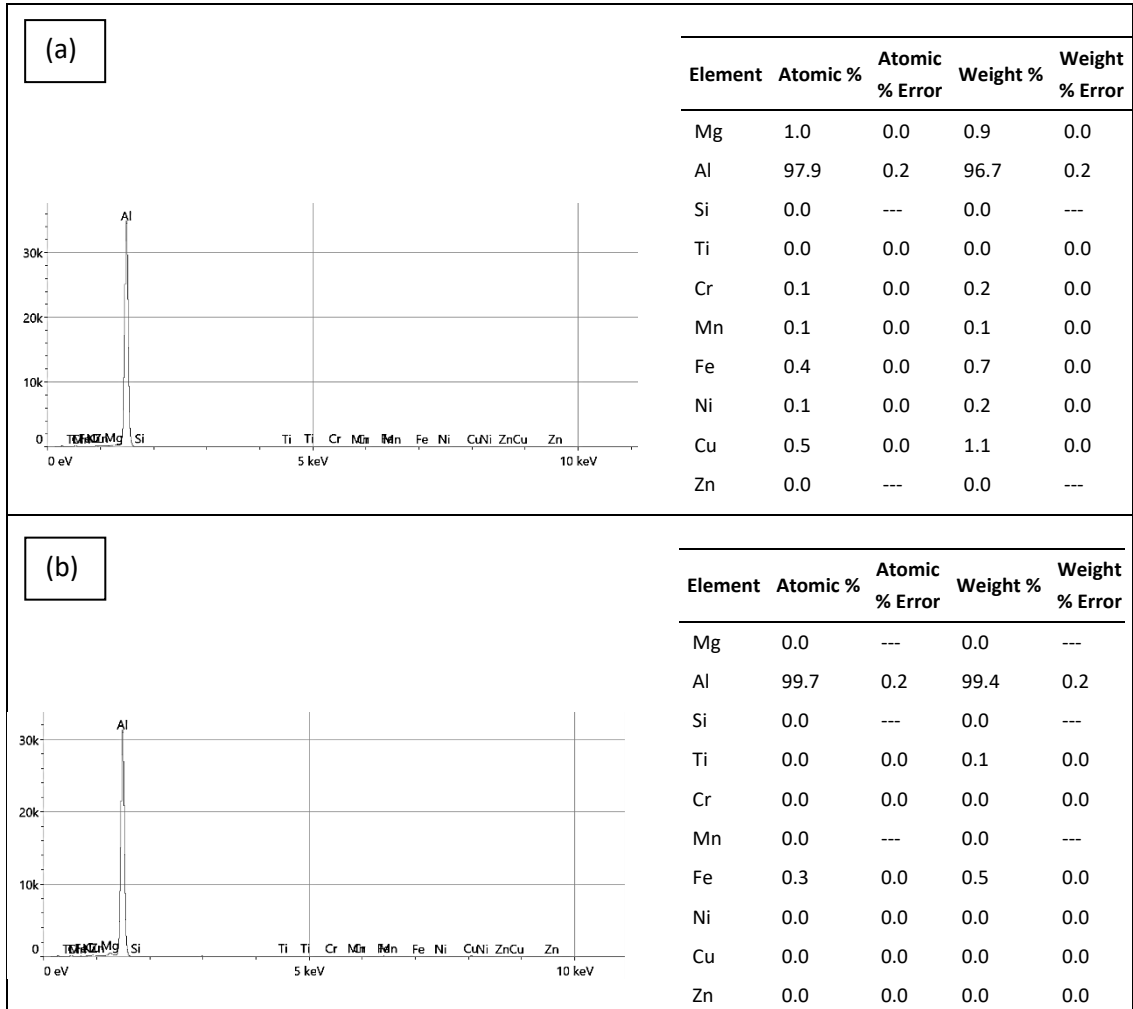
Figure 5.12. EDS for dissimilar weld AA6061-AA2024 at (a) nugget zone (b) at HAZ

5.5. XRD ANALYSIS of WELDMENTS

XRD analysis was performed to recognize the reaction phases shaped on the joint due to the limitations of EDS for quantify some phases. The main phase presented for all weldments are pure aluminum. As a result, XRD analysis may not confirm the presence of new reaction phases at the aluminum-aluminum interface, with the exception of a new phase named Al1.1Ni0.9 observed in sample 11. This, however, is hard to confirm due to the low percentage fraction of volume and tiny size of the possible interfacial reaction regions. Figure 5-13 presents the XRD test for AA6061-T6, AA2024-T3, AA6061-AA6061 sample 3, AA6061-T6 AA2024 sample 12. The original copies of reports analysis enclosed in the Annex A.
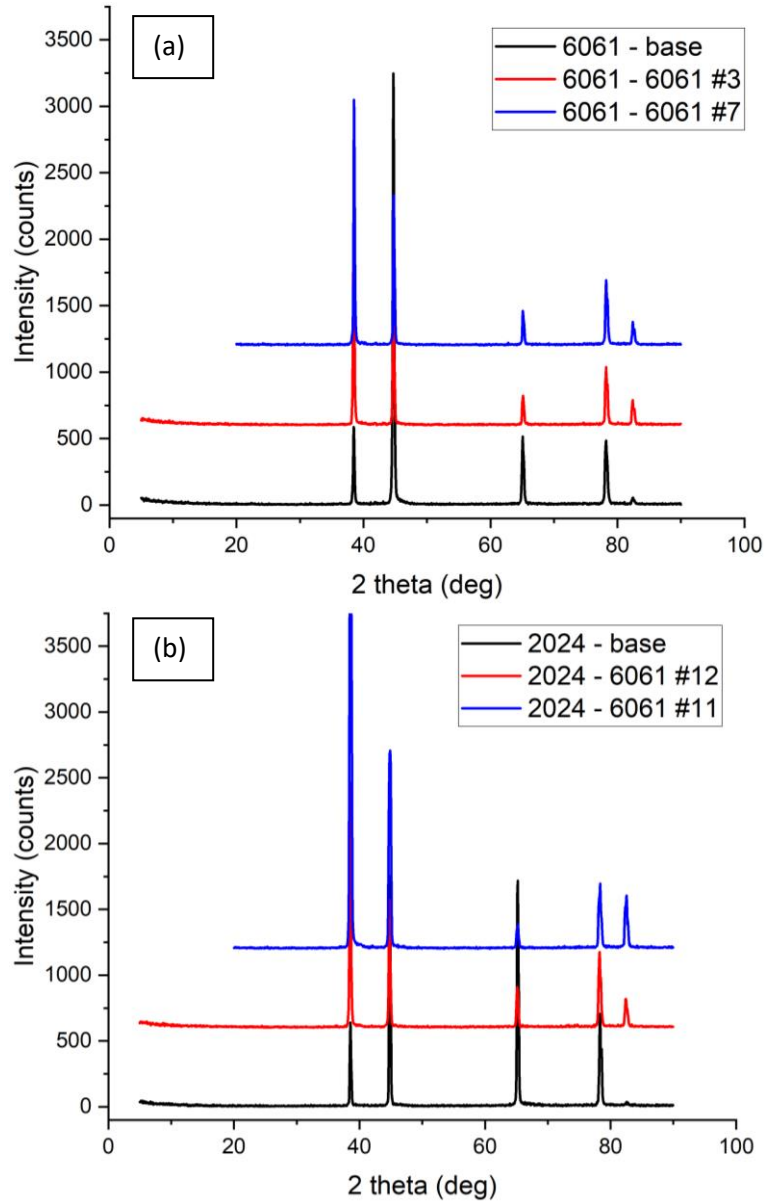
Figure 5.13. XRD analyses for a) AA6061-T6 and similar welded, b) AA2024-T3 and dissimilar welded samples.

5.6. TENSILE STRENGTH RESULTS

5.6.1. Similar Tensile Strength AA6061-T6 to AA6061-T6

The welded specimens with similar welding which include a three rotating speed and three travel speed were tested by tensile test under testing machine speed of 1mm/min.

The outcomes of tensile test are listed in Table 5-1. Generally, both yield and ultimate tensile strength are lower in the region of welding in contrast to that of the source material (before Annealing) due to a localized deformation or combination of dissolution, coarsening and precipitation of strengthening precipitates during FSW. The first operation conditions of welding, with Rotating Speed 0f 710 RPM and different travel speed of 45, 71 and 112 mm/min illustrations that the perfect elongation and ultimate tensile strength can be attained at 112 mm/min travel speed. This examination was repeated for other Rotating Speed s of 450 and 1400 RPM.

Figure 5-1 Relationship between the UTS and Travel Speed at different travel speeds for similar FSW and Figure 5-2 displays the relationship between the UTS and the travel speeds at different rotational speeds for dissimilar FSW. From the two figures it can be found that the optimum combinations of Rotating Speed and travel speed occurs at 710 RPM and 112 mm/min according to UTS tensile.
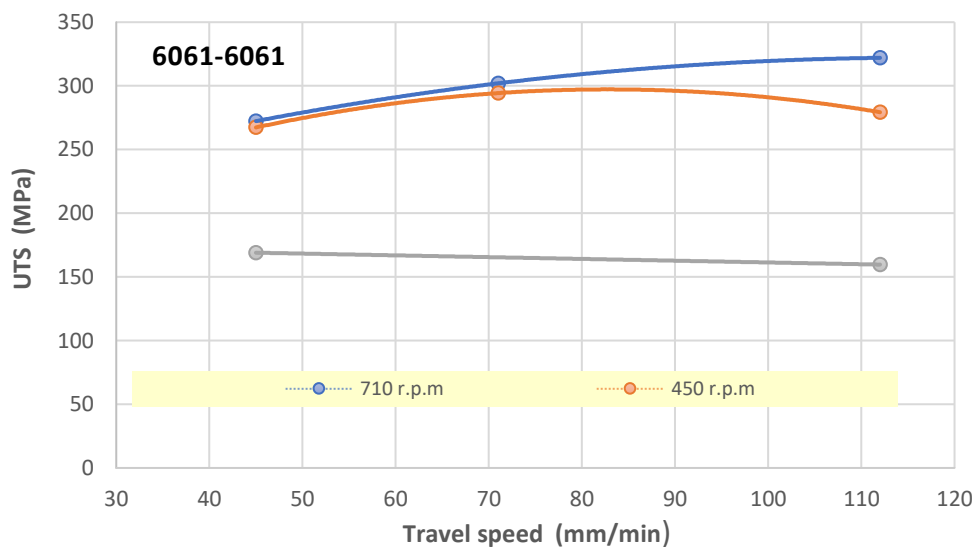
Figure 5.14 Relationship between the UTS and Travel Speed for similar weld.
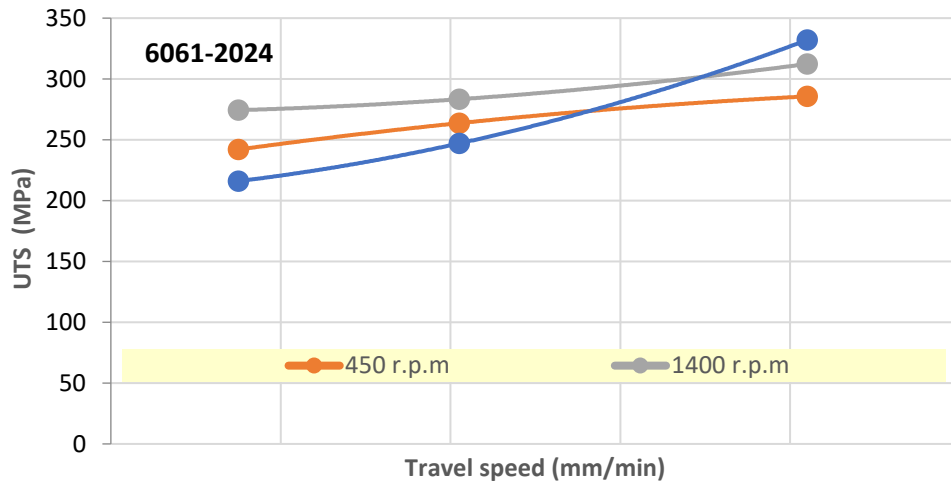
Figure 5. 15. Relationship between the UTS and travel speed for dissimilar FSW
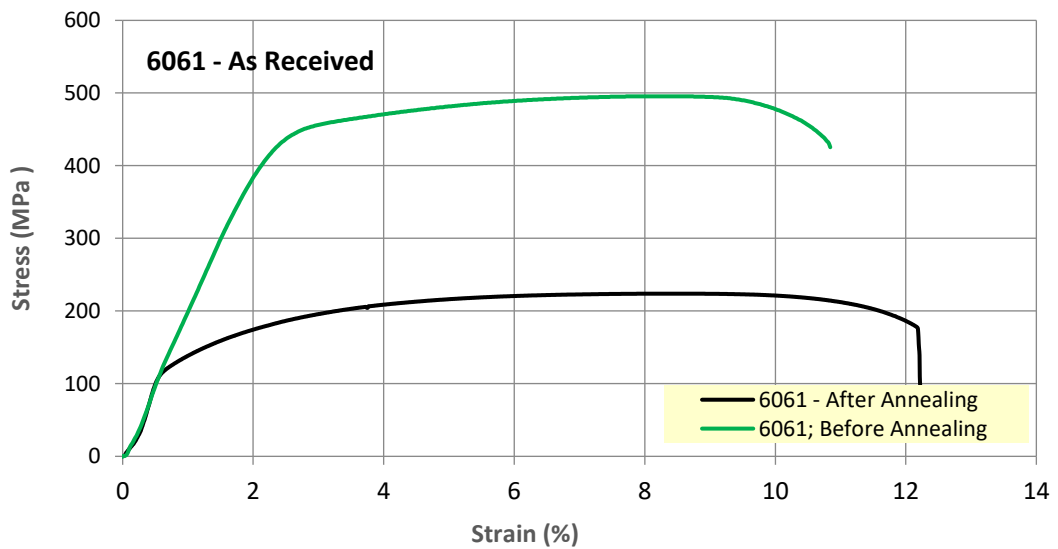
Figure 5.16. Stress-Strain curve for the base metal AA6061-T6 before and after annealing

Results of the tensile test for similar type weld (AA6061-T6) are listed in Table 5.1. Maximum ultimate tensile stress was found at value was 322 MPa compared with the base metal AA6061-T6 224 MPa; After Annealing, that because the annealing process results to relief the residual stresses from manufacturing process and increase the elongation. This value gives a higher efficiency (144%) compared with the other weldment.

Table 5.1. Tensile test result for similar FSW joints (AA6061-T6).

No.	Rotating Speed (RPM)	Travel Speed (mm/min)	UTS-1 (MPa)	UTS-2 (MPa)	UTS-3 (MPa)	UTS Mean
1	710	45	272	272	273	272
2	710	71	301	300	305	302
3	710	112	320	323	323	322
4	450	45	299	241	262	267
5	450	71	270	309	304	294
6	450	112	288	276	274	279
7	1400	45	210	136	161	169
8	1400	71	269	302	308	293
9	1400	112	146	176	157	160
AA6061 After Heat Treatment (Annealing)						224
AA2024 After Heat Treatment (Annealing)						384

Figures from 5.18 to 5.20 represent the tensile tests of similar welding for material (AA6061-T3) at three rotating speeds (N=710, 450 and 1400 RPM) and travel speeds (v=45, 71 and 112 mm/min). It was observed that the tensile ultimate stress of weldment was greater than that of the base alloy (after annealing) that because the fine in grain size in the welding zone. But the overall extension of the base material was less than those of each weldment at each welding conditions. Approximately, the yield tensile stress values are at the same strain range ($\epsilon < 1\%$).
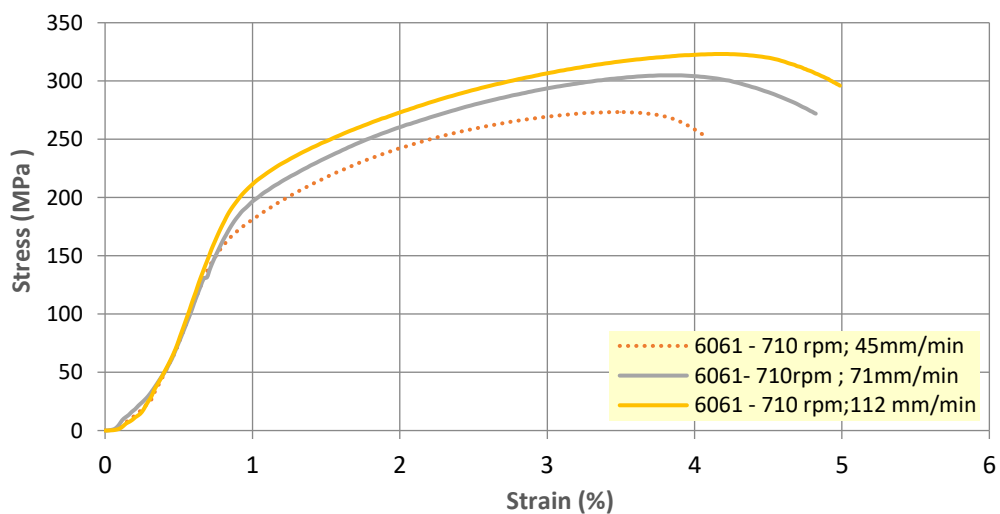
Figure 5. 17. Stress-Strain Curve for similar FSW at rotating speed (710 RPM)
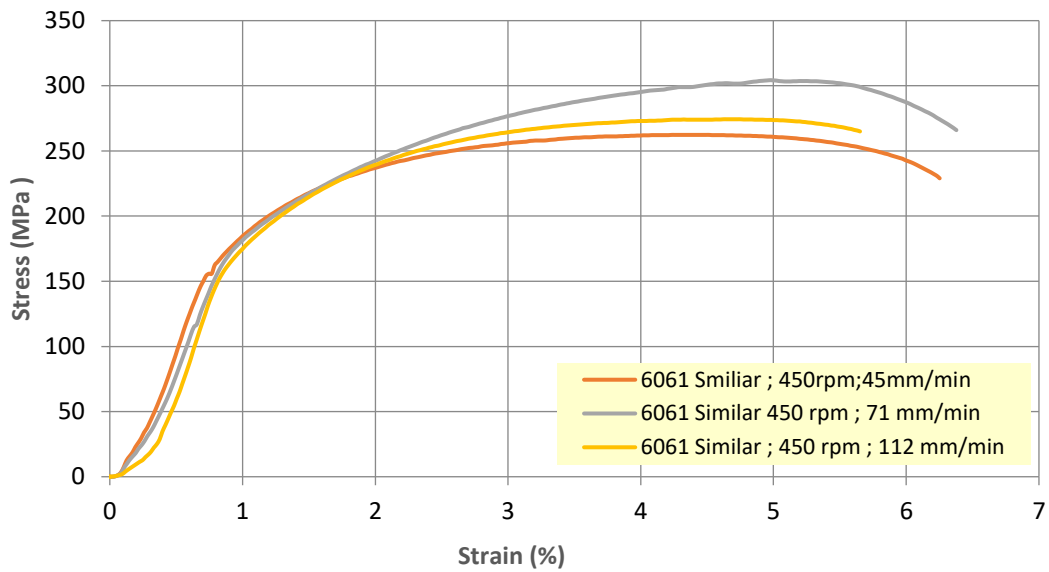
Figure 5. 18. Stress-strain % for similar FSW at rotating speed 450 RPM.

Figure 5. 19. Stress-strain % curve for similar FSW at 1400 RPM

In order to achieve high quality FSW welded joints with high mechanical properties, in other words high welding efficiency, the most dominated operational conditions for welding are (Rotating Speed and travel speed), this has to be carefully chosen to balance the effect of each parameter on the quantity of heat input during stir welding.

The shape and location of the tensile specimens' fractures can be used to make the following findings. First, the majority of the FSW joints failed in the heat affected zone (HAZ) on the advancing side. This is compatible with research deal with FSW of aluminum alloys such as Ren S. R. et al. [75], observed that the fracture of FSW of heat treatable aluminum alloys typically happens in the (HAZ), the softest zone in the FSW joints because of essential coarsening of the precipitates, also it matches to the findings of Mishra R. S. et al. [76], who obtained that the (HAZ) has the lowest degree of strength due to significant coarsened precipitates and the development of free precipitates zones (FPZs) and that also conforms to the conclusion of Sutton M. A. [60].

Second, failure took place in a plane almost perpendicular to the tensile axis. the third failure, under the same travel speed, a change in rotation rate did not modify the fracture mechanism, which is agreements with the observations of Ren et al [75].

Ren et al. [61] establish that for FSW both tool rotation rate and travel speed employ a substantial influence on the mechanical properties and thermal input. It was stated that the rising tool rotation rate in aluminum alloys AA6061-T6, AA6063-T5 led to higher heat input. This investigation adapts to the results in Table 5.1.

In order to explain the effect of each rotating and travel speed on the ultimate stress of weldment, Figures 5.21 and 5.22 have been taken into account. It has been observed from Figure 5.21 the ultimate stress was increase during the rising of rotating speed as in 710 RPM. Increasing the rotating speed increase the generated input heat as a consequence of the developed friction between tool and specimens but it reduced again due the high temperature that generated, as results, plastic deformation formation can be happened especially at the welding zone which leads to reduce the mechanical properties of weldments.

It may conclude that the friction stir welding required sufficient input heat to give best mechanical properties, increasing the rotating speed may negative results in high heat input which is high plastic deformation and stress remaining.
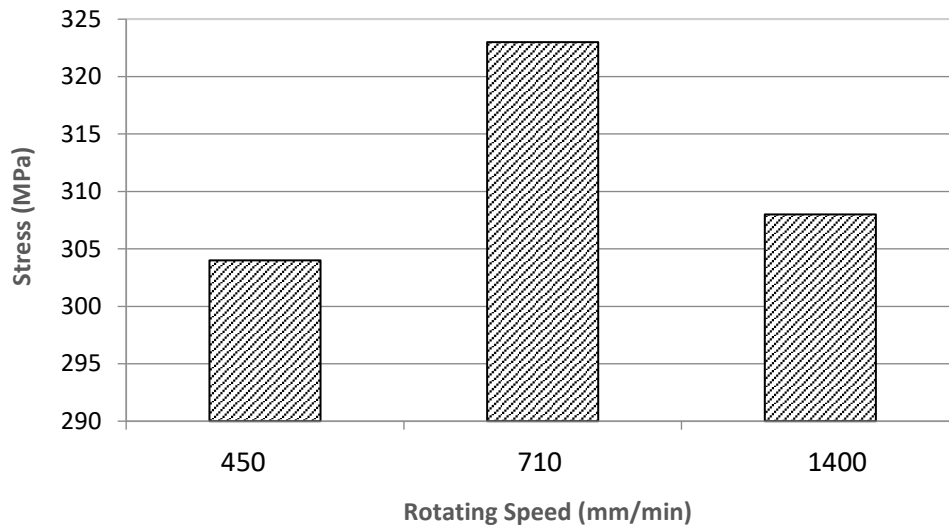
Figure 5. 20. Relationship between rotating speed and ultimate tensile strength for similar weld
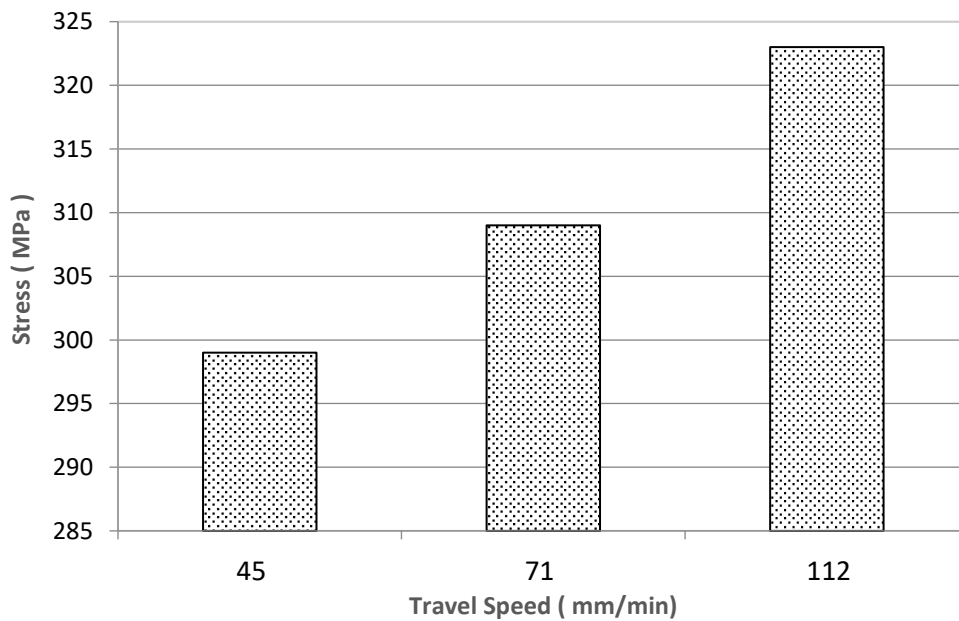
Figure 5. 21. Demonstrate the relationship between travel speed and ultimate tensile strength for similar weld

The travel speed has an effect on the tensile strength of the weldment as illustrated in Figure 5.6. The higher travel speed 112mm/min gives the highest tensile strength while lower (45mm/min.) speeds give a minimal tensile strength.

5.6.2. Dissimilar Welds (AA6061-T6 to AA2024-T3)

The results of tensile strength for dissimilar welding (AA6061-AA2024) were examined. Table 5.2 presents the findings of tensile test.

Table 5.2. Tensile test result for dissimilar FSW joints (AA6061-T6 to 2024-T3)

No.	Rotating Speed (RPM)	Travel Speed (mm/min)	UTS-1 (MPa)	UTS-2 (MPa)	UTS-3 (MPa)	UTS Mean
10	710	45	221	235	310	255
11	710	71	255	264	222	247
12	710	112	328	330	338	332
13	450	45	264	289	304	286
14	450	71	243	210	273	242
15	450	112	293	294	204	264
16	1400	45	308	311	306	308
17	1400	71	286	264	300	283
18	1400	112	287	327	323	312
AA6061 After Heat Treatment (Annealing)						224
AA2024 After Heat Treatment (Annealing)						384
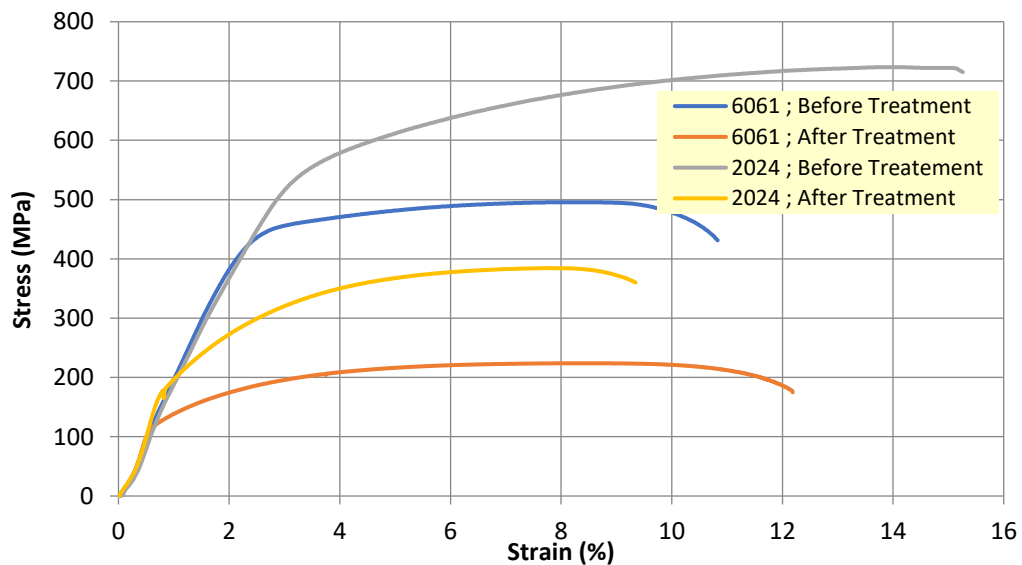
Figure 5. 22. Stress-Strain curve for the base materials before and after heat treatment (Annealing)

Figure 5.23 present the behavior of stress-strain curves of base metal (AA2024-AA6061). AA2024 had gotten the highest value σ=725 MPa before the heat treatment (as received -T6) while it reduced to (σ =384 MPa) after processing the heat treatment, that because the stresses accompanied to the rolling processes during the production, while the AA6061 registered (σ =497 and 224 MPa) before and after annealing respectively.
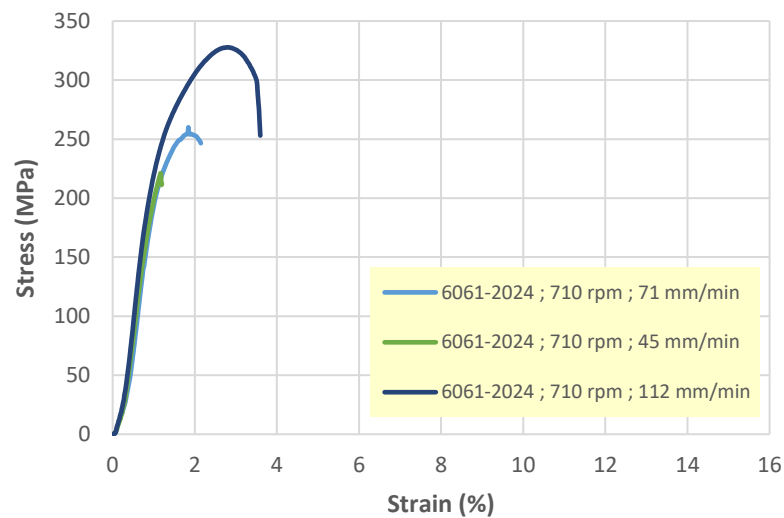
Figure 5. 23. Stress -Strain curve for the dissimilar FSW at rotation at speed 710 RPM

Figures from 5.24 to 26 presents the behavior of stress-strain curves of dissimilar welding (AA6061-AA2024) at different rotating and travel speed. They have been the same behavior of stress-strain curves for each specimen approximately for a wide range of stress (σ<300 MPa).

The results show that travel speed 112 mm/min and rotation speed 710 RPM gives the best tensile strength among the other parameters which is matching similar FSW.
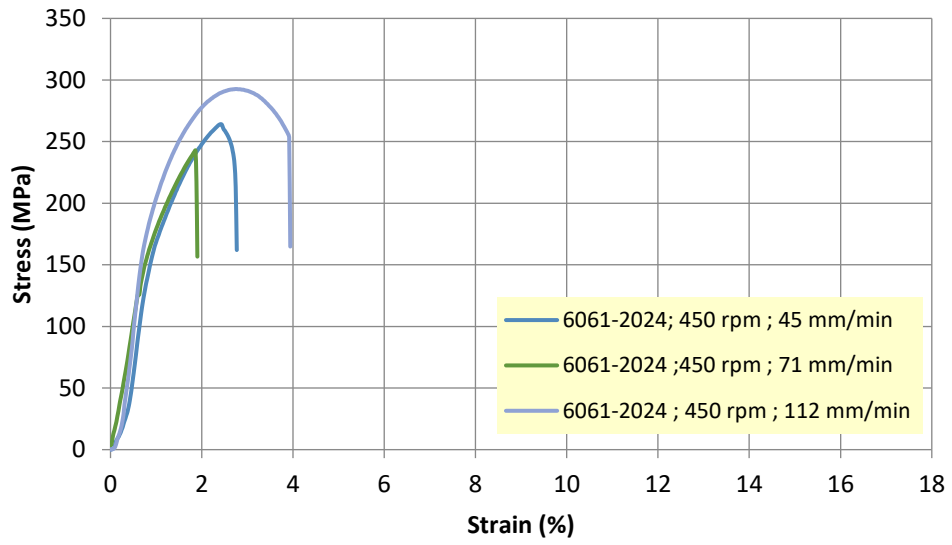
Figure 5. 24. Stress-strain curve for dissimilar FSW at rotating speed 450 RPM

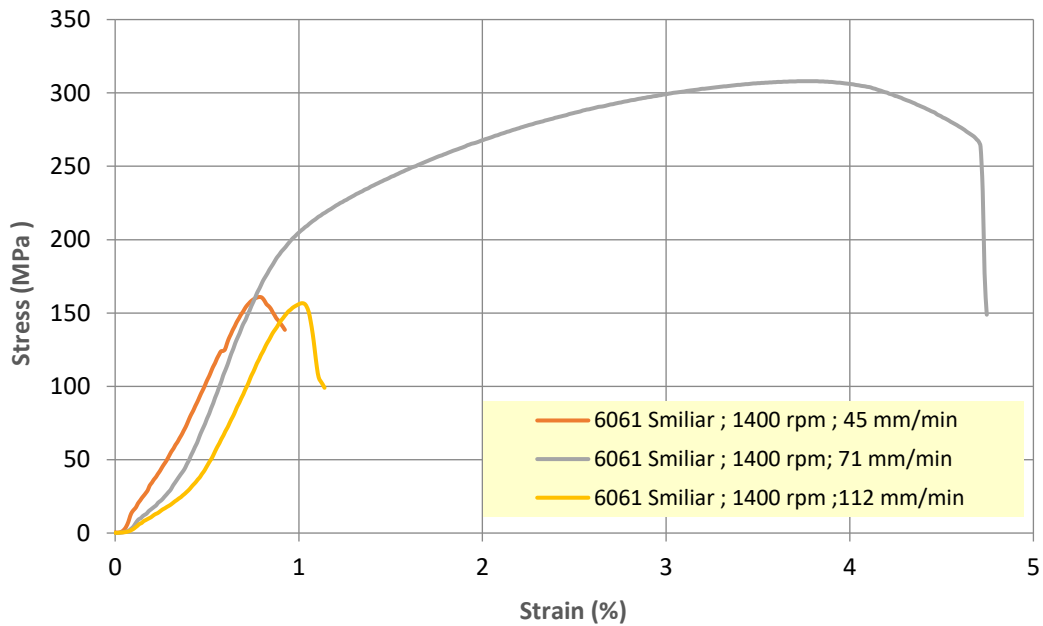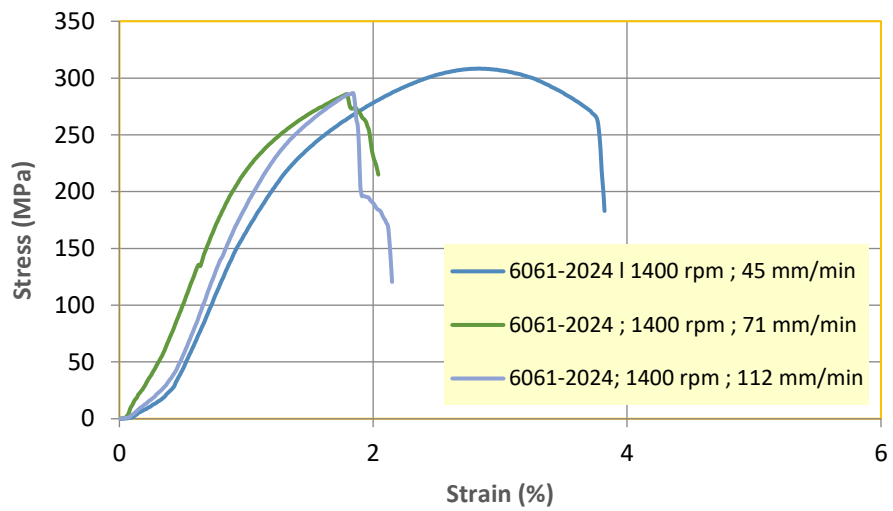Figure 5. 25. Stress-strain curve of dissimilar FSW at rotating speed 1400 RPM
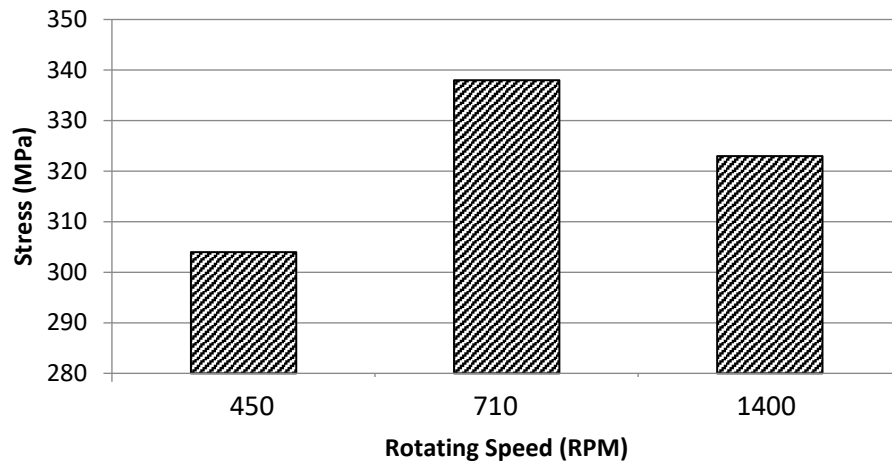
Figure 5. 26. Ultimate tensile stress vs. rotating speed for dissimilar weld

It has been observed from Figure 5.27 the ultimate tensile stress was increase during the rising in the rotating speed. Increasing the rotating speed increase the generated input heat because of the developed friction between tool and specimens. As results, plastic deformation formation can be happened especially at the welding zone which leads to reduce the mechanical properties of weldments. Figure 5.27 shows the highest stress has gotten when the Travel Speed 112 RPM, which is the same to the best condition in similar FSW.
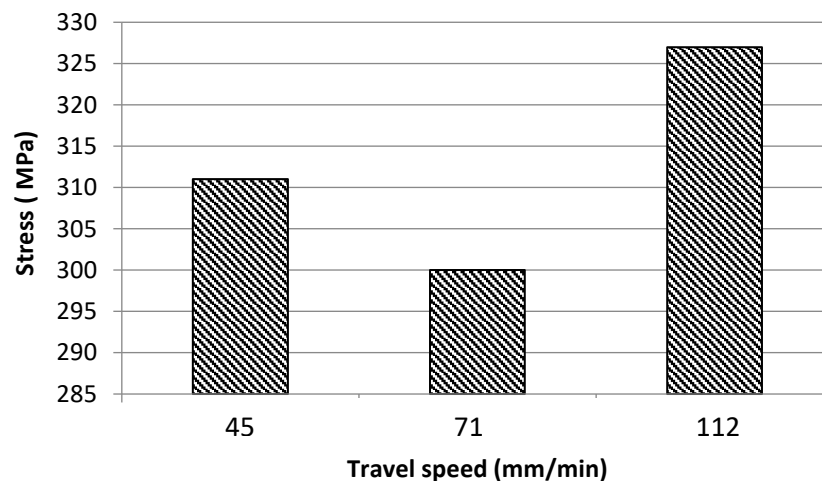
Figure 5.27. Effect of travel speed on tensile strength for dissimilar sheets

5.7. BENDING TEST RESULTS

The ultimate flexural stress is the maximum stress achieved before fracture (or before the stress decreases if the sample does not fracture). Figure 5.29 demonstrations the bend test for specimens consist of both AA6061-to-AA6061 Sample # 3 and AA6061 to AA2024 sample # 12 in addition to the base metals (as received).

The findings obtained from the bending tests were carried out in accordance with the tensile test results. Most of the bending specimens show V-shape. The bending angle was reached 120-140 and that mean in the bend test of the joints, some if cracks was observed with the weld root or face under any of the test conditions. All the specimens that tested were formed as a straight sided shape instead of a dog bone shape to save time and money.

The displacement control was 0.5 mm/min. The bending results indicated that most of specimens tested did not break completely except AA6061-AA2024 #12. This indicates that the specimens acted like brittle material. This is actually because of the presence of essential microcracks and kissing bond type defect in the stirred zone of this joint.

Table 5.3. Bending result for similar ad dissimilar FSW joints

Sample ID	Sample #1	Stress (MPa)	Load kN	Sample #2	Stress (MPa)	Load kN	Mean
6061-6061 # 03	Rbb	480	0.16	Rbb	454	0.15	467/0.155
	Rpb	-	-	Rpb	-	-	-
6061-2024 #12	Rbb	360	0.12	Rbb	420	0.14	390/0.13
	Rpb	-	-	Rpb	-	-	-
6061	Rbb	600	0.2	Rbb	600	0.2	600/0.2
	Rpb	360	0.12	Rpb	360	0.12	360/0.12
2024	Rbb	690	0.23	Rbb	690	0.23	690/0.23
	Rpb	420	0.14	Rpb	420	0.14	420/0.14
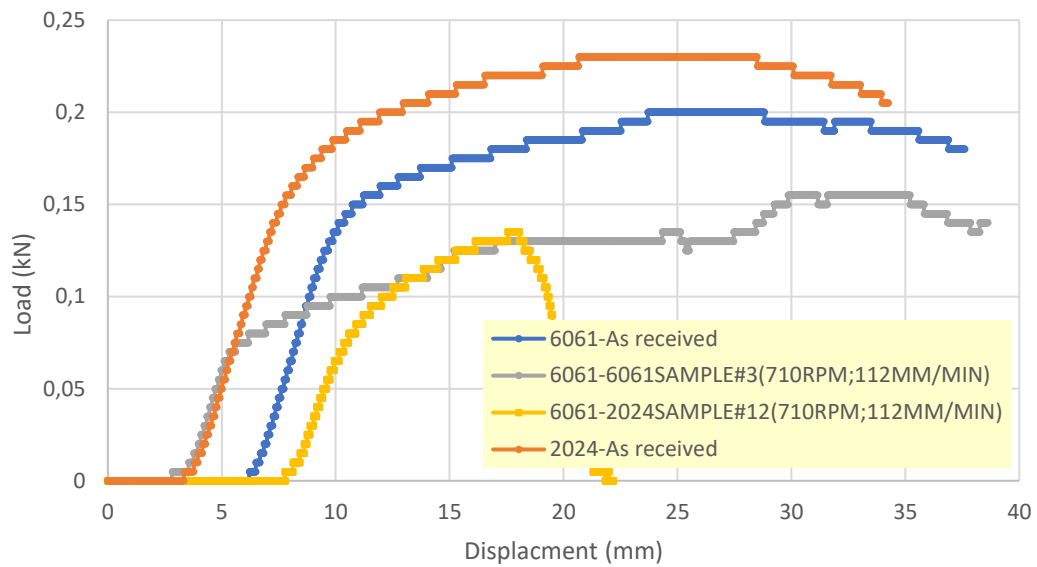
Figure 5. 28. Load –displacement curves for bending test
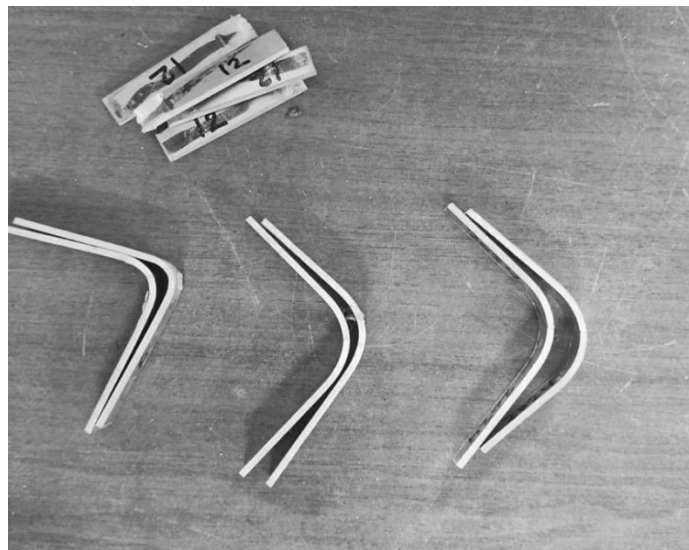
Figure 5. 29. Bended samples.

Figure 5-29 shows there is a substantial difference in bending strength for the specimens #3, #12 in comparison to the base metals, the specimens were welded under the similar operation conditions (rotation and travel speeds) demonstrating essential negative effect. The figure shows the strength of (AA6061-AA2024 # 12) is less than (AA6061-AA6061 # 3) that because formation microcracks during the FSW process which is weakened the bending strength.

5.8. MICRO HARDNESS RESULTS of SIMILAR and DISSIMILAR

As stated by the obtained finding of tensile and bending tests, the 710 RPM rotational speed at travel speeds 112 mm/min was selected to investigate the distribution of the microhardness at the mid thickness in the x-axis direction and along the thickness in the y-axis direction. Figure 5.31 illustrations the hardness distribution in the x-axis direction

Generally, the microhardness values in all welding areas are lower than that at the base metal. This indicates that the heat generated during FSW results in softening of the welded area because of grain coarsening or precipitate dissolution, which is consistent with the findings of Terry Khaled [54], who realized that for heat treatable aluminum alloys, FSW temperatures arriving at the NZ and parts of the (TMAZ) cause at least partial dissolution of the hardening phases. As a result, some softening within the NZ is to be expected in heat treatable metals welded in T-tempers. Some grain coarsening and softening may also occur in the HAZ.

Figure 5.31 demonstrates that the Vickers micro-hardness number, which was measured in numerous spots along the transverse centerline of the metallographic specimens of each welding base material.
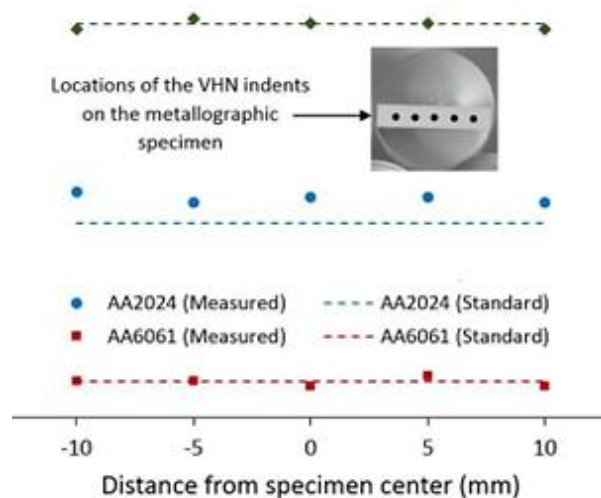
Figure 5. 30. Micro-hardness of the base materials
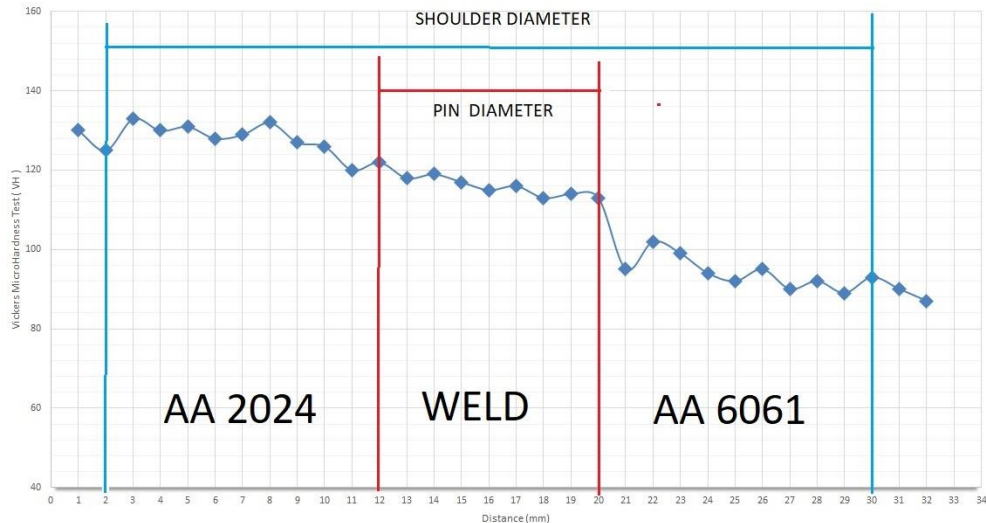
Figure 5. 31. Hardness for specimens #3 and # 12. The specimens were welded using the same travel and rotating speed which is 112 mm/min and 710 RPM respectively.

The reduction in weld hardness Figure 5.31 can be related to precipitate dissolution, which takes place when weld cooling rates discourage the nucleation and growth of all precipitates [14]. Mishra et al. [76] reported that FSW forms a softened zone surrounding the weld center in a variety of precipitation-hardening aluminum alloys. They propose that such softening is produced by the coarsening and dissolution of strengthening precipitates during the FSW's thermal cycle, and that the reported hardness profile is significantly affected by precipitate distribution rather than grain size in the weld.

Figure 5.31 indicates that the minimum hardness values exist on all sides of the weld in the HAZ. Owing to the post weld thermal cycle, pre-precipitation can occur in the material, where the precipitates dissolved in the matrix thus the hardness is able to be enhanced. However, hardness cannot be improved in the region where precipitates grow. The reappearance of precipitates in the NZ and TMAZ is a cause for hardness improvement. Precipitates in the HAZ matrix are not dissolved, hence there is no reappearance of precipitates because of the post-weld thermal cycle. This results in the lowest hardness and, as a result, fractures occur during tensile testing in the HAZ. This validates Kumar K. [78]'s conclusion. The width of the HAZ in most joints appears to be very small and only slightly influenced by process variables.

The average value of hardness of 105.15 HV was attained across the weldment for cylindrical threaded pin, the hardness of weld nugget was significantly lower than that of AA2024; on the other hand, the hardness is comparatively higher than 6061 base material and TMAZ.
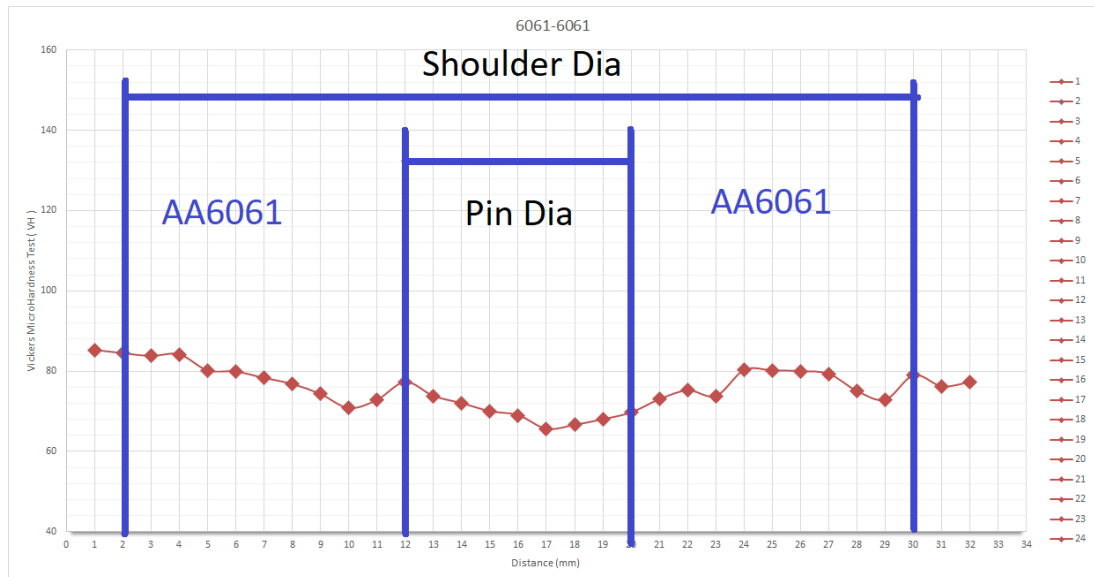
Figure 5. 32. Hardness for specimen #3, The specimens were welded using the same travel and rotating speed which is 112 mm/min and 710 RPM respectively.

While in similar, the graph of hardness was no substantial difference between among positions, because the similarity of metal but it also registered a little decrease in hardness of FSW zone due to the heat generated during the welding process. This means that fluctuations in temperature throughout the friction stir welding procedure influence the mechanical characteristics of welded region such as hardness.

The FSW technique parameters have been optimized based on the weldments' mechanical and metallurgical characteristics. According to the findings of this study, the most efficient rotating speed is 710 RPM, with a travel speed of 112 mm/min.

PART 6

CONCLUSION AND RECOMMENDATION FOR FUTURE WORKS

6.1. CONCLUSIONS

1. Friction stirs welding (FSW) of dissimilar Al-alloys 6061-T6 and 2024-T3 was successfully performed.

2. The best welding parameters were 710 RPM of tool rotation and 112 mm/min welding speed depending on tensile strength of similar welding.

3. The hardness results showed that the nugget zone has lower value than other welding zones in all welded joints for similar and dissimilar aluminum alloys.

4. The ultimate tensile strength and joint efficiency for dissimilar FSW joints were 338 MPa while for similar joint were 323 MPa for AA6061-T6.

5. SEM micrographs show formation micro cracks, some striation with cleavage fracture type dissimilar joints, while some specimens show ductile fracture type in similar joints.

6. SEM-EDS elemental analysis indicate, good mixing in stir zone sufficient diffusion of alloying elements Mg and Si between AA6061-T6 and AA2024-T3 alloys.

6.2. RECOMMENDATIONS FOR FUTURE WORK

1. Study the effect of mechanical properties such as impact test for similar and dissimilar joints.

2. Study mechanical properties (Residual Stress) for similar and dissimilar Al-alloys.

3. Study effect of shot peening and laser peening behavior of similar and dissimilar joints.

4. Study the effect of FSW parameters on corrosion resistance of Al- Joint.

5. Investigation of fatigue behavior of friction stir welded weld similar and dissimilar Al-Alloy.

6. Experimental and theoretical analysis for crack propagation in fracture surfaces for similar and dissimilar joints.

REFERENCES

[1] Murphy, A., Ekmekyapar, T., Özakça, M., Poston, K., Moore, G., & Elliott, M., " Buckling/post-buckling strength of friction stir welded aircraft stiffened panels .," *Journal of Aerospace ,* vol. Part G:, no. Proceedings of the Institution of Mechanical Engineers,, (2014)..

[2] Senthil Kumar T, Balasubramanian V, Sanavullah, "Influences of pulsed current tungsten inert gas welding parameters on tensile properties of AA6061 aluminium alloy," p. pp2080–2092., (2007).

[3] P.M.G.P. Moreira, T. Santos, , " Materials and Design," in *"Mechanical and metallurgical characterization of friction stir welding joints of AA6061-T6 with AA6082-T6",* (2009), p. pp.180–187..

[4] A.K.Lakshminarayanan, V. Balasubramanian &K. Elangovan, "Effect of Welding Processes in Tensile Properties of AA6061aluminum alloy joints," *",Int J Adv. Manuf.Technol., ,* pp. Vol. 40, PP.286-296,, (2009)..

[5] Sadeesh Pa, Venkatesh Kannan M, Rajkumar V , Avinash P and Arivazhagan N., " Studies on friction stir welding of AA 2024 and AA 6061 dissimilar metals"," *Procedia Engineering ,,* pp. Vol.75, PP:145 – 149, (2014).

[6] Colligan, K. J., & Mishra, R. S. , "A conceptual model for the process variables related to heat generation in friction stir welding of aluminum," *Scripta Materialia, ,* vol. 58, no. (5), pp. 327-331., (2008).

[7] J. Adamowski and M. Szkodo ," , "Friction Stir Welds (FSW) of aluminium alloy AW6082-T6," *, Journal of Achievements in Materials and Manufacturing Engineering ,* pp. Vol.20, Issue 1-2, , pp.403-406, 2007.

[8] G. Raghu Babu, K. G. K. Murti and G. Ranga Janardhana,, "An experimental study on the effect of welding parameters on mechanical and microstructural properties of AA 6082-T6 friction stir welded butt joints"," *ARPN Journal of engineering and applied sciences,* pp. vol.3 ,No.5, PP.68, , 2008..

[9] N. T. Kumbhar and K. Bhanumurthy, "Friction Stir Welding of Al 6061 Alloy," *Asian J. Exp. Sci.,,* vol. 22, no. 2, pp. 63-74, 2008.

[10] S. J. Al_Joudi, "The Influence Of Tool Geometry Of Friction Stir Weld On Mechanical Properties and Microstructure Of 2218_T72 Aluminum Alloy," *M.Sc. thesis, University of Baghdad, 2009.,* 2009.

[11] S. Rajakumar, C. Muralidharan, and V. Balasubramanian,, "“Establishing empirical relationships to predict grain size and tensile strength of friction stir welded AA 6061-T6 aluminium alloy joints," *Trans. Nonferrous Met. Soc. China,,* Vols. vol. 20, no.10,, p. pp. 1863.

[12] Perumalla J. Ramula and A.Satish Babu, , "The behavior of friction stir welding (FSW) sheet of AA6061-T6 during in-plane stretching test"," *International and conference on design and manufacturing of Icon DM, ,* (2013).

[13] H. Jamshidi Aval & S. Serajzadeh, "A study on natural aging behavior and mechanical properties of friction stir-welded AA6061-T6 plates," *Int J Adv Manuf Technol,* vol. 71, p. 933–941, 2014.

[14] M. L. Saad, "The Effect of Tool Geometry on the Strength of AA2024-T3 of Friction Stir Welding”," *M.Sc. thesis, Middle Technical University,,* (2015)..

[15] A. W. Shafey, "Determination of Residual Stress in Friction Stir welding of Alumium Alloy," 2016 .

[16] S. Malopheyev, I. Vysotskiy, V. Kulitskiy, S. Mironov, and R. Kaibyshev,“, "Optimization of processing-microstructure-properties relationship in friction-stir welded 6061-T6 aluminum alloy," *Mater. Sci. Eng.,* Vols. vol. 662, , pp. pp. 136–143, , 2016..

[17] "Friction Stir Welding of 2024 Aluminum Alloy to 2198 Aluminum-Lithium Alloy," MONTREAL, M.Sc Thesis , 2017.

[18] Munaf Hashim Ridha, Sohaib Khlil Alkhazraji, and Isam Tareq Abdullah, "Investigation of Friction Stir Welding of AA2024-T4 Thin," in *3rd International Conference on Sustainable Engineering Techniques*, 2020.

[19] Ying Li, L.E. Murr , J.C. McClure, "Flow visualization and residual microstructures associated with the friction-stir welding of 2024 aluminum to 6061 aluminum," *Materials Science and Engineering,* vol. A271, p. 213–223, 1999.

[20] P.Vilaça, J.P. Santos, A. Góis, L. Quintino, "JOINING ALUMINIUM ALLOYS DISSIMILAR IN THICKNESS BY FRICTION STIR WELDING AND FUSION PROCESSES," *Instituto Superior Técnico – Technical University of Lisbon (Portugal),* vol. 49, no. 3/4, 2005.

[21] Hidetoshi Fujii and Ling Cui, Masakatsu Maeda and Kiyoshi Nogi, "Effect of tool shape on mechanical properties and microstructure of friction stir welded

aluminum alloys," *", Materials Science and Engineering ,,* no. Vol. 419, PP: 25–31, , (2006).

[22] V. Balasubramaian, "'Relationship between base metal properties and friction stir welding process parameters",," *'Center of material joining research, Materials science, and engineering, ,* vol. Vol. 480, pp. PP. 397-403,, 2008. .

[23] S.T. Amancio-Filhoa, S. Sheikhia,J.F. dos Santosa, C. Bolfarini, "Preliminary study on The microstructure and mechanical properties of dissimilar friction stir welds in aircraft aluminium alloys 2024-T351 and 6056-T4," *Journal of materials processing technology,* vol. 206, pp. 132-142, 2008.

[24] R. M. Leal and A. Loureiro, " "Material flow in heterogeneous friction stir welding of thin aluminium sheets: Effect of shoulder geometry '," *Materials science and engineering, ,* Vols. Vol.A498,, pp. PP.384-391,, (2008)..

[25] P. M. G. P. Moreira, Jesus, A.M.P.and Ribeiro, A.S.,, " "Fatigue crack _growth behavior of the friction stir welded 6082_T6 aluminum alloy",," *Mecânica Experimental, ,* Vols. Vol.16, , pp. pp.99-106,, (2008). .

[26] Sadeesh Pa, Venkatesh Kannan M, Rajkumar V , Avinash P and Arivazhagan N.,, "Studies on friction stir welding of AA 2024 and AA 6061 dissimilar metals"," *Procedia Engineering,* Vols. Vol.75,, p. PP:145 – 149, (2014)..

[27] Nazar ABDULWADOOD1, Burak SAHIN1, Nihat YILDIRIM1, "EFFECT OF WELDING PARAMETERS ON THE MECHANICAL PROPERTIES OF DISSIMILAR ALUMINUM ALLOYS 2024-T3 TO 6061-T6 JOINTS PRODUCED BY FRICTION STIR," *Nigde Universities Muhendislik Bilimleri ,* vol. 3, no. 1, pp. 25-36, 2014.

[28] S Venkadesh and M Shunmathi, "Friction stir welding of AA2024 and AA6061 using various pin profile," *International Journal of Circuit, Computing and Networking,* vol. 2, no. 2, pp. 47-54, 2021.

[29] Svetsaren, ""A welding Review," *ESAB,,* Vols. 54,, no. 2, pp. 12-13,, 2000.

[30] J. R. Croteau et al, "Microstructure and mechanical properties of Al-Mg-Zr alloys processed by selective laser melting," *Acta Mater,* vol. 153, pp. 35-44, 2018.

[31] "A. Association, Aluminum ;properties and physical metallurgy ASM," 1984.

[32] J. R. Davis, "Aluminum and aluminum alloys," *ASM international,* 1993.

[33] S. Murali and M. S. Yong, "Liquid forging of thin Al-Si structures,," *J. Mater.Process. Technol,* Vols. 210,, no. 10, p. 1276–1281, 2010.

[34] H. Ardianto, "EFEK FRICTION STIR SPOT WELDING DALAM PEMASANGAN RIVET TERHADAP SIFAT MEKANIK MATERIAL ALMUNIUM SERI 2024," *Tek. STTKD J. Tek. Elektron. Engine,* vol. 7, no. 2, p. 184–192, 2021..

[35] R. Z. Wu, Z. K. Qu, and M. L. Zhang,, "Reviews on the influences of alloying elements on the microstructure and mechanical properties of Mg-Li base alloys,","" *Rev. Adv. Mater. Sci.,,* vol. 24, no. 1-2, pp. 35-43, 2010.

[36] C. K. S. Moy, M. Bocciarelli, S. P. Ringer, and G. Ranzi, "Identification of the material properties of Al 2024 alloy by means of inverse analysis and indentation tests,","" *Mater. Sci. Eng. A,,* vol. 529, no. 1, pp. 119-130, 2011,.

[37] Z. Zhao et al.,, "An overview of graphene and its derivatives reinforced metal matrix composites: Preparation, properties and applications," *Carbon N. Y.,,* vol. 170, pp. 302-326, 2020.

[38] B.F. Jogi , P.K. Brahmankar, "Some studies on fatigue crack growth rate of aluminum alloy 6061," *journal of materials processing technology,* vol. 201, p. 380–384, 2008.

[39] Jeom Kee Paik, "Mechanical properties of friction stir welded aluminum alloys 5086 and 5383","" *Inter J nav archit Oc Engng,* vol. 1, pp. 39-49, 2009.

[40] Mursal Luaibi Saad, "The Effect of Tool Geometry on the Strength of AA2024-T3 of Friction Stir Welding," *M.Sc. thesis ; Middle Technical University,* 2015.

[41] G.C.Jadhav, R.S.Dalu, "Friction Stir Welding – Process Parameters and its Variables","" *International Journal Of Engineering And Computer Science,* vol. 3, pp. 6325-6328, 2014.

[42] R. S. Mishra and Z. Y. Ma, "Friction Stir Welding and Processing," *Materials and engineering,* vol. R50, pp. 1-78, 2005.

[43] Livan Fratini , and Gianluca Buffa,, "CDRX modeling in Friction Stir Welding of aluminum alloys," *International Journal of Machine Tools and Manufacture,,* vol. 45, pp. 1189-1194, 2005.

[44] H. K. Mohanty, P. Biswas, N. R. Mandal, "Effect of Tool Shoulder and Pin Probe Profiles on Friction Stirred Aluminum Welds – a Comparative Study," vol. Vol.11, pp. 200-207, , 2012.

[45] ASTM A681, " Standard Specification for Tool Steels Alloy," (2008)..

[46] Salih careem, Using of Computer to Study the Hardening of Steel by Polymeric Solutions, M.Sc Thesis, The University of Technology , Baghdad , 2002.

[47] Hoile, S., "Processing and properties of mild interstitial free steels," *Materials Science and Technology,* vol. 16, no. 10, pp. 1079-1093, 2000.

[48] Liang, Y. L., Wang, Z. B., Zhang, J. B. & Lu, K., "Formation of interfacial compounds and the effects on stripping behaviors of a cold-sprayed Zn–Al coating on interstitial-free steel," vol. 3(40), pp. 89-95, 2015.

[49] A. K. &. K. D. R. Gupta, "Formability of galvanized interstitial-free steel sheets," vol. 172(2), pp. 225-237, 2006.

[50] Kenter, J. O., O'Brien, L., Hockley, N., Ravenscroft, N., Fazey, I., Irvine, K. N. & Williams, S.,, "What are shared and social values of ecosystems," no. 11(1), pp. 86-99, 2015.

[51] R. P. S. K. &. S. S. B. Jain, "A study on the variation of forces and temperature in a friction stir welding process , A finite element approach.," *Journal of Manufacturing Processes,* 2016.

[52] I. F. J. &. J. P. Garcia, "Electrodeposition and sliding wear resistance of nickel composite coatings containing micron and submicron SiC particles," vol. 148(3), pp. 171-178, 2001 .

[53] Erler, F., Jakob, C., Romanus, H., Spiess, L., Wielage, B., Lampke, T., & Steinhäuser,, "Interface behaviour in nickel composite coatings with nanoparticles of oxidic ceramic," vol. 48(22), pp. 3063-3070, 2003 .

[54] ASTM E747, "Standard Practice for Design Manufacture and Material Grouping Classification of Wire Image Quality Indicators Used forRadiology," 2008.

[55] ASTM E407-99,, "Standard Practice for Microetching Metals and Alloys," 2008.

[56] AWS D17.3/D17.3M, "Specification for Friction Stir Welding of Aluminum Alloys for Aerospace Applications," *American National Standards Institute,* pp. 14-25, 2010.

[57] ASTM B557M-02a, Standard Test Methods of Tension Testing Wrough and Cast Aluminum- and Magnesium-Alloy Products [Metric]",, (2008)..

[58] ASTM E986-97, "Scanning Electron Microscope Beam Size Characterization," 2008.

[59] J. H. L. S. J. C. H. Z. L. &. Z. J. Zuo, "Effect of deformation induced precipitation on grain refinement and improvement of mechanical properties AA 7055 aluminum alloy," 2017.

[60] Sutton M. A., Yang B., Reynolds A. P. and Taylor R.,, " "Microstructural studies of friction stir welds in 2024-T3 aluminum",," *Materials Science and Engineering A323, ,* pp. pp. 160-166, March 2001,.

[61] Ren S. R., Ma Z. Y. and Chen L. Q., "Effect of welding parameters on tensile properties and fracture behavior of friction stir welded Al-Mg-Si alloy," *Scripta Materialia,* Vols. 56, October , , no. , pp. 69-72. , 2006.

[62] Rajat Gupta, Sumit Jain, Arvinder Singh, in *"Friction Stir Welding"*, July (2013), pp. Vol.2, No.7, pp 1-2..

[63] A. S. H. J. R. Davis, Aluminum & Aluminum Alloys, 1993.

[64] A. H. Musfirah and A. G. Jaharah, "Magnesium and aluminum alloys in," *J. Appl. Sci. Res,* vol. 8, no. 9, p. 4865–4875, 2012..

[65] B. Stojanovic, M. Babic, S. Mitrovic, A. Vencl, N. Miloradovic, and M. Pantic,, "Tribological characteristics of aluminium hybrid composites reinforced with silicon carbide and graphite. A review,"," *J. Balk. Tribol. Assoc,* vol. 19, no. 1, pp. 83-96, 2013.

[66] A. Skulić and M. Bukvić,, "Tribological properties of piston-cylinder set in," *Appl. Eng. Lett,* vol. 1, no. 1, pp. 29-33, 2016.

[67] A. M. A. Al-Doori, "Fatigue Properties of Friction Stir Welded Aluminum Alloys," *M.Sc Thesis, Al-Nahrain University/ College of Engineering, Iraq, December,* 2010..

[68] R. a. Al-taie, "Residual Stress Effect on Fatigue Behavior of 2024- Aluminum Alloy,"," vol. 29, no. 3, 2011.

[69] M. Mahendra Boopathi, K. P. Arulshri, and N. Iyandurai, "Evaluation of mechanical properties of Aluminium alloy 2024 reinforced with silicon carbide and fly ash hybrid metal matrix composites," *Am. J. Appl. Sci.,,* vol. 10, no. 2, p. 219–229, 2013,.

[70] Z. Huda, N. I. Taib, and T. Zaharinie, "Characterization of 2024-T3: An aerospace aluminum alloy," *Mater. Chem. Phys,* vol. 113, no. 2-3, p. 515–517, 2009.

[71] in *ASM Metals Handbook*, 1992, p. 646.

[72] Ringer, S. P., & Hono, K,, "Microstructural Evolution and Age Hardening in Aluminium Alloys," *Elsevier Science Inc,* vol. 44, pp. 101-131, 2000..

[73] T. Khaled, *An Outsider Looks at Friction Stir Welding" Ph. D. Thesis,,* July 2005, pp. 1-71. .

[74] Hisham Elabd, Islam AbdelGhani, Michael Bushra. , "Friction stir welding Senior thesis II," *The American University in Cairo, ,* 2001.

[75] Jauhari T. Khairuddin, Jamaluddin A.", "Principles and Thermo-Mechanical Model of Friction Stir Welding," Vols. chapter 6,, pp. pp:25-26 ., 2012.

[76] ASM Metals Handbook,, vol. 04, 1992, p. 1568.

[77] Gupta, A. K., & Kumar, D. R., "Formability of galvanized interstitial-free steel sheets",," vol. 172(2), pp. 225-237, 2006.

[78] K. M. Y. &. M. Tachibana, "Hot dip fine Zn and Zn–Al alloy double coating for corrosion resistance at coastal area",," vol. 49(1), pp. 149-157, 2007 .

[79] Kumar K., Kailas S. V.,, "On the role of axial load and the effect of interface position on the tensile strength of a friction stir welded aluminum alloy," *Material and Design,* vol. 29, pp. 791-797..

[80] SHAO Qing, HE Yuting, ZHANG Teng and WU Liming, "Numerical Analysis of Static Performance Comparison of Friction Stir Welded versus Riveted 2024-T3 Aluminum Alloy Stiffened Panels," *CHINESE JOURNAL OF MECHANICAL ENGINEERING,* vol. 27, no. 4, pp. 761-, 2014.

[81] Safa M. Lafta , Maan A. Tawfiqb, "Experimental and Numerical Investigation into Residual Stress During Turning Operation for Stainless Steel AISI 316," *Engineering and Technology Journal,* vol. 38, no. A, pp. 1862-1870, 2020.

[82] Assefa Asmare , Raheem Al-Sabur and Eyob Messele, "Experimental Investigation of Friction StirWelding on 6061-T6 Aluminum Alloy using Taguchi-Based GRA," *Metals ,* vol. 1480, no. 10, pp. 1-21, 2020.

[83] Alexander Kalinenko a, Vasiliy Mishin b, Ivan Shishov b, Sergey Malopheyev a, Ivan Zuiko Vseslav Novikov a,c, Sergey Mironov a,*, Rustam Kaibyshev a,

Sheldon Lee Semiatin, "Mechanisms of abnormal grain growth in friction-stir-welded aluminum," *Materials Characterization,* vol. 194, 2022.

[84] Haining Yao , Ke Chen , Katsuyoshi Kondoh , Xianping Dong b, Min Wang , Xueming Hua , "Microstructure and mechanical properties of friction stir lap welds between FeCoCrNiMn high entropy alloy and 6061 Al alloy," *Materials & Design,* vol. 224, 2022.

[85] Y.J. Kwon , I. Shigematsu , N. Saito, "Dissimilar friction stir welding between magnesium and aluminum alloys," *Materials Letters,* vol. 62, p. 3827–3829, 2008.

[86] S. K. HUSSEIN, "ANALYSIS OF THE TEMPERATURE DISTRIBUTION IN FRICTION STIR WELDING OF AA 2024-T3 AND AA 6061-T6 USING FINITE ELEMENT METHOD," *U.P.B. Sci. Bull., Series,* vol. 78, no. 4, pp. 119-132, 2016.

[87] C. H. Bumgardner, B. P. Croom, N. Song, Y. Zhang, and X. Li, "Low energy electroplasticity in aluminum alloys," *Mater. Sci. Eng. A,* Vols. 798,, pp. 140235,, 2020..

[88] B. P. D. &. R. Xu, "Role of silicon in solidification microstructure in hot-dipped 55 wt% Al–Zn–Si coatings," vol. 473(2), pp. 76-80, 2008.

[89] V. F. K. S. V. A. A. P. &. A. N. Kosarev, "On some aspects of gas dynamics of the cold spray process," vol. 12(2), pp. 265-281, 2003.

[90] F. G. J. M. a. M. R. C. Leonardi, "Method of manufacturing electromagnetic devices using kinetic spray ; US Patent 7,097,885,Washigton USA," vol. 2006)..

[91] M. S. J. R. B. D. E. D. W. S. &. D. Grujicic, "Computational analysis of the interfacial bonding between feed-powder particles and the substrate in the cold-gas dynamic-spray process," vol. 219(4), pp. 211-227, 2003.

[92] H. G. F. S. T. &. H. Assadi, ""Bonding mechanism in cold gas spraying",," vol. 51(15), pp. 4379-4394, 2003.

[93] Gray, J., & Luan, B.,, "Protective coatings on magnesium and its alloys—a critical review",," vol. 336(2), pp. 88-113, 2002.

[94] Z. S. L. L. &. D. W. J. Wei, "Al arc spray coating on AZ31 Mg alloy and its corrosion behavior," vol. 48(8), pp. 685-688, 2005 .

[95] Ren S. R., Ma Z. Y. and Chen L. Q., " "Effect of welding parameters on tensile properties and fracture behavior of friction stir welded Al-Mg-Si alloy",," *Scripta Materialia,,* Vols. Vol, 56, , , pp. pp. 69-72, October 2006.

[96] Mishra R. S. and Ma Z., "Friction Stir Welding and Processing," *Material Science and Engineering R50,,* pp. pp. 1-78, August 2005,.

APPENDIX

Appendix A

XRD Reports
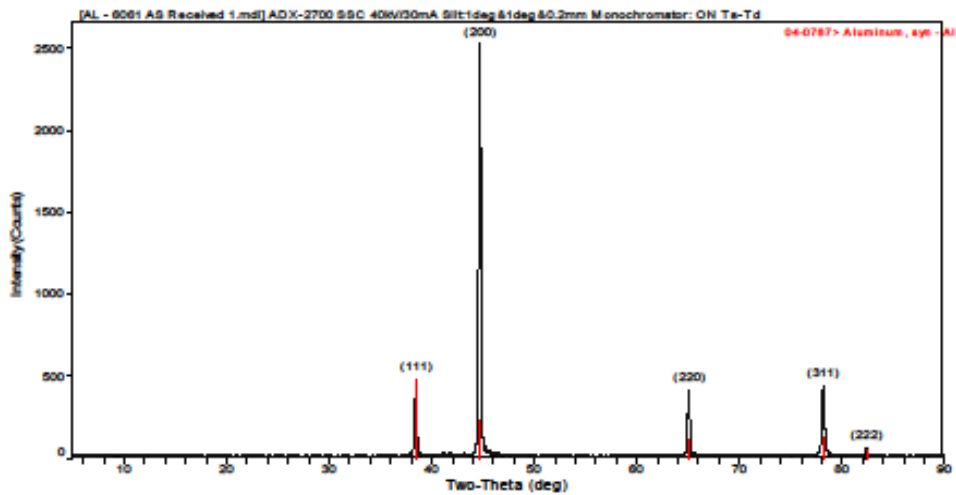
Peak ID Extended Report (5 Peaks, Max P/N = 25.1)

[AL - 6061 AS Received 1.mdi] ADX-2700 SSC 40kV/30mA Slit:1deg&1deg&0.2mm Monochromator: ON Ts-Td

PEAK: 11-pts/Parabolic Filter, Threshold=3.0, Cutoff=0.1%, BG=3/1.0, Peak-Top=Summit

2-Theta	d(nm)	Height	Height%	Phase ID	d(nm)	I%	(h k l)	2-Theta	Delta
38.447	0.23394	469	18.6	Al	0.2338	100 (1 1 1)		38.472	0.025
44.696	0.20258	2524	100	Al	0.2024	47 (2 0 0)		44.738	0.042
65.086	0.14319	402	15.9	Al	0.1431	22 (2 2 0)		65.133	0.047
78.152	0.1222	428	17	Al	0.1221	24 (3 1 1)		78.227	0.075
82.361	0.11699	45	1.8	Al	0.1169	7 (2 2 2)		82.435	0.074

Peak Search Report (5 Peaks, Max P/N = 25.1)

[AL - 6061 AS Received 1.mdi] ADX-2700 SSC 40kV/30mA Slit:1deg&1deg&0.2mm Monochromator: ON Ts-Td

PEAK: 11-pts/Parabolic Filter, Threshold=3.0, Cutoff=0.1%, BG=3/1.0, Peak-Top=Summit

2-Theta	d(nm)	(h k l)	BG	Height	I%	Area	I%	FWHM	XS(nm)
38.447	0.23394	(1 1 1)	7	469	18.6	2221	16.4	0.201	42
44.696	0.20258	(2 0 0)	9	2524	100	13513	100	0.228	38
65.086	0.14319	(2 2 0)	8	402	15.9	2302	17	0.243	38
78.152	0.1222	(3 1 1)	9	428	17	2868	21.2	0.285	36
82.361	0.11699	(2 2 2)	6	45	1.8	275	2	0.26	40

Peak ID Extended Report (7 Peaks, Max P/N = 20.9)
[AL 2024 -1.mdi] ADX-2700 SSC 40kV/30mA Slit:1deg&1deg&0.2mm Monochromator: ON Ts-Td
PEAK: 13-pts/Parabolic Filter, Threshold=3.0, Cutoff=0.1%, BG=3/1.0, Peak-Top=Summit

2-Theta	d(nm)	Area	Area%	Phase ID	d(nm)	I%	(h k l)	2-Theta	Delta
38.551	0.23334	3760	34.8	Al	0.2338	100	(1 1 1)	38.472	-0.079
44.846	0.20194	9810	90.7	Al	0.2024	47	(2 0 0)	44.738	-0.108
65.197	0.14297	10820	100	Al	0.1431	22	(2 2 0)	65.133	-0.064
67.541	0.13857	141	1.3						
75.761	0.12545	261	2.4						
78.339	0.12195	5757	53.2	Al	0.1221	24	(3 1 1)	78.227	-0.112
82.585	0.11673	428	4	Al	0.1169	7	(2 2 2)	82.435	-0.15

Peak Search Report (7 Peaks, Max P/N = 20.9)
[AL 2024 -1.mdi] ADX-2700 SSC 40kV/30mA Slit:1deg&1deg&0.2mm Monochromator: ON Ts-Td
PEAK: 13-pts/Parabolic Filter, Threshold=3.0, Cutoff=0.1%, BG=3/1.0, Peak-Top=Summit

2-Theta	d(nm)	(h k l)	BG	Height	I%	Area	I%	FWHM	XS(nm)
38.551	0.23334	(1 1 1)	4	637	36.4	3760	34.8	0.251	33
44.846	0.20194	(2 0 0)	0	1751	100	9810	90.7	0.238	36
65.197	0.14297	(2 2 0)	7	1712	97.8	10820	100	0.269	35
67.541	0.13857		9	17	1	141	1.3	0.355	27
75.761	0.12545		2	17	1	261	2.4	0.655	15
78.339	0.12195	(3 1 1)	7	700	40	5757	53.2	0.35	29
82.585	0.11673	(2 2 2)	6	31	1.8	428	4	0.587	18

[Sampel AL3 6061 - 1.mdi] ADX-2700 SSC 40kV/30mA Slit:1deg&1deg&0.2mm Monochromator: ON Ts-Td

04-0787> Aluminum, syn - Al
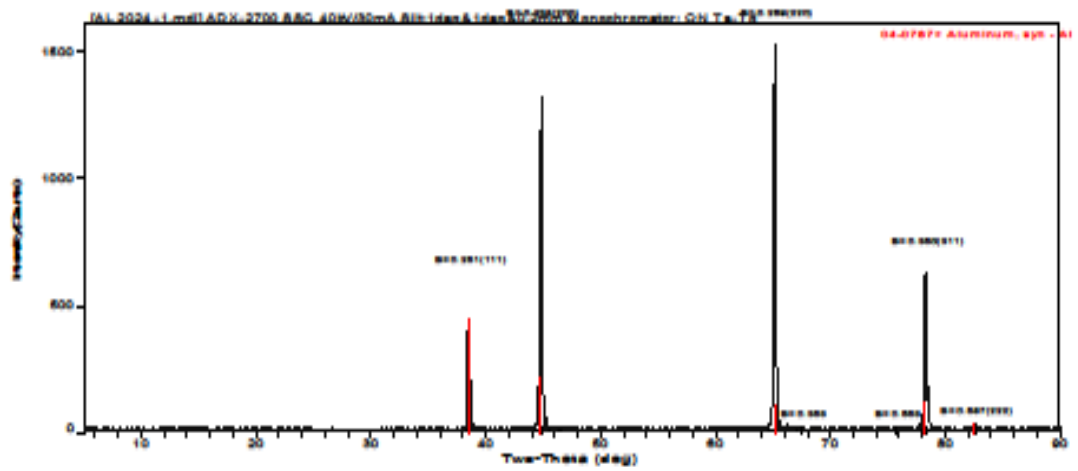
Peak ID Extended Report (6 Peaks, Max P/N = 19.9)

[Sampel AL3 6061 - 1.mdi] ADX-2700 SSC 40kV/30mA Slit:1deg&1deg&0.2mm Monochromator: ON Ts-Td
PEAK: 13-pts/Parabolic Filter, Threshold=3.0, Cutoff=0.1%, BG=3/1.0, Peak-Top=Summit

2-Theta	d(nm)	Height	Height%	Phase ID	d(nm)	I%	(h k l)	2-Theta	Delta
38.454	0.2339	1592	100	Al	0.2338	100	(1 1 1)	38.472	0.018
41.762	0.21611	17	1.1						
44.708	0.20253	1087	68.3	Al	0.2024	47	(2 0 0)	44.738	0.031
65.144	0.14308	223	14	Al	0.1431	22	(2 2 0)	65.133	-0.01
78.201	0.12213	439	27.6	Al	0.1221	24	(3 1 1)	78.227	0.026
82.395	0.11695	187	11.7	Al	0.1169	7	(2 2 2)	82.435	0.04

Peak Search Report (6 Peaks, Max P/N = 19.9)

[Sampel AL3 6061 - 1.mdi] ADX-2700 SSC 40kV/30mA Slit:1deg&1deg&0.2mm Monochromator: ON Ts-Td
PEAK: 13-pts/Parabolic Filter, Threshold=3.0, Cutoff=0.1%, BG=3/1.0, Peak-Top=Summit

2-Theta	d(nm)	(h k l)	BG	Height	I%	Area	I%	FWHM	XS(nm)
38.454	0.2339	(1 1 1)	7	1592	100	9393	100	0.251	33
41.762	0.21611		1	17	1.1	195	2.1	0.488	17
44.708	0.20253	(2 0 0)	2	1087	68.3	6785	72.2	0.265	32
65.144	0.14308	(2 2 0)	0	223	14	1764	18.8	0.336	28
78.201	0.12213	(3 1 1)	1	439	27.6	3998	42.6	0.387	26
82.395	0.11695	(2 2 2)	3	187	11.7	1772	18.9	0.403	26
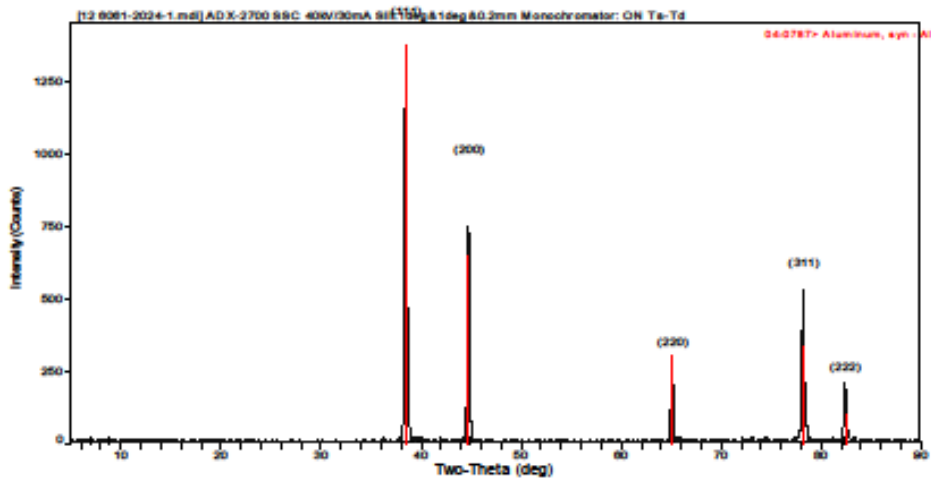
[12 6061-2024-1.mdi] ADX-2700 SSC 40kV/30mA Slit:1deg&1deg&0.2mm Monochromator: ON Ts-Td
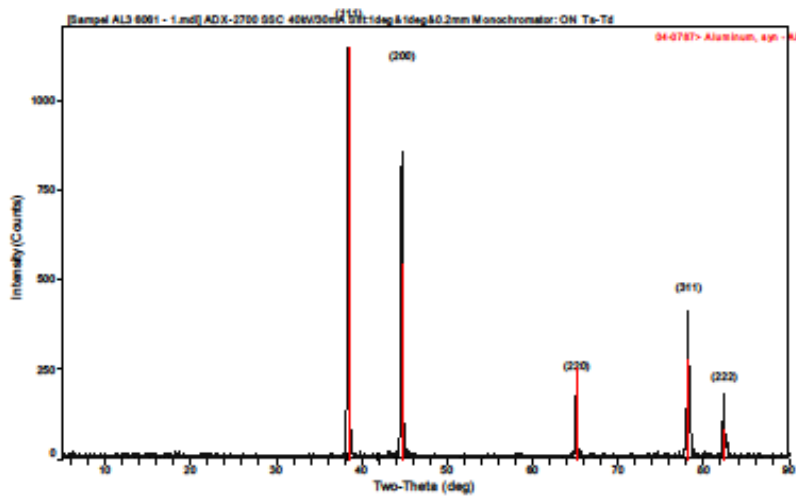
04-0787> Aluminum, syn - Al

Peak ID Extended Report (7 Peaks, Max P/N = 21.6)
[12 6061-2024-1.mdi] ADX-2700 SSC 40kV/30mA Slit:1deg&1deg&0.2mm Monochromator: ON Ts-Td
PEAK: 13-pts/Parabolic Filter, Threshold=3.0, Cutoff=0.1%, BG=3/1.0, Peak-Top=Summit

2-Theta	d(nm)	Height	Height%	Phase ID	d(nm)	I%	(h k l)	2-Theta	Delta
7.096	1.24469	21	1.1						
8.698	1.01578	23	1.2						
38.502	0.23363	1863	100	Al	0.2338	100	(1 1 1)	38.472	-0.029
44.792	0.20217	969	52	Al	0.2024	47	(2 0 0)	44.738	-0.054
65.15	0.14307	310	16.6	Al	0.1431	22	(2 2 0)	65.133	-0.017
78.245	0.12208	575	30.9	Al	0.1221	24	(3 1 1)	78.227	-0.018
82.406	0.11693	216	11.6	Al	0.1169	7	(2 2 2)	82.435	0.029

Peak Search Report (7 Peaks, Max P/N = 21.6)
[12 6061-2024-1.mdi] ADX-2700 SSC 40kV/30mA Slit:1deg&1deg&0.2mm Monochromator: ON Ts-Td
PEAK: 13-pts/Parabolic Filter, Threshold=3.0, Cutoff=0.1%, BG=3/1.0, Peak-Top=Summit

2-Theta	d(nm)	(h k l)	BG	Height	I%	Area	I%	FWHM	XS(nm)
7.096	1.24469		18	21	1.1	297	2.6	0.601	13
8.698	1.01578		14	23	1.2	152	1.3	0.281	28
38.502	0.23363	(1 1 1)	0	1863	100	11423	100	0.261	32
44.792	0.20217	(2 0 0)	3	969	52	6397	56	0.281	30
65.15	0.14307	(2 2 0)	0	310	16.6	2411	21.1	0.331	28
78.245	0.12208	(3 1 1)	2	575	30.9	5322	46.6	0.393	26
82.406	0.11693	(2 2 2)	4	216	11.6	2283	20	0.449	23

SEYKOÇ ALÜMİNYUM "TÜRKİYE'NİN LİDER ALÜMİNYUM TEDARİKÇİSİ"	UYGUNLUK SERTİFİKASI (Certificate of Conformity)	Document No : FR.061 Publishing Date : 01.10.2016 Revision Date : 15.03.2018 Revision No : 2 Page No : 1/1

Sertifika No (Certificate Number)	89246089		Tarih (Date)	22.11.2021

Genel Bilgi (General Information)

Formu (Form)	LEVHA		Lot No (Lot/Batch No)	69054
Ölçüleri (Dimensions)	2X1200X2500		Miktar (Kg) (Quantity)	1066
Alaşım (Alloy)	2024		Adet (Pieces)	64
Temper (Temper)	T3		Standartlar (Standards)	AIMS 03-04-011, ABS 5043 D

Kimyasal Analiz (Chemical Analysis)

DEĞERLER (VALUES)	ELEMENTLER (%) (Elements)										
STANDART (STANDARD)	Fe	Si	Mn	Cr	Ti	Cu	Mg	Zn	Each	Total	Al
Min.	-	-	0,30	-	-	3,8	1,2	-	-	-	-
Max.	0,50	0,50	0,90	0,10	0,15	4,9	1,8	0,25	0,05	0,15	
TEST SONUÇLARI (%) (Test Results)											
	0,05	0,05	0,46	0,03	0,02	4,4	1,4	0,03			

Mekanik Özellikler (Mechanical Properties)

1 Mpa = 1 N/mm² = 0.145 ksi =0.102 kgf/mm²

STANDART (STANDARD)	Çekme Dayanımı (MPa) (Tensile Strength)	Akma Dayanımı (MPa) (Yield Strength)	Uzama (%) (Elongation)	Sertlik (HB) (Hardness)
Min.	430	310	-	-
Max.				
TEST SONUÇLARI (%) (Test Results)				
	443	335	18	-

Ultrasonik Muayene (Ultrasonic Inspection)

Uygulandı (Done)	Uygulandı İse, Standardı (If Done, Standarts)		Uygulanmadı (Not Done)	X

Onay (Approval)

Seykoç Alüminyum bu uygunluk sertifikası ile, müşteriye teslim edilen ve yukarıda özellikleri tanımlanan ürünlerin; müşteri sipariş şartlarını sağladığını, rapor üzerinde belirtilen teknik değerlerin doğruluğunu ve uluslararası standart şartlarına uygunluğunu beyan ve taahhüt eder.
Seykoç Alüminyum with this conformity certificate, the products delivered to the customer and defined above features; customer order conditions, the accuracy of the technical values stated on the report and compliance with international standard requirements.
Bu Uygunluk Sertifikası, TS EN 10204 standardının 3.1 formatına uygun olarak hazırlanmıştır.
This Conformity Of Certificate was prepared in format 3.1 in accordance with TS EN 10204 standart
Bu Uygunluk Sertifikası, üretici firmanın orijinal sertifika bilgilerini içermektedir.
This Conformity of Certificate contains the information of the manufacturer's original certificate.

Kalite Kontrol Departmanı
(Quality Control Department)

Şahin ARSLAN

QUALITY CONTROL DEPT.
SEYKOÇ ALÜMİNYUM

العدد : ١٦٢٩٢/
التاريخ م:٢٩/٢/٢٢هـ

الدائرة : السيطرة النوعية
القسم : الصناعات الهندسية

الى/ وزارة الصناعة والمعادن / الشركة العامة للزجاج والحراريات/
القسم / الصيانة

م/ تسهيل مهمة

ندرج في ادناه نتائج الفحوص والتحاليل المختبرية التي اجريت على النماذج المرافقة لكتابكم ذي العدد
٣١٠٤ في ٢٠٢٢/١٢/١٤

التقييم	المواصفة المعتمدة	النموذج
- النموذج من الالمنيوم ومطابق للسبيكة (٧٠٧٥) (نتائج الفحص مرافقة).	BS EN 573-3	١. عينة من سبيكة الالمنيوم سمك (٣ مم) رمز النموذج: S/EG/2022/12/15/1427
- النموذج من الالمنيوم ومطابق للسبيكة (٦٠٦١) (نتائج الفحص مرافقة) .	BS EN 573-3	٢. عينة من سبيكة الالمنيوم سمك (٢ مم) رمز النموذج: S/EG/2022/12/15/1428

العائد للمهندس : حامد محمد كودي

- تم تسديد اجور الفحص البالغة (١٥٠٠٠٠) مائة وخمسون الف دينار .
- تم اتلاف النماذج وفقاً لمتطلبات الفحص علما ان مدة الحفظ للنماذج اسبوعين من تاريخ اصدار الكتاب اعلاه
وبخلافه يسقط حقكم بالمطالبة بالنماذج .
- لا يعتمد هذا الكتاب مالم يكن مختوما بختم الجهاز .

للتفضل بالاطلاع ٠٠٠ مع التقدير

المرافقات :
تقرير اختبار عدد (٢)

المهندس
وسام سعيد عاصي
مدير عام دائرة السيطرة النوعية
٢٠٢٢/١٢/ ١٩

صورة عنه الى/
- مكتب رئيس الجهاز / للتفضل بالاطلاع ٠٠٠ مع التقدير
- دائرة السيطرة النوعية/ مكتب المدير العام / للتفضل بالاطلاع ٠٠٠ مع التقدير
- قسم الصناعات الهندسية / ت٣/ ٥٣٣ (٥ خمسة)

RESUME

His name is Hamid Mohammed Kodi KODI primary and elementary education in Iraq. He is a mechanical engineer who graduated from the Faculty of Engineering, University of Technology – Iraq. He received his bachelor's degree in 1990. He currently works as Director General in the General State Company of Glass and Refectories at Ministry of Industrial and Minerals – Iraq. He is currently studying for his master's degree at Karabuk University in the field of Metallurgical Engineering.